eport No. FHWA-RD-79-42

UNDAMENTAL STUDIES
.N AUTOMATIC VEHICLE CONTROL

May 1978
Interim Report

Document is available to the public through
the National Technical Information Service,
Springfield, Virginia 22161

Prepared for
FEDERAL HIGHWAY ADMINISTRATION
Offices of Research & Development
Traffic Systems Division
Washington, D.C. 20590

FOREWORD

This report presents the achievements of the first year of a three year program to develop critical technologies for automatic lateral and longitudinal control for ground vehicles. These technologies are those essential for maneuvers such as switching, lane changing, and merging under both normal and emergency conditions. The vehicles will be capable of operating in high-speed, small time-headway situations through complex guideway networks.

The results are being distributed to researchers in automatic vehicle control through annual interim reports so that the achievements can be made available on a timely basis.

Charles F. Scheffey
Director, Office of Research

NOTICE

Technical Report Documentation Page

1. Report No.	2. Government Accession No.	3. Recipient's Catalog No.
FHWA-RD-79-42		

4. Title and Subtitle
Fundamental Studies in Automatic Vehicle Control

5. Report Date
May 31, 1978

6. Performing Organization Code
784712

8. Performing Organization Report No.
784712-1

7. Author(s)
R.E. Fenton, R.J. Mayhan, G.M.Takasaki, J.Glimm

9. Performing Organization Name and Address
Transportation Control Laboratory
Department of Electrical Engineering
The Ohio State University
Columbus, Ohio 43210

10. Work Unit No. (TRAIS)

11. Contract or Grant No.
DOT-FH-11-9257

13. Type of Report and Period Covered
Interim Report
April 1977-April 1978

12. Sponsoring Agency Name and Address
Office of Research and Development
Federal Highway Administration,
Department of Transportation
Washington, D.C. 20590

U.S.

14. Sponsoring Agency Code

15. Supplementary Notes
FHWA Contract Manager: Fred Okano (HRS-32)

16. Abstract

During the past year, which was the first year of a planned three-year program, the research efforts were focused principally on the development of a physical test facility which would be employed to study control and communication problems at, and below, the sector level. These studies would be focused on the automatic control of high-speed (to 28.1 m/s), traffic operations at time headways as small as 1 s.

The primary activites undertaken were: a) The implantation of both lateral and longitudinal information sources at the 6.4-km, skid-pad facility at the Transportation Research Center of Ohio (TRCO); b) The specification of a sector-level controller which would be comprised of a commercially available microprocessor and a considerable amount of special-purpose hardware; c) A study of automatic longitudinal control, both in the normative and emergency modes of operation; d) The evaluation of a "flattened" helical-line information source for providing continuous position information to each controlled vehicle in a sector; and e) A study of automatic steering with an emphasis on high-speed, lane-changing operations. The status of items (a), (c) and (d) are discussed in detail, while (b) and (e) will be discussed in two forthcoming papers.

The secondary activities included a reevaluation of a headway safety policy for automated highway operations, and the development of a methodology to determine the accident costs associated with a particular policy choice.

17. Key Words	18. Distribution Statement
Automatic highway, dual-mode, automatic longitudinal control, information source, headway policy, sector communications, sector computer	This document is available to the public through the National Technical Information Service, Springfield, Virginia, 22161

19. Security Classif. (of this report)	20. Security Classif. (of this page)	21. No. of Pages	22. Price
unclassified	unclassified	197	

Form DOT F 1700.7 (8-72)

Reproduction of completed page authorized

ACKNOWLEDGMENTS

Prof. Karl Olson and Mr. Ronald Ventola played a vital role in several activities, most especially the instrumentation of the test track at TRCO. Mr. Richard Bishel performed many of the required computations and some of the artwork, and Ms. June Barrington and Joanne Alt typed the manuscript. Their assistance was very much appreciated.

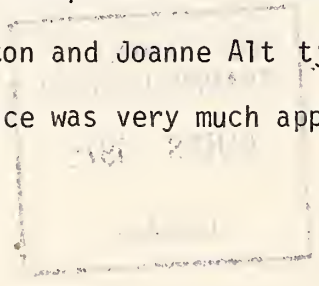

FUNDAMENTAL STUDIES

IN

AUTOMATIC VEHICLE CONTROL

EXECUTIVE SUMMARY

The control required for an automated highway system can be achieved via a hierarchy wherein a centralized computer would oversee network operations with this including the coordination of activities in the individual geographic regions comprising the network. A second level of control would be at the regional level. Each regional controller would supervise the activity of a number of sectors and control the vehicles in those sectors via appropriate commands to the sector computers which comprise the third level of control. The fourth level of control is that of the individual vehicle. In this study, the focus is on the following essential aspects of the latter two levels:

a) The specification of the desired state of each vehicle;

b) The determination of the actual state of each vehicle;

c) Communications between each vehicle and sector-control; and

d) The control of each individual vehicle.

Each of the facets can be viewed in the context of either longitudinal or lateral control.

During the past year, which was the first year of a planned three-year program, The Ohio State University efforts were focused principally on the development of a physical test facility which will be employed

to study control and communication problems at, and below, the sector level. These studies will be focused on the automatic control of high-speed traffic (to 28.4 m/s) operating at time headways as small as 1 s.

Within this framework, the principal accomplishments over the first year of this study include:

a) The implantation of sources to provide each controlled vehicle with a continuous measure of its lateral and longitudinal state over the complete extent of the 6.4 km, skid-pad facility at the Transportation Research Center of Ohio (TRCO). (Some 27,500 m (90,000 ft) of wire were inserted in specially cut slots in the pavement and sealed in place);

b) The development and laboratory testing of an approach employing audio frequencies and a "flattened" helical information source to provide continuous, absolute position information within an accuracy of ±0.33 cm, to a string of moving vehicles; and

c) The design of a vehicle longitudinal controller for both normal and emergency modes of operation, and the preliminary evaluation of that controller under full-scale conditions.

In addition, substantial progress was made on the following:

a) The design and evaluation of a steering controller which is adaptive to changes in vehicle speed; and

b) The development of a sector-level controller which is

comprised of a commercially available microprocessor and a considerable amount of special-purpose hardware. These items will be discussed in a subsequent report.

The secondary accomplishments included the reevaluation of a headway safety policy for automated highway operations, and the development of a methodology to determine the accident costs associated with a particular policy choice.

The second-year efforts will be focused on the following six topics with the primary emphasis being on the first four:

a) The continued development of the automated vehicle test facility of TRCO;

b) The implementation of a sector-level controller;

c) Studies in automatic longitudinal control under both normative and emergency conditions;

d) Studies in vehicle lateral control with an emphasis on lane-changing operations; and

e) The specification and development of a sector-level communication system; and

f) The instrumentation of a third test vehicle.

TABLE OF CONTENTS

LIST OF FIGURES

Figures (Cont.)

Figures (Cont.)

Figures (Cont.)

Figures (Cont.)

LIST OF TABLES

CHAPTER I

INTRODUCTION

A. Introduction

In recent years much attention has been focused on various forms of individual-vehicle, automated ground transport as one promising approach toward the solution of both present and anticipated future transportation problems. The suggested systems have generally fallen into three categories:

1) Captive-vehicle systems for use in restricted geographical areas;
2) Dual-mode systems for general coverage of urban areas; and
3) Dual-mode systems for intercity automated highways.

The potential advantages associated with each category are well known and will only be briefly summarized here. The first offers transportation to all citizens in a limited area--such as downtown business district--and the partial or complete elimination of privately owned vehicles from that area with an attendant reduction in noise, air pollution, and congestion. The feasibility of this class is currently being evaluated via the operational system at Morgantown, West Virginia (1).

The general class of dual-mode systems offers the prospects of high flow capacities, enhanced vehicle safety, door-to-door movement in either a public conveyance, such as dial-a-bus, or in a privately owned

vehicle, and extended mobility to the poor, the aged, and the infirm. DOT had planned to develop a prototype dual-mode system by 1980 (2); however, this plan has been indefinitely postponed.

The initial studies on the automated highway were conducted in the late 1950's and subsequently limited efforts were undertaken, both here and abroad, by various industrial organizations, government laboratories and academic institutions (3)-(18). This type of system would probably be first considered for an already congested network (e.g., the Northeast corridor) because of its prospects for substantially increasing both flow capacity and highway safety.

B. Automated Highway System Concept

The general dual-mode concept involves a roadway complex which consists of both automated and nonautomated roads. Various main arteries would probably be equipped for automation while various secondary streets/roads would not be equipped. Ultimately, it would be expected that public vehicles and both individual private vehicles and commercial traffic would use the system; however, it seems likely that initially only mass transit vehicles would be employed.

An individual vehicle would enter the system at a special entrance point where it would first undergo a rapid automatic checkout, and the driver would indicate his destination. If it "passed" the checkout, the vehicle would move to an entrance ramp from which it would be automatically merged into the traffic stream. However, if it "failed" the vehicle would not be allowed to merge into the traffic stream; instead,

it would be rejected and guided to a nearby service facility for repair.

The traffic stream velocity would be fixed by a central traffic controller and would be dependent on weather, roadway conditions, the state of the traffic stream, etc. Once in the traffic stream, the vehicle would remain under automatic control until the driver's preselected exit was reached. Then the vehicle would be guided off the roadway onto an exit ramp, and control would be returned to the driver.

In the event of vehicle disability, the vehicle would be ejected from the main traffic stream. If it were controllable, it would be routed to the nearest emergency exit. If it were not, the use of one lane would be lost until the vehicle could be moved off the highway. Hence, it would be temporarily necessary to direct the mainstream vehicles around the disabled one. Clearly, some provision must be made for clearing the roadway as quickly as possible.

C. Dual-Mode Control Hierarchy

The control required for the automated part of a dual-mode system is comprised of two intimately related facets. The first, macro-control, embodies the entire hierarchy of control which is necessary for system coordination. This is, of course, the "systems" level of control, and it includes such operations as vehicle scheduling and routing, the determination and specification of traffic speeds, and system response to abnormal and emergency situations. The second facet, micro-control, is explicitly concerned with individual vehicle position regulation and

maneuvering and encompasses both vehicle lateral control and longitudinal control.

A general control hierarchy, which could be employed with an automated vehicle system, includes a central controller to oversee network operations with this including the coordination of activities in the individual geographic regions comprising the network (see Fig. 1). A second level of control would be at the regional level. Each regional controller would supervise the activity in a number of sectors and control the vehicles in those sectors via appropriate commands to the sector computers which comprise the third level of control. The fourth, and lowest, level of control is that of the individual vehicle.[1]

Note from Fig. 2 that a sector-level, control configuration would be comprised of four basic elements:

1) A sector computer;
2) A communication link for achieving both computer-to-vehicle and vehicle-to-computer transmissions;
3) An information source for directly providing the computer with state information on each vehicle;

---

[1]This hierarchy could be employed in conjunction with either a synchronous or a quasi-synchronous control strategy. With the former, slots of H_t in time units move through a network, generally at a fixed speed for each link, so that synchronization is obtained at all merge points. A vehicle, before entering the system, is assigned a sequence of synchronized slots that will, under normal operating conditions, provide an uninterrupted trip from origin to destination. The quasi-synchronous approach is less rigid in that an incoming vehicle doesn't require an a priori assigned sequence of slots prior to entering the network. Instead, it is merged into mainline traffic, possibly into the first available empty slot and then is moved in synchronization with other traffic until a conflict point (e.g., an intersection) is reached; then maneuvering may be required to effect safe and efficient operations.

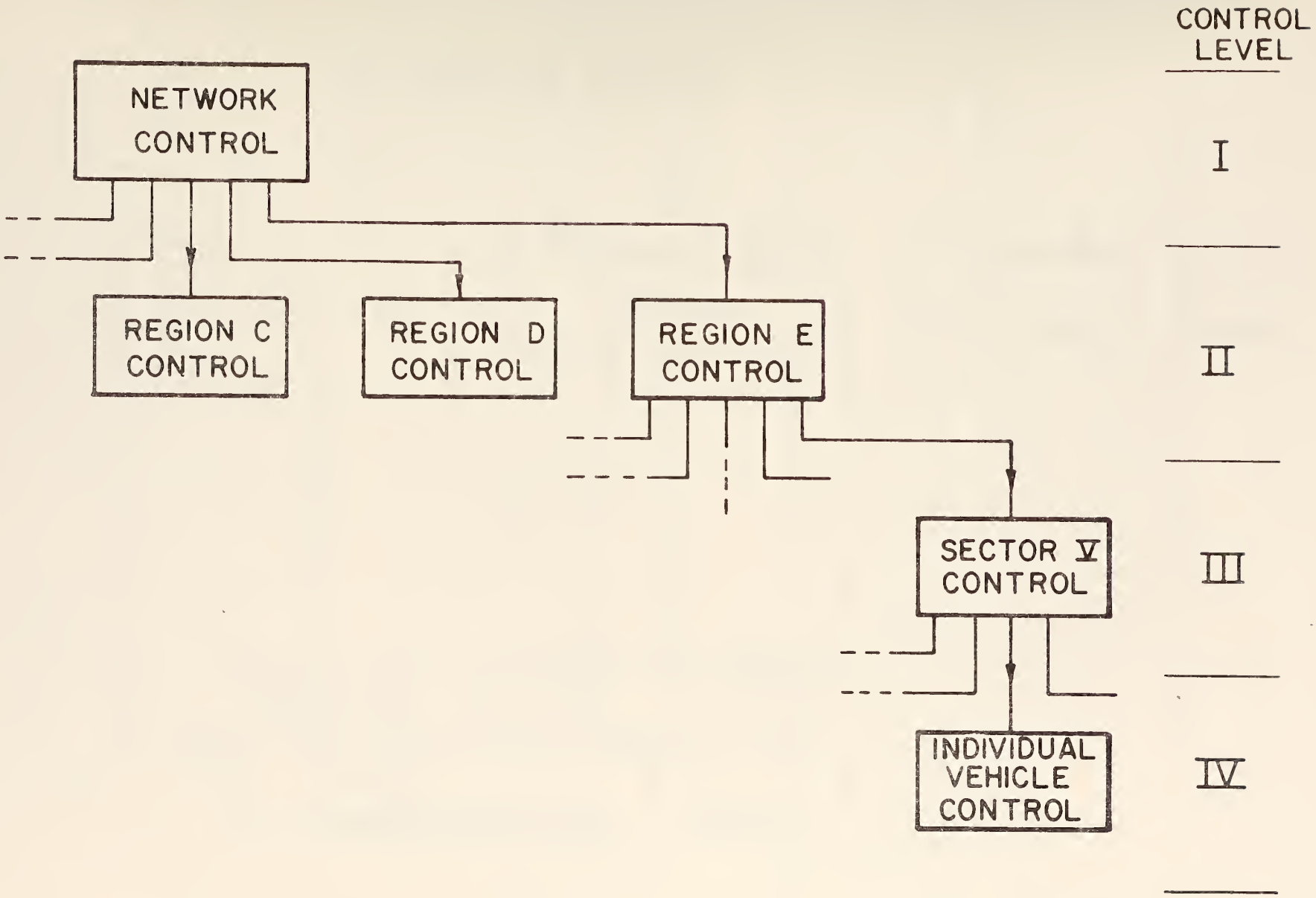

Fig. 1. A general control hierarchy.

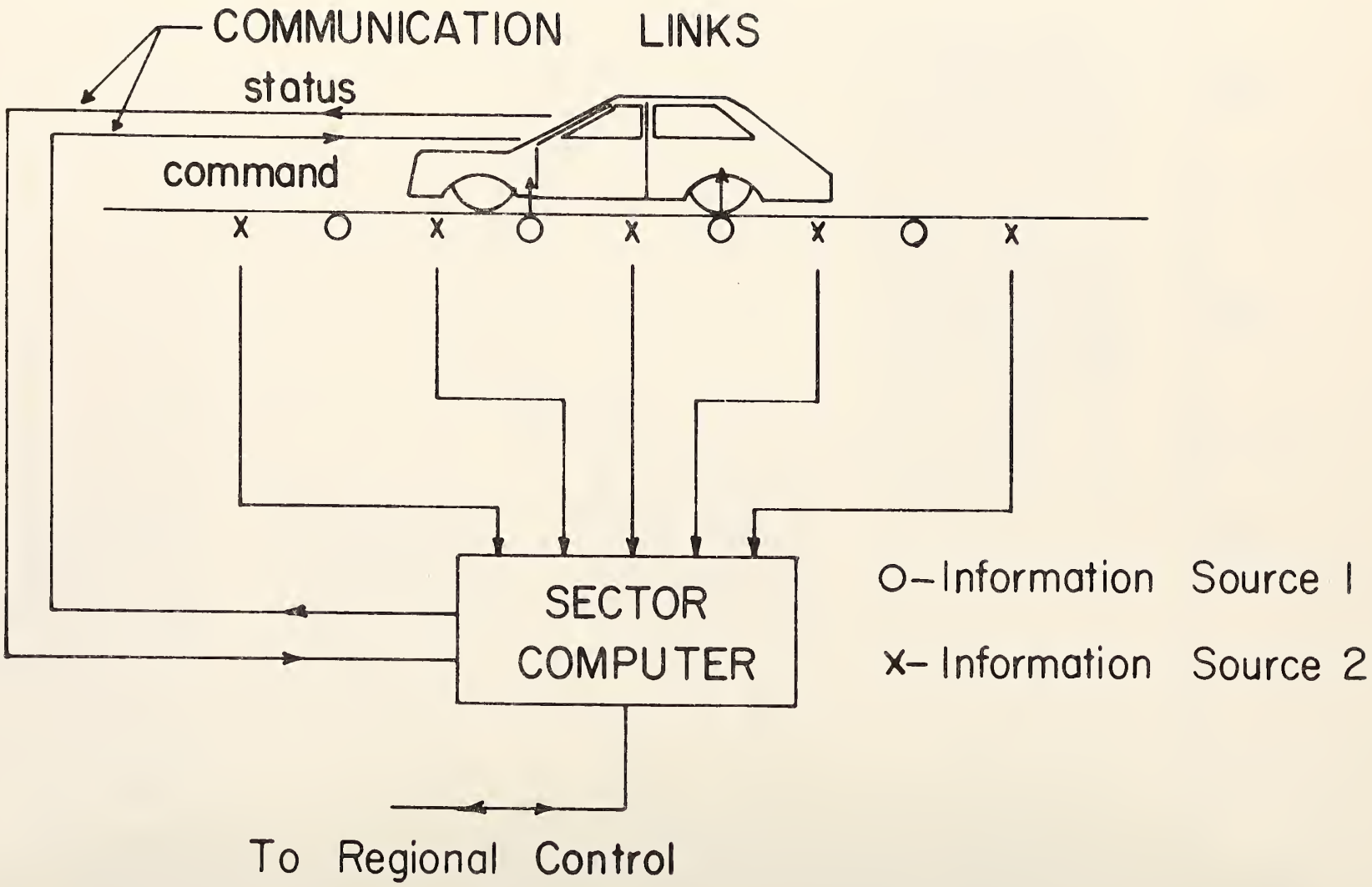

Fig. 2. A sector-level, control configuration.

4) An information source embedded in, or located nearby, the guideway and intended to supply state information to each controlled vehicle.

With this general configuration, the sector computer would have two independent indications of the state of each vehicle--one from the guideway-to-sector computer information source and one transmitted from the vehicle. This would provide desired redundancy. Further, if the information received were of sufficient accuracy and timeliness, the system could be designed for a quick response to an anomalous situation.

D. Overview

During the past year, which was the first year of a planned three-year program, The Ohio State University efforts were focused principally on the development of a physical test facility which will be employed to study control and communication problems at, and below, the sector level. This would be done in the context of high-speed (to 28.4m/s (93f/s) operations at time headways as small as 1 sec. The primary activities undertaken were:

a) The implantation of both lateral and longitudinal information sources at the 6.4-km, skid-pad facility at the Transportation Research Center of Ohio (TRCO);

b) The specification of a sector-level controller which would be comprised of a commercially available microprocessor and a considerable amount of special-purpose hardware.

c) A study of automatic longitudinal control both in the normative and emergency modes of operation;

d) The evaluation of a "flattened" helical line information source for providing continuous position information to each controlled vehicle in a sector; and

e) A study of automatic steering with an emphasis on high-speed, lane-changing operations.

The secondary activities included a re-evaluation of a headway safety policy for automated highway operations, and the development of a methodology to determine the accident cost of a particular policy choice.

A survey of the accomplishments during this year are contained in the following chapters, and certain detailed information is included in the attached appendices.

CHAPTER II

AN AUTOMATED VEHICLE TEST FACILITY

A. Introduction

During the spring of 1977, efforts were started toward developing an automated vehicle test facility which, when completed, would be employed to study control and communication problems at, and below, the sector level.[1] It was decided, after consultation with Transportation Research Center of Ohio (TRCO) officials, to instrument the TRCO skid-pad for this purpose.

The skid-pad geometrics are shown in Fig. 3. The length of the "dashed" closed-loop path is some 6.4km (21,000 ft), with this including a path around each turn-around loop and two straight sections--each of which includes a standard braking surface (as defined by a roughness number). This configuration was considered sufficient to approximate a "typical" single-lane highway sector.[2] A control center will be located next to the pad as shown, and it will house both the sector computer and the computer-to-vehicle communication system.

---

[1] Some of the efforts described here were undertaken on Contract DOT-FH-77-28.

[2] In addition to the closed-loop path, it is planned to provide additional paths for merging, diverging and lane-changing operations.

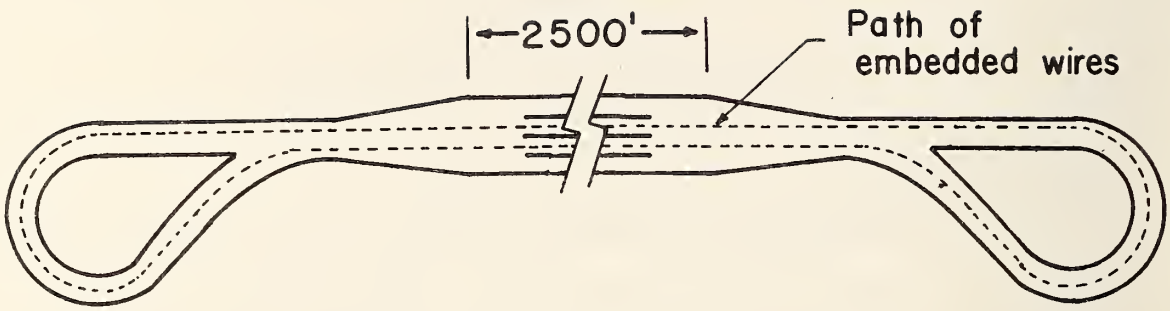

1 ft = 0.305 m

Fig. 3. Geometrics of automated-vehicle test facility.

B. Sector Computer

The tasks to be performed by the sector computer include the following:

a) The generation of acceleration, speed, position, and lateral motion commands for each vehicle within the sector. (under normative conditions, these commands would be selected at a regional (or higher) level, generated at the sector level, and transmitted to the controlled vehicles in a condensed form.)

b) The initiation of emergency operations when necessary (such a decision would be based on status information received from various sources such as a regional computer, adjacent sector computers, the controlled vehicles within a sector, and guideway-

based information sources. The actions taken would include (a) The revision of previously specified vehicle command trajectories, and (b) The communication of an "emergency alert" to other control sources).

c) The accomplishment of vehicle transfer via communications with adjacent sector computers, the vehicles, and/or the regional computer.[3]

The required functions could be performed by a general-purpose microprocessor provided appropriate special-purpose hardware (digital processors, memories, interfaces, etc.) were also employed. A commercially available unit (a DEC LSI - 11/03) was selected for implementation, and it is currently being interfaced with the necessary external units. The composite unit, when completed, should be a flexible, high-performance controller capable of handling up to 256 vehicles simultaneously.[4]

C. Sector-Level Communications

In general, little effort has been devoted to studying communications between a sector-level computer and the vehicles under its control, and the efforts here have thus far been confined to the

---

[3]When a vehicle leaves one sector and enters another, the control must be transferred from one sector computer to a second. This involves coordination of both sector computers, the vehicle and the regional computer.

[4]A detailed discussion of this controller will be contained in a forthcoming working paper (19).

specification of the communication requirements for a typical sector.

Note from Fig. 2 that the computer is the source of command information (command acceleration, command speed, and command position) and the controlled vehicle(s) is a source of status information--vehicle acceleration A(t), vehicle speed V(t), vehicle position X(t) and other data. The information content of these sources is largely dependent on the operating policy of a sector, and is thus strongly influenced by technical and economic constraints and safety considerations. For one particular policy, it was estimated that a two-way bit rate of approximately 300 bits/sec/vehicle would be required (18).

As reliable communications must be maintained at all times, a large signal-to-noise ratio (>20 db) would be necessary to decrease the probability of random errors; also, cyclic block codes should be employed to protect against spurious (burst) noise sources. In addition, strict synchronization must be maintained for two reasons:

a) To provide effective clocked communications between all transmitters and receivers; and

b) To provide the necessary time reference for the vehicles' commands.

Initially, it is planned to achieve communications via a radio-frequency link. Subsequently, it is planned to employ an induction-field approach--if the required bit rates can be achieved in a safe and efficient manner.

D. Information Sources--Longitudinal Control

There are two types of information-source configurations for longitudinal control--one to provide static information to each controlled vehicle, and a second to provide this information directly to the sector computer (see Fig. 2). The efforts undertaken, both under this contract and on previous ones, have dealt only with the former.[5] Several sources have been evaluated in terms of the following requirements:

1) The signal(s) available at the receiver onboard each vehicle should be easily processable to yield accurate measurements of $X(t)$ and $V(t)$ (e.g., to within 0.1 ft and 0.5 ft/sec, respectively);
2) This signal should have a large signal-to-noise ratio and be essentially unaffected by the environment;
3) The signal should be available in an unambigious form over the expected range of vehicle state deviations--both in the lateral and longitudinal direction; and
4) The information source must be highly reliable so that the probability of a failure is extremely low.

---

[5]Even if sufficient control information were available form this type, the second type would still be highly desirable for purposes of redundancy, and hence reliability.

The general approach taken toward obtaining a continuous measurement of X is depicted in Fig. 4. Here, widely spaced position markers, hereafter referred to as absolute position markers, would be employed to provide a positive indication of a vehicle's absolute position when that vehicle passed over a given marker. This would be achieved by employing the detected signal to zero a vehicle-borne counter. Intermediate position markers would be located between the absolute markers, and the vehicle counter would be advanced as it passed each such marker.

The probability of an error buildup could be greatly reduced if a unique signal were available at every nth marker as shown. Between markers, position interpolation would be employed.

A number of devices, including permanent and ac-excited magnets and laterally positioned, current-carrying wires could be employed as guideway-mounted position markers. A desirable choice for an absolute marker is a magnet because of its high reliability, good reported position resolution (within 1 in), insensitivity to environmental factors, and low-noise properties. Permanent magnets would have the additional advantage of being passive and requiring no maintenance. Another desirable choice is a very narrow, current-excited loop. The position of one side of this loop can be detected to within ±0.15 cm at high speeds (17) and, if desired, the loops could be excited so that a vehicle's passage over a specific loop could be uniquely identified.

It was decided to employ very narrow (1-ft wide in the longitudinal direction), current-excited loops, spaced at 152.4m (500 ft) intervals for the absolute markers (see Fig. 5). Two such loops, spaced 0.61m

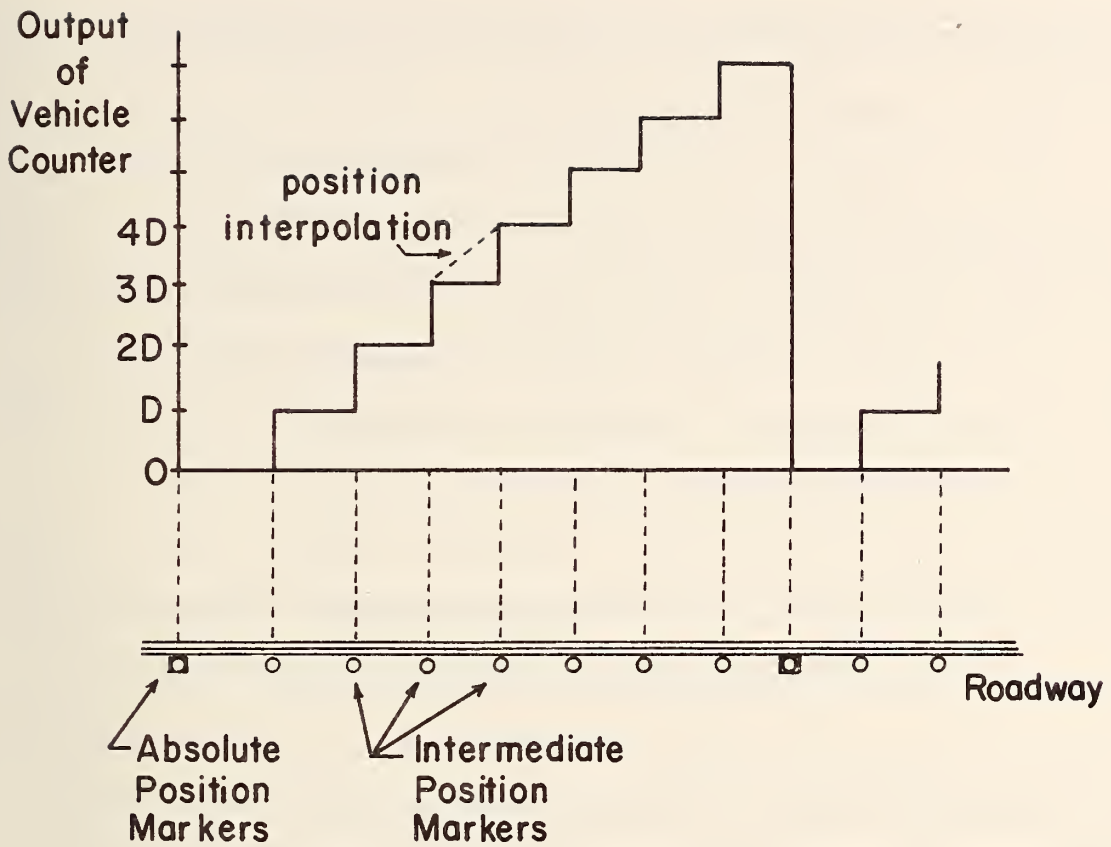

Fig. 4. A discrete-element, information source with position interpolation.

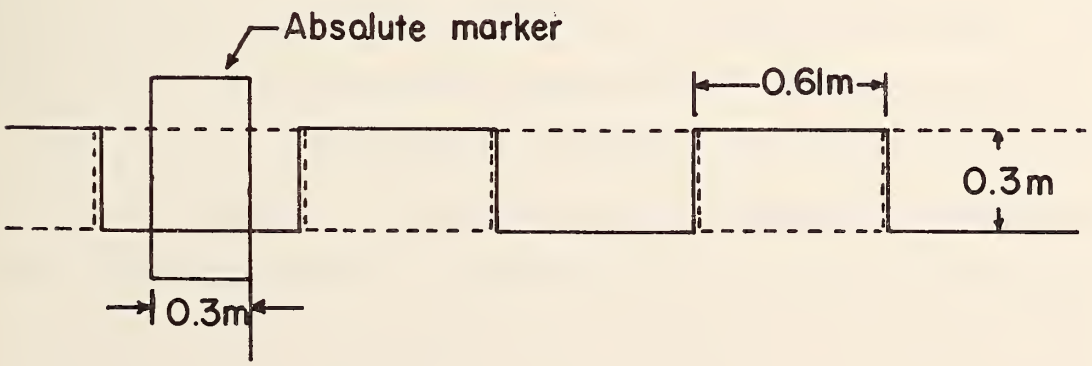

Fig. 5. Spatial square waves of wire installed under the roadway surface.

(2 ft) apart, are employed to mark the beginning (and end) of the 6.4-km "sector."

After evaluating a number of approaches for the realization of intermediate position markers (18), the approach depicted in Fig. 5 was selected.[6] Here, a pair of wires, in a spatial, square-wave configuration, are employed to provide a position signal every 0.61m (2 ft). Here the phase reversal of the vertical component of the magnetic field, which occurs at each crossover (every .61m in Fig. 5), is sensed by appropriate vehicle-mounted coils. These phase reversals tend to remain directly above the wires, even when steel-reinforced, roadway materials are present, and wire position can be measured to an accuracy within 0.15cm at speeds up to 31m/s. This configuration has been installed over the complete extent of the path shown in Fig. 3. The frequency (50kHz) of the current flowing in these lines is different from that employed in the loops spaced every 500 ft; thus, a unique signal is available from the latter.[7]

Position interpolation between the 0.61m marks can be accomplished in various ways with virtually any of these being satisfactory insofar as normative control is concerned. One approach is to use a wheel tachometer, filter the noise, and appropriately integrate to obtain the required interpolation. This works well in situations where V is not

---

[6]The evaluation of another approach, a helical, transmission-line configuration, is presented in Chapter IV.

[7]A detailed specification of the positioning of these lines at the TRCO skid pad is given in Appendix A.

rapidly changing, as one can employ dynamic calibration procedures to obtain a good estimate. Such effects as slipping wheels would not be especially critical here.

However, the effects of wheel slippage are exceedingly important in one essential mode of vehicle control--emergency operation. There are two primary reasons for this importance:

a) The need for an accurate V signal in the control of a rapidly decelerating vehicle; and

b) The need for such a signal in the detection of an emergency situation.

Thus, one concern was obtaining as accurate a measurement as possible. Given such a measurement, it can be used for position interpolation under normal conditions and in emergency detection and subsequent control.

Several approaches toward obtaining an accurate velocity measurement were previously evaluated, and two of these appeared quite promising (17). The first involved a Doppler radar speedometer used in conjunction with small metallic reflectors beneath the roadway surface. The latter resulted in an extremely strong returned signal which could be processed to yield V to within ± 0.5 ft/sec under both normal and high-deceleration situations (18). In addition, the returned signal was virtually unaffected by vehicle pitch and roll; i.e., a JANUS configuration was not required. A major drawback of this approach was the difficulty of installing the reflectors in the roadbed.

A second approach, which is the one to be employed, would involve a conditional-feedback scheme wherein an accelerometer, tachometer, and crossed-wire detector would be employed to yield continuous estimates of A, V, and X. The signals would be processed in a manner which would reduce (or eliminate) the effects of various measurement errors (accelerometer bias, wheel-slip, variations in the crossed-wire spacing, etc.).

E. Information Sources--Lateral Control

In a previous study (14), a detailed approach was made of various approaches toward achieving "electronic" steering. This included the evaluation of magnetic fields set up by various configurations of current-carrying conductors, the magnetic-distortion effects caused by nearby steel structures, and data-processing techniques to overcome the effects of such distortion and provide an accurate indication of a vehicle's lateral state.

This effort culminated in the selection of a one-wire configuration--primarily since the magnetic-field distortion was relatively small in this case. This configuration was installed over the closed-loop path of Fig. 3, and it is located in the "center" of the spatial, square-wave configuration as shown in Fig. 6.

At present, an evaluation of two or more lines, each excited at a different frequency, and intended for use at lane changing and/or diverge points, is being conducted under both laboratory and full-scale conditions as is described in a forthcoming paper (20).

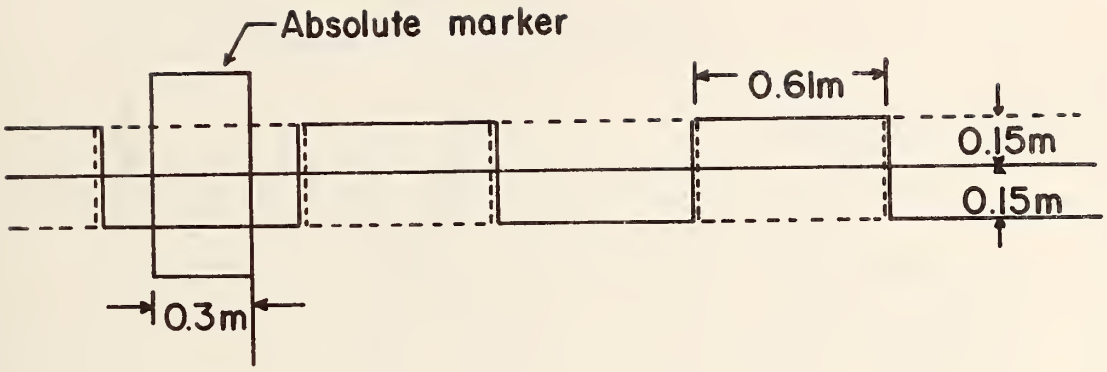

Fig. 6. Orientation of steering wire relation to spatial, square-wave configuration.

F. Current Status

The facility described here is partly finished as the information sources for both lateral and longitudinal control have been installed, checked out, and employed for both the lateral and longitudinal control of individual vehicles. However, the lines are not yet loaded and/or terminated in an optimal manner.

It will be at least 12 months before the sector computer and the communication link are installed, and the complete facility will not be operational until the Fall of 1979.

CHAPTER III

ON VEHICLE LONGITUDINAL CONTROL

A. Introduction

In this investigation, a vehicle longitudinal control system was designed and constructed for small-time-headway, point-follower operation.[1] A simple block diagram of this system is illustrated in Fig. 7. Here, a vehicle-borne command generator is employed to produce X_c, V_c and A_c, which are the vehicle's command position, velocity and acceleration, respectively. The outputs of onboard sensors (i.e., a wire-detector, a tachometer and an accelerometer) are collectively processed by a state estimator to provide suitable feedback signals for the controller circuit. These feedback signals are $\hat{X}$, $\hat{V}$ and $\hat{A}$, which are estimates of the vehicle's position, velocity and acceleration, respectively. Each feedback signal is subtracted from the corresponding command signal, and the resulting state error signals ($X_c - \hat{X}$, $V_c - \hat{V}$, $A_c - \hat{A}$) and $\hat{V}$ are processed by a nonlinear controller to obtain V_i, which is the voltage input to an electrohydraulic actuator controlling the throttle-valve position. Other velocity and acceleration estimates $\hat{\hat{V}}$ and $\hat{\hat{A}}$, which are low-passed versions of V_c and A_c, respectively, are also utilized in the controller circuit. Each element of this block diagram will be subsequently discussed in detail.

---

[1]This study was restricted to the vehicle propulsion system. Braking studies are currently being conducted by R. Fling.

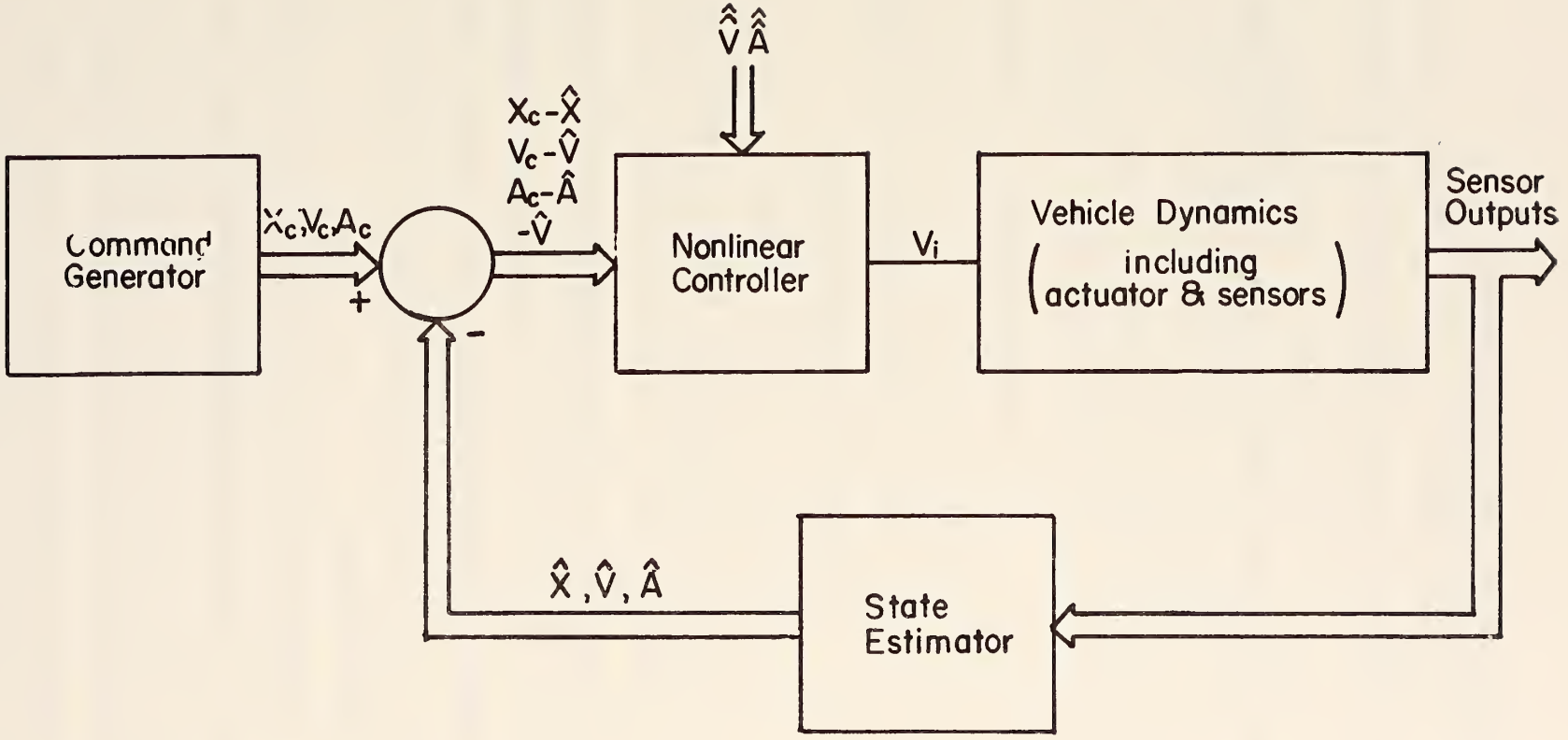

Fig. 7. A block diagram of the vehicle longitudinal control system.

B. Vehicle Propulsion System Dynamics

In previous studies (21 - 23) a model of the propulsion system dynamics of a 1969 Plymouth sedan was developed and subsequently used, with good success, in the design of a longitudinal controller for that vehicle. In this study, a different test vehicle, a 1965 Plymouth sedan, was employed. Because these vehicles were not physically identical, much of the modeling process had to be repeated for the latter. However, some obvious similarities (e.g., the tire-road interface, the vehicle mass and the frictional characteristics) did exist; thus some of the modeling results, which had been obtained for the 1969 Plymouth, were used in the model for the 1965 Plymouth.

Consider the model of vehicle propulsion system dynamics shown in Fig. 8. This relatively complex, acceleration- and velocity-dependent model is a realistic simplification of a more complex model which explicitly accounts for such phenomena as a transport delay in the fuel-air intake system, lags associated with the engine-drivetrain combination, the nonlinear effects of slipping tires, and the variety of forces which act, linearly and nonlinearly, on a moving vehicle.

The model input is V_i, the throttle-actuator input, and the output is V which is the vehicle's velocity with respect to the roadway. The intermediate quantity V_w is the driven-wheel velocity as measured via a tachometer mounted on the drive shaft. One acceleration- and velocity-dependent function $k_p(A,V)$ and three velocity-dependent functions $t_p(V)$, $k_f(V)$ and $\xi(V)$ are included.

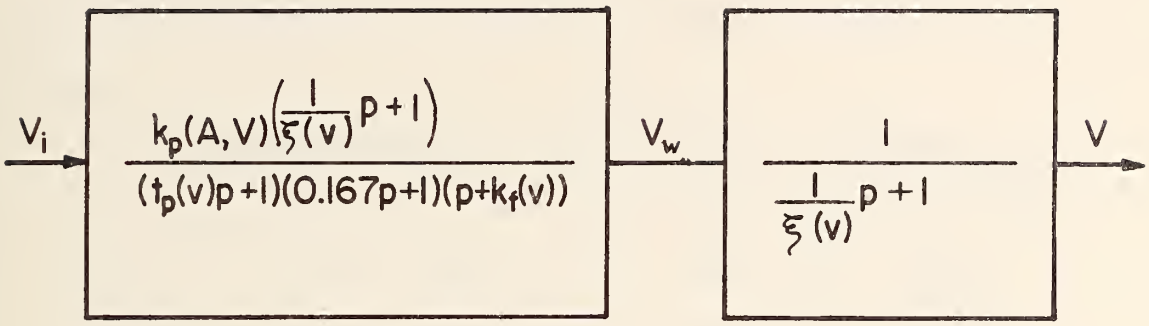

Fig. 8. A nonlinear model of a vehicle propulsion system dynamics.

The first two are associated with the nonlinear properties of the engine-drivetrain combination; the third with the vehicle's mass and frictional characteristics, and the fourth with the tire-roadway interface. Average values of the latter, which were specified in a previous study (16), are shown in Fig. 9. In another study (22), estimates of $k_f(V)$ ranging from 0.0 to 0.2 were obtained, and later, in (23). it was shown that the closed-loop responses of practical Type 1 and Type 2 systems were insensitive to variations of k_f in [0.0, 0.2]. Thus, in this study, k_f was conveniently fixed at 0.0.

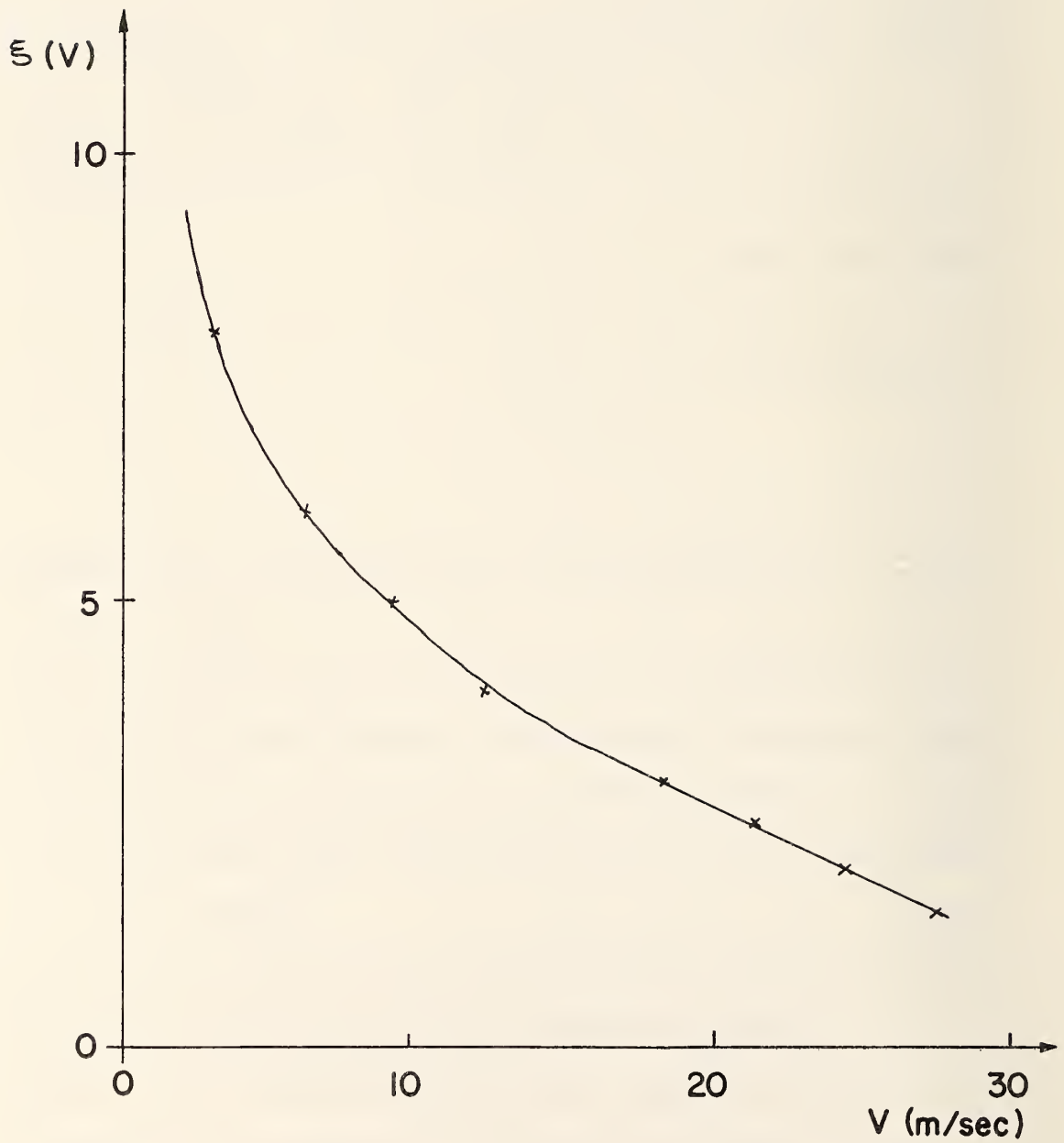

Fig. 9. $\xi(V)$ versus V.

Some data pertaining to $k_p(A,V)$ and $t_p(V)$ were obtained via a model-matching approach, in which the following procedure was employed:

> The command input, $V_c = 0.61\ t$ (m/sec), was applied to the controller/vehicle system shown in Fig. 10, while the vehicle was initially traveling at a fixed speed, and the signal e(t), which is defined in this figure, was recorded. This procedure was repeated several times at that speed to verify that a true response indication was obtained. This was done for eleven initial speeds: 0, 1.52, 3.05, 6.10, 9.14, 12.2, 15.2, 18.3, 21.3, 24.4, and 27.4 m/sec.
>
> The full-scale tests were subsequently replicated using an analog computer. The system model was excited with the same command, and the response e(t) was matched with that obtained in the corresponding full-scale test by appropriately adjusting t_p and k_p. Thus, these quantities were assigned values for each selected speed.

Typical full-scale and model responses are compared in Fig. 11. Three comparisons are shown, corresponding to initial speeds of 6.10, 12.2 and 24.4 m/sec. Note that good correlation exists in these cases. However, at speeds below 6.1 m/sec, the full-scale responses were noisy and highly erratic, and good response matches were not obtained; thus, the results for this speed range were not reliable.

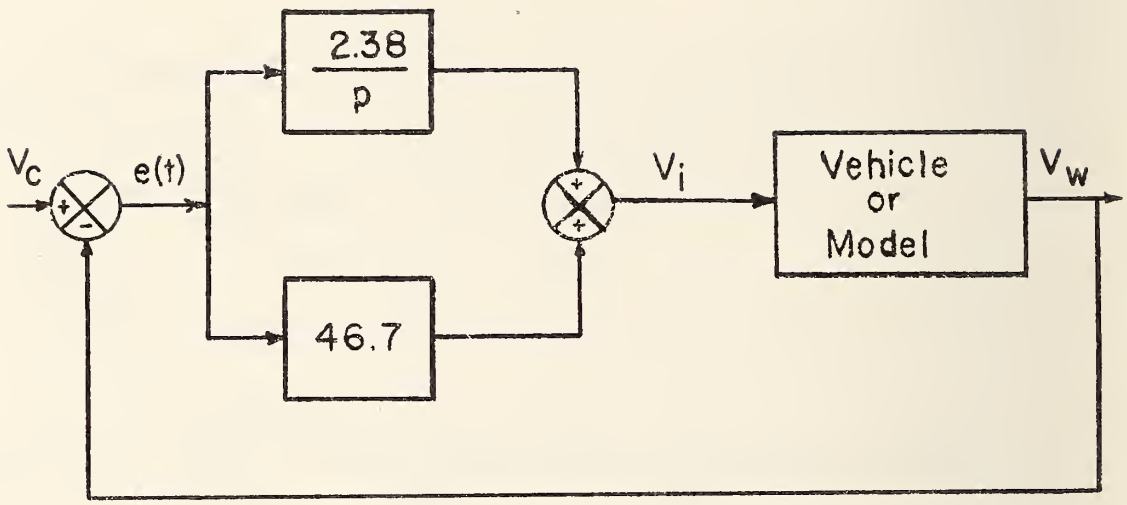

Fig. 10. Velocity controller used for modeling.

The composite results $t_p(V)$ vs. V and $k_p(A,V)$ vs. V for A = 0.61 m/sec^2 are specified in Figs. 12 and 13, respectively. Note that both quantities change substantially with V (as does $\xi(V)$, which was shown in Fig. 9). These results are generally consistent with those previously specified for a 1969 Plymouth, and indicate the need for accounting for nonlinearities when dealing with rubber-tired vehicles driven by internal combustion engines.

Documented data pertaining to $k_p(A,V)$ for other values of A were not obtained. However, an estimate of this function, based on past controller studies, is presented in the next section. In Section G, a method for obtaining a more accurate model will be suggested.

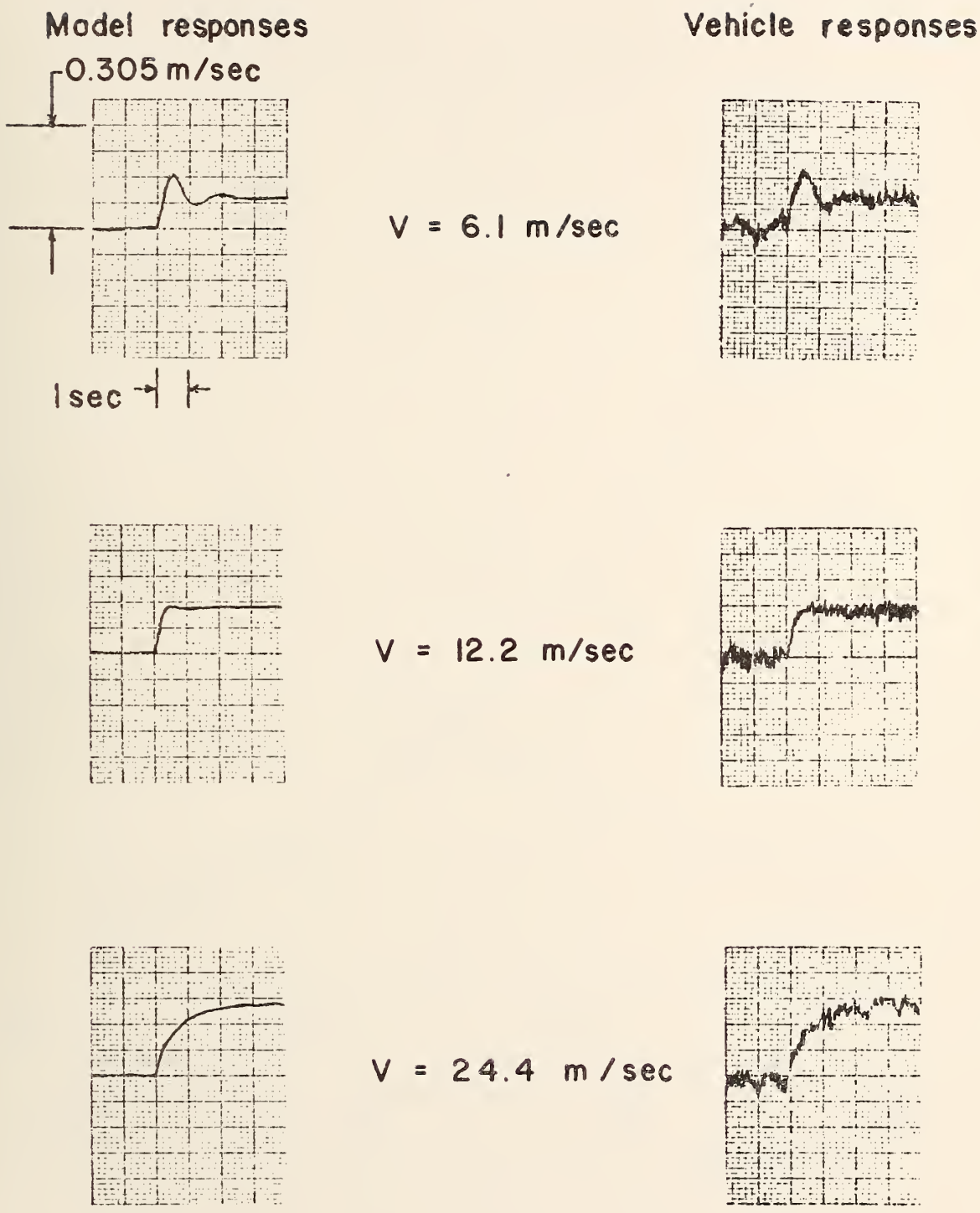

Fig. 11. Comparison of model and vehicle responses.

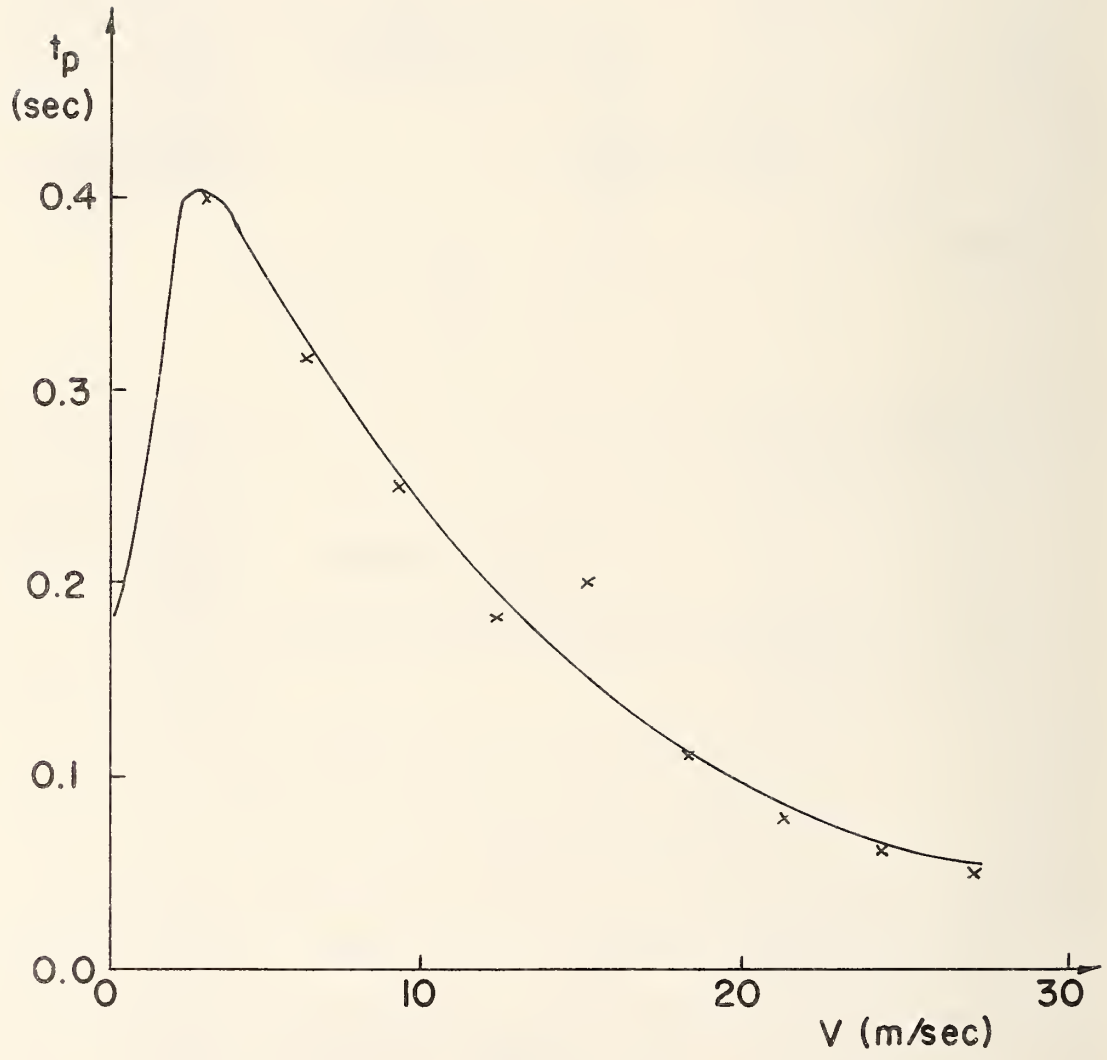

Fig. 12. $t_p(V)$ vs. V.

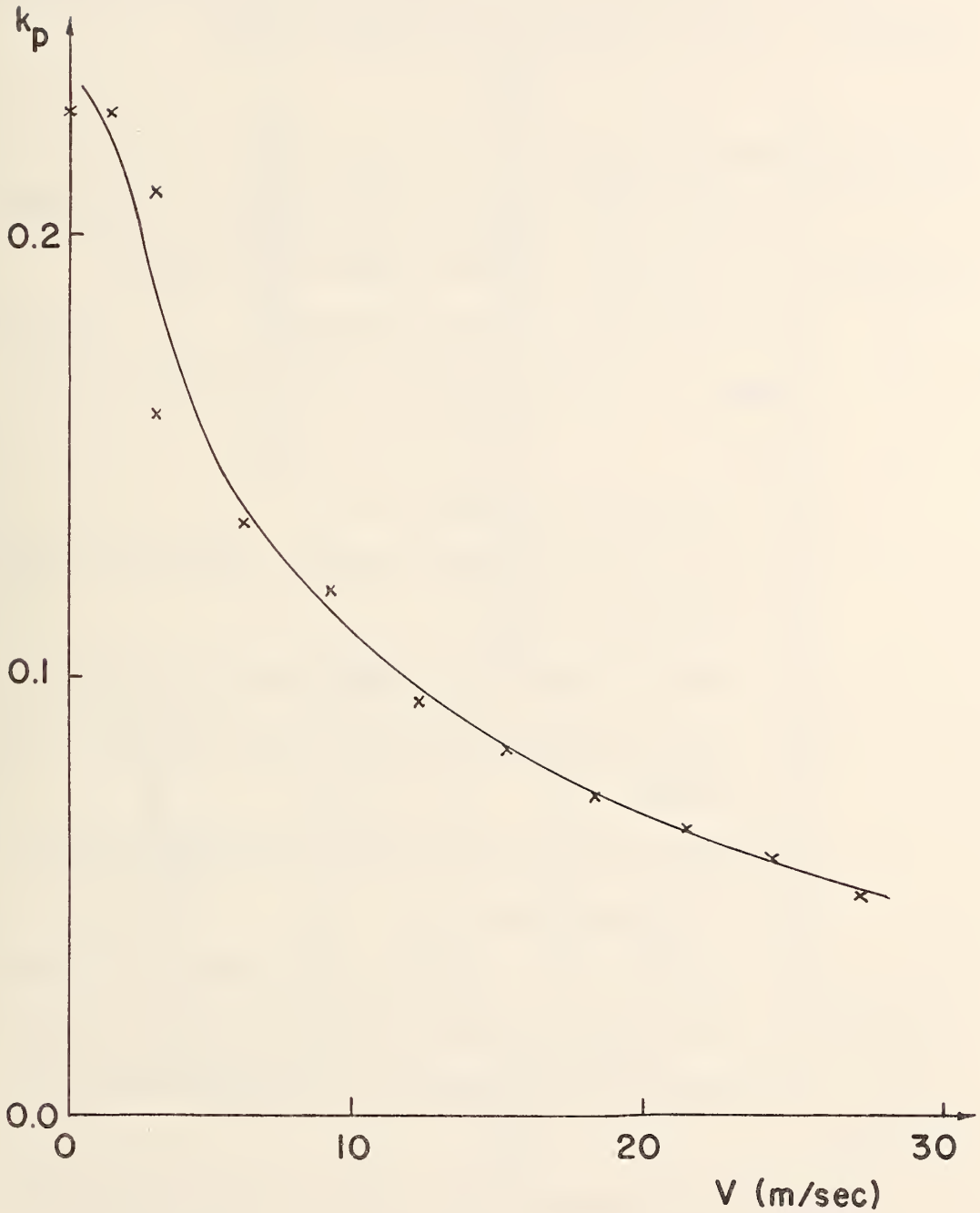

Fig. 13. $k_p(A,V)$ vs. V for A = 0.61 m/sec^2.

The model specified here was used in the design of a position controller, which is described in the next section.

C. A Nonlinear Controller

A longitudinal control system for an individual vehicle must be designed to satisfy the following general requirements:

1. The system must be physically realizable, i.e., any required response must be written within the capabilities of the vehicle.
2. The ride must be comfortable.
3. The tracking errors should be small -- especially during mainstream operation.
4. The effects of disturbance inputs should be minimized.
5. The required ramp length for entry merging maneuvers should be minimized.
6. The system should respond quickly and accurately to an emergency command input.

The general class of position controllers was chosen to meet these requirements because good control of a vehicle's position would result in correspondingly good control of its acceleration and velocity.

The specific controller shown in Fig. 14 was selected for reasons of simplicity, the availability of the required feedback and command signals, and its general ease of implementation. The inputs X_c, V_c and A_c are available from a command generator (see Section D), and X, V and A are available as estimates:

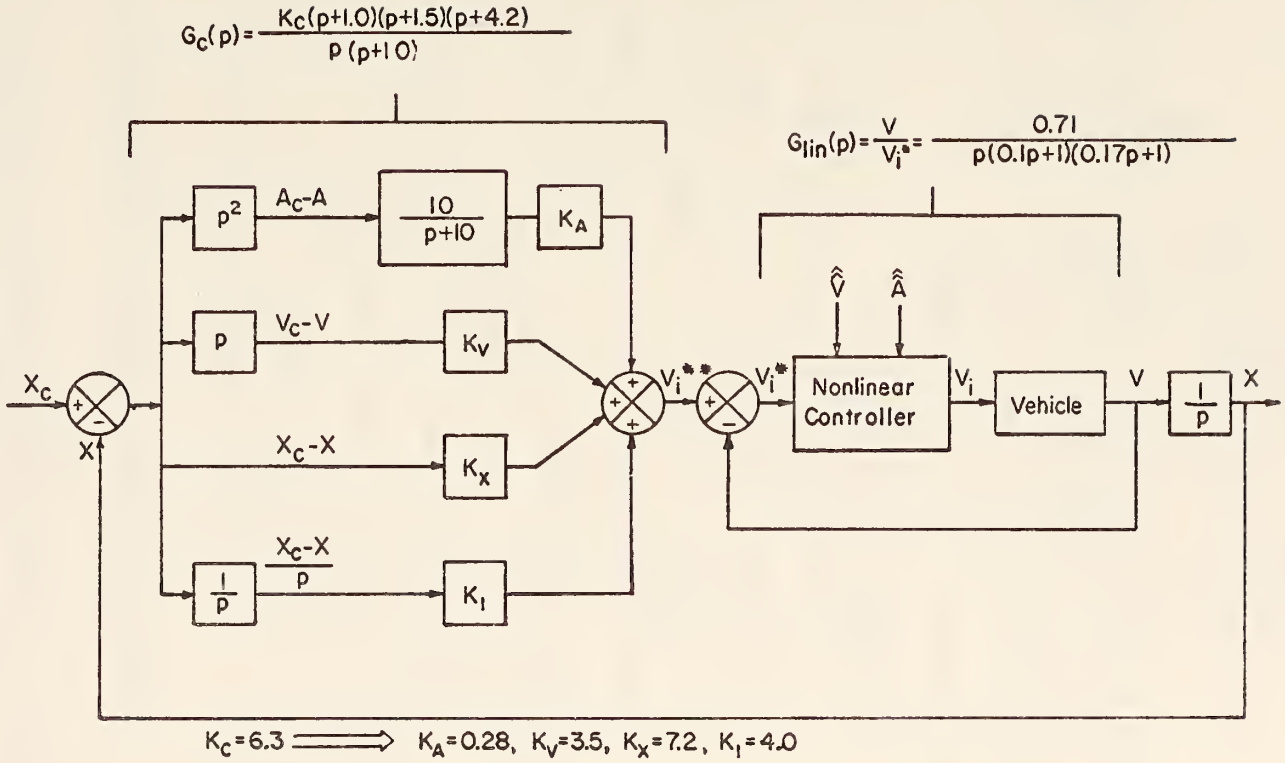

Fig. 14. A vehicle longitudinal control system.

$\hat{X}$, $\hat{V}$ and $\hat{A}$, respectively. If the state estimator discussed in Section E were used, $\hat{X}$ and $\hat{V}$ would be unbiased and relatively noisefree, and

$$\hat{X} \doteq X \quad \text{and} \quad \hat{V} \doteq V.$$

As $\hat{A}$ would contain a substantial amount of high-frequency noise (e.g., that due to vehicle vibration), the function $(\frac{10}{p+10})$ was selected to filter $A_c - \hat{A}$. Then, one could assume $\hat{A} \doteq A$ with no appreciable effect on controller design.

The nonlinear compensator shown in Fig. 15 was selected to nullify the acceleration- and velocity-dependencies of k_p and t_p which were specified in the previous section. Here, $\hat{V}$ and $\hat{A}$ are derived from V_c and A_c, respectively, through low-pass filters $(\frac{10}{p+10})$, which are employed to insure smooth gain changes. The piecewise linear approximations for $\frac{1}{k_p}$ and t_p in Figs. 16 and 17 were employed. Here, $t_p(V)$ and $\frac{1}{k(A,V)}\Big|_{A = 0.61 \text{ m/sec}^2}$ were primarily based on the experimental data of the previous section. However, no documented data were available for $\frac{1}{k(A,V)}\Big|_{A = 0.0 \text{ m/sec}^2}$; this function was estimated on the basis of past controller studies [19]. The resulting linearized propulsion model was

$$G_{lin}(p) = \frac{V}{V_i^*} = \frac{0.71}{p(0.1\,p + 1)(0.17\,p + 1)}$$

Internal velocity feedback was used to speed up the response of this linearized model, and to reduce the effects of model inaccuracies at low frequencies. The resulting transfer function was

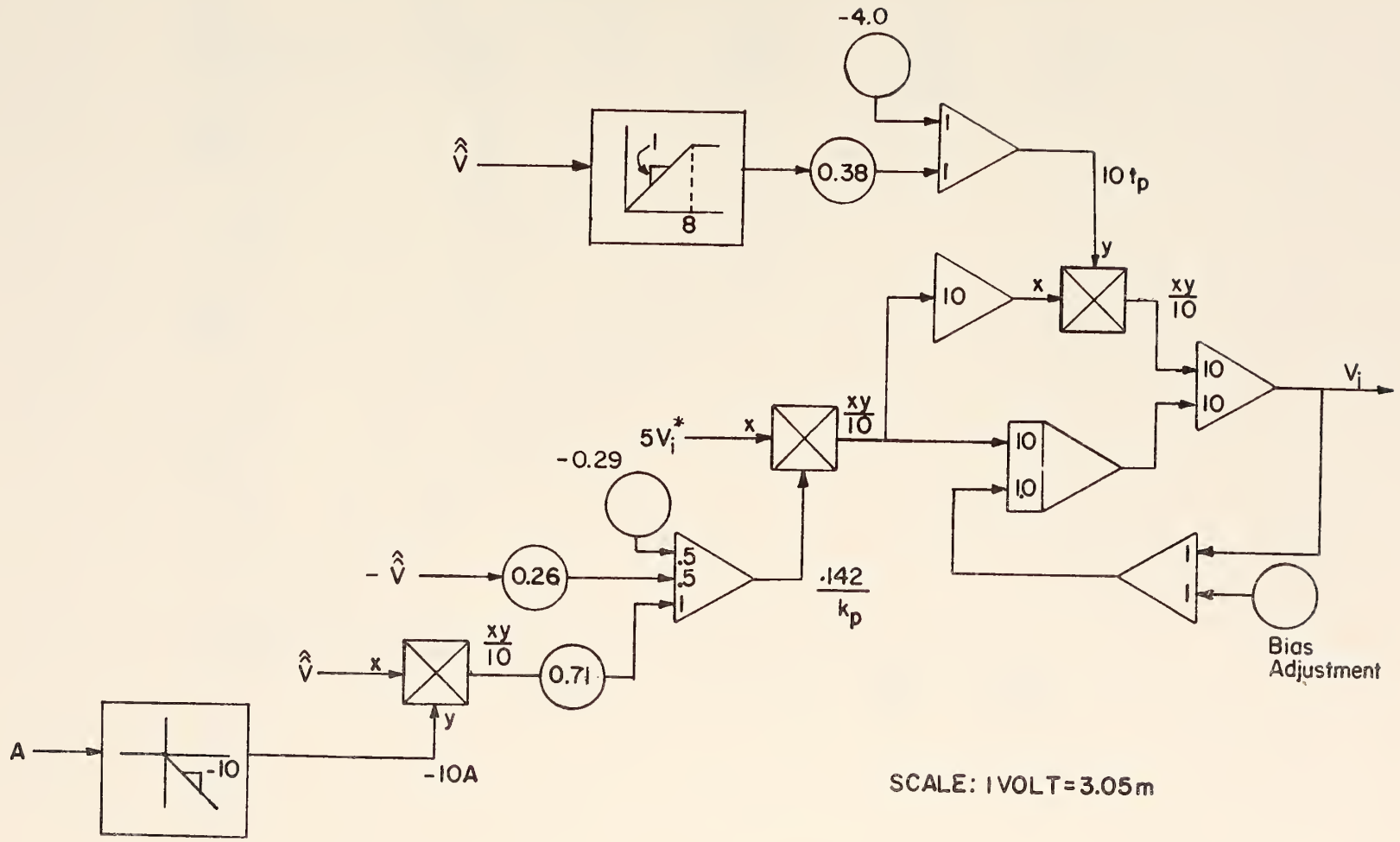

Fig. 15. A nonlinear compensator.

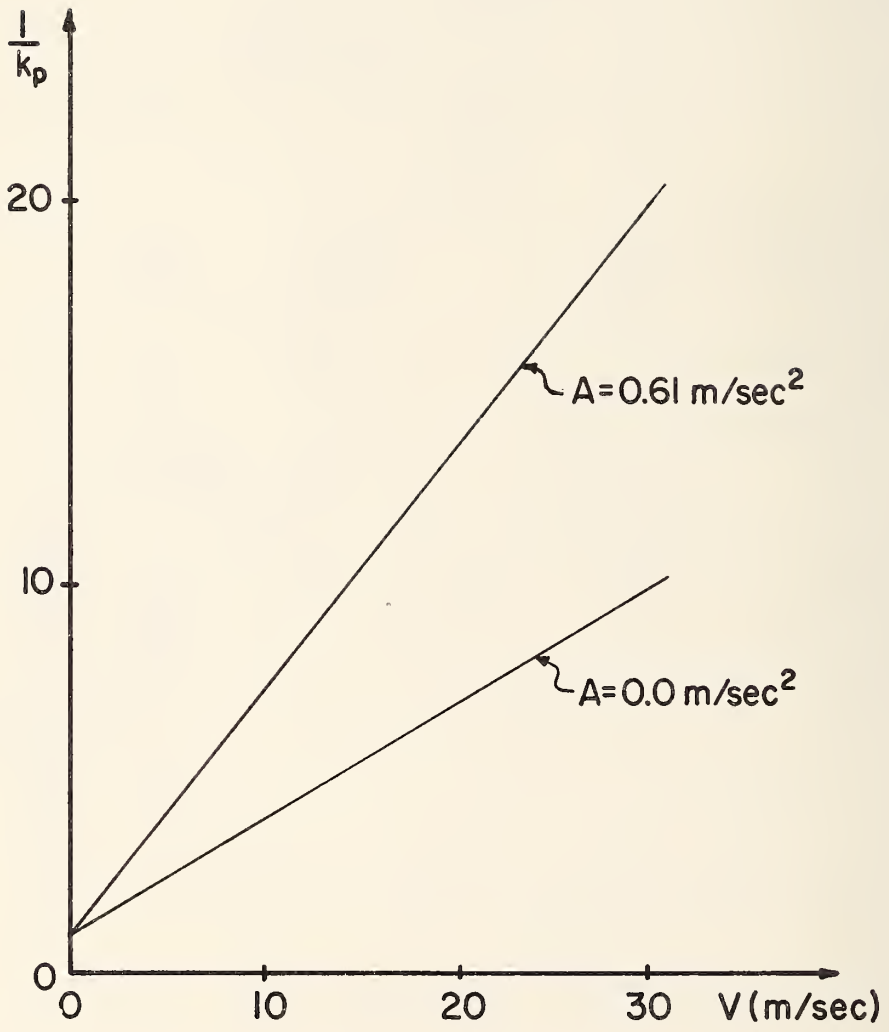

Fig. 16. A linear approximation of $\frac{1}{k_p}$.

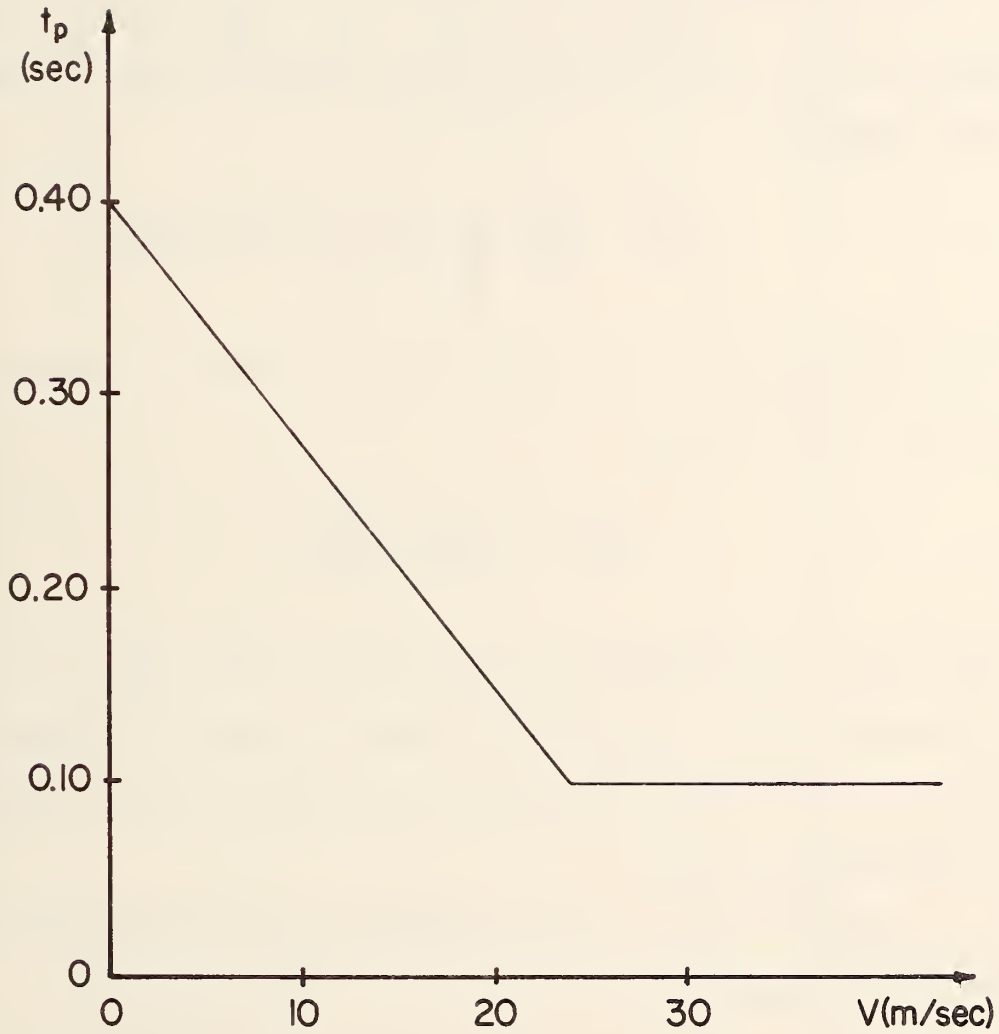

Fig. 17. A piecewise linear approximation of t_p.

$$\frac{X}{V_i^{**}} = \frac{1}{p} \frac{G_{lin}(p)}{1 + G_{lin}(p)} = \frac{41.8}{p(p + 10.79)(p + 4.14)(p + 0.94}$$

where V_i^{**} is defined by Fig. 14.

The composite linear compensator $G_c(p)$ was selected to insure small position errors to both ramp- and parabolic-position commands. This selection,

$$G_c(p) = \frac{K_c\ (p + 1.0)(p + 1.5)(p + 4.2)}{p\ (p + 10)}$$

resulted in the root loci shown in Fig. 18, where the open-loop transfer function was

$$G_o(p) \cong \frac{K\ (p + 1.5)}{p^2\ (p + 10)^2}$$

Note that K = 270 would result in adequate damping and a fast-responding system. Since this is a Type 2 system, the steady-state position error to a ramp-position (constant-speed) command is theoretically zero.

The response $(X_c - X)$ of a simulation model to the move-up maneuvering command

$$X_c(t) = X_c(0) + V_c(0)t + 0.305t^2 \text{ (m)} \quad (0 < t < 10\text{s}).$$

which was applied to vehicle initially moving at a constant speed, is shown in Fig. 19. The response peak is 0.19 m, and $X_c - X$ quickly approached zero after the maneuver was completed. Note that this response should be speed independent.

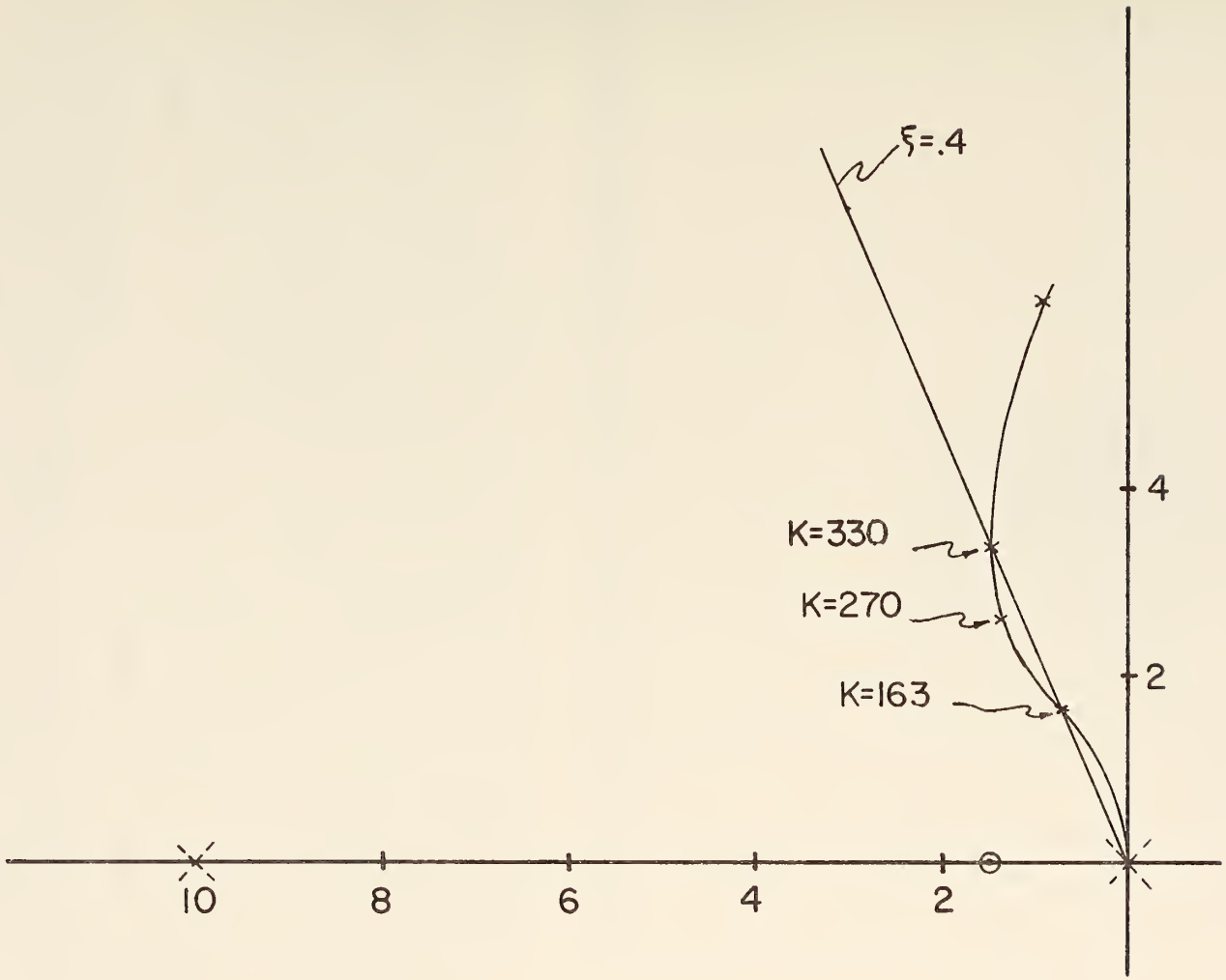

Fig. 18. The root-locus plot corresponding to $G_o(p) = \frac{K(p + 1.5)}{p^2 (p + 10)^2}$

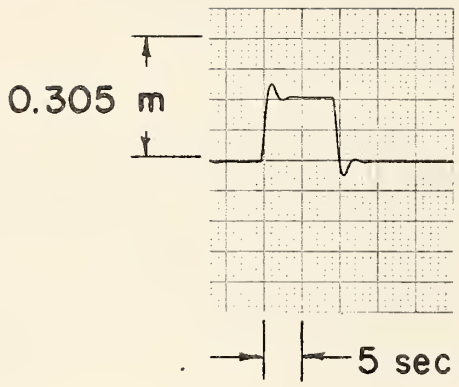

Fig. 19. Simulation response (X_c - X) to a maneuvering command.

The response to a disturbance input, equivalent to a sudden 13.4 m/sec headwind, is shown in Fig. 20. The response deviation reached a maximum of 0.076 m, and thereafter rapidly decreased to zero. Thus, this design is relatively insensitive to such inputs.

The circuit shown in Fig. 21 is one possible realization of the controller design presented in this section. Here, sample-and-hold devices are used because X_c, V_c and A_c would be available only at discrete times (i.e., a digital command generator is used). In a previous study [19], involving a very similar controller, no noticeable deterioration in system performance was observed if the sampling interval T_s were 0.1 sec or less. For T_s > 0.2 sec, the responses were underdamped (or unstable), and the ride was generally uncomfortable. Thus, T_s was chosen to be 0.1 sec.

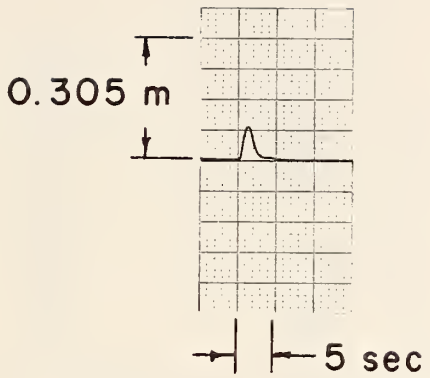

Fig. 20. Simulation response (X_c - X) to a disturbance input.

The simulation studies were followed by full-scale tests; the description and results of these tests are given in Section F. The detailed circuit diagrams of the controller circuit, corresponding to the analog representations of Figs. 15 and 21, are given in Reference (24).

D. A State Estimator

One approach to the measurement of vehicle position is shown in Fig. 22. Here, widely spaced position-reference markers (e.g., magnets or current loops), hereafter referred to as absolute position markers, would be placed at convenient points on the roadway. Numerous, equally-spaced intermediate position markers would be

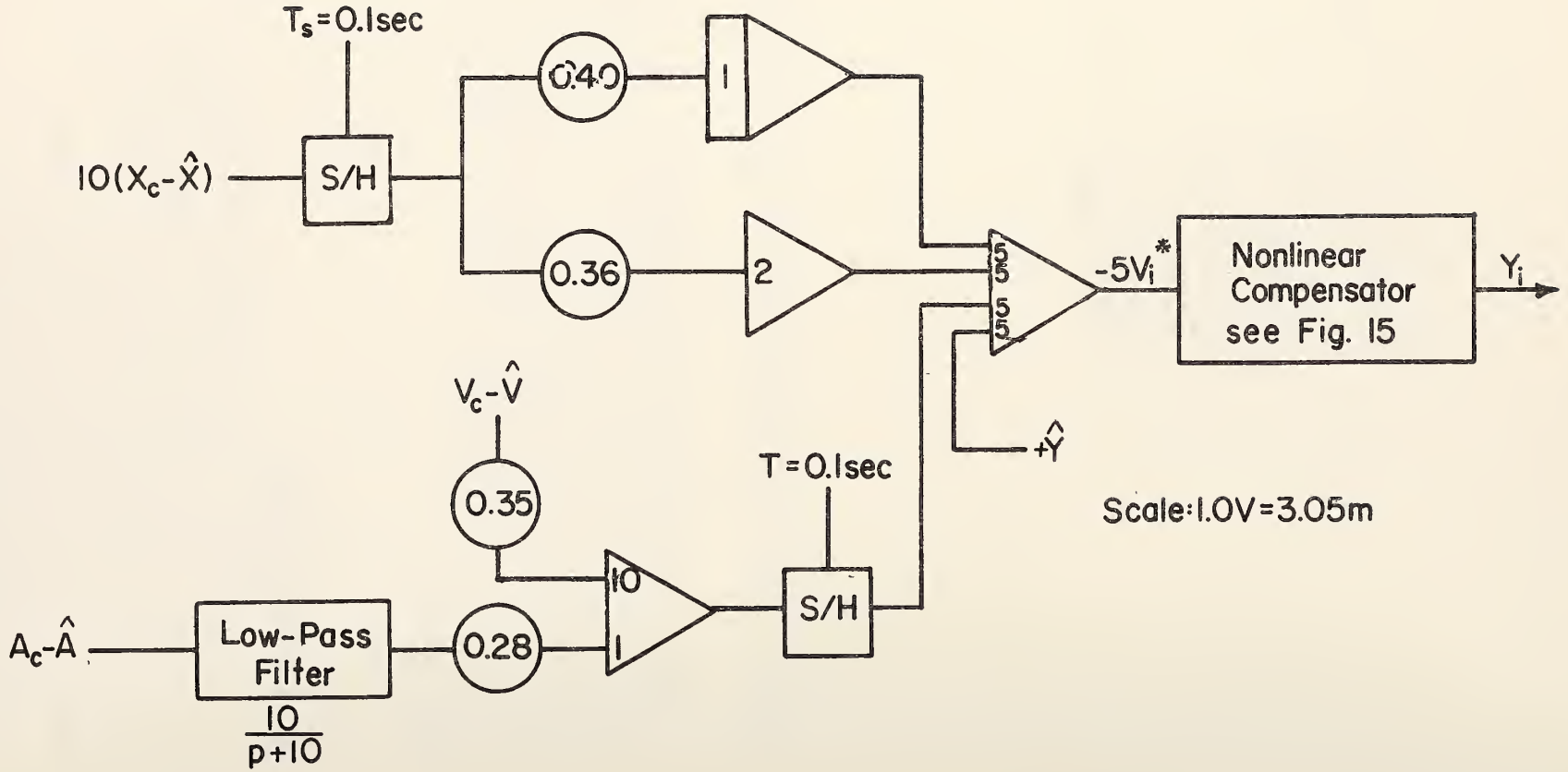

Fig. 21. The vehicle longitudinal controller.

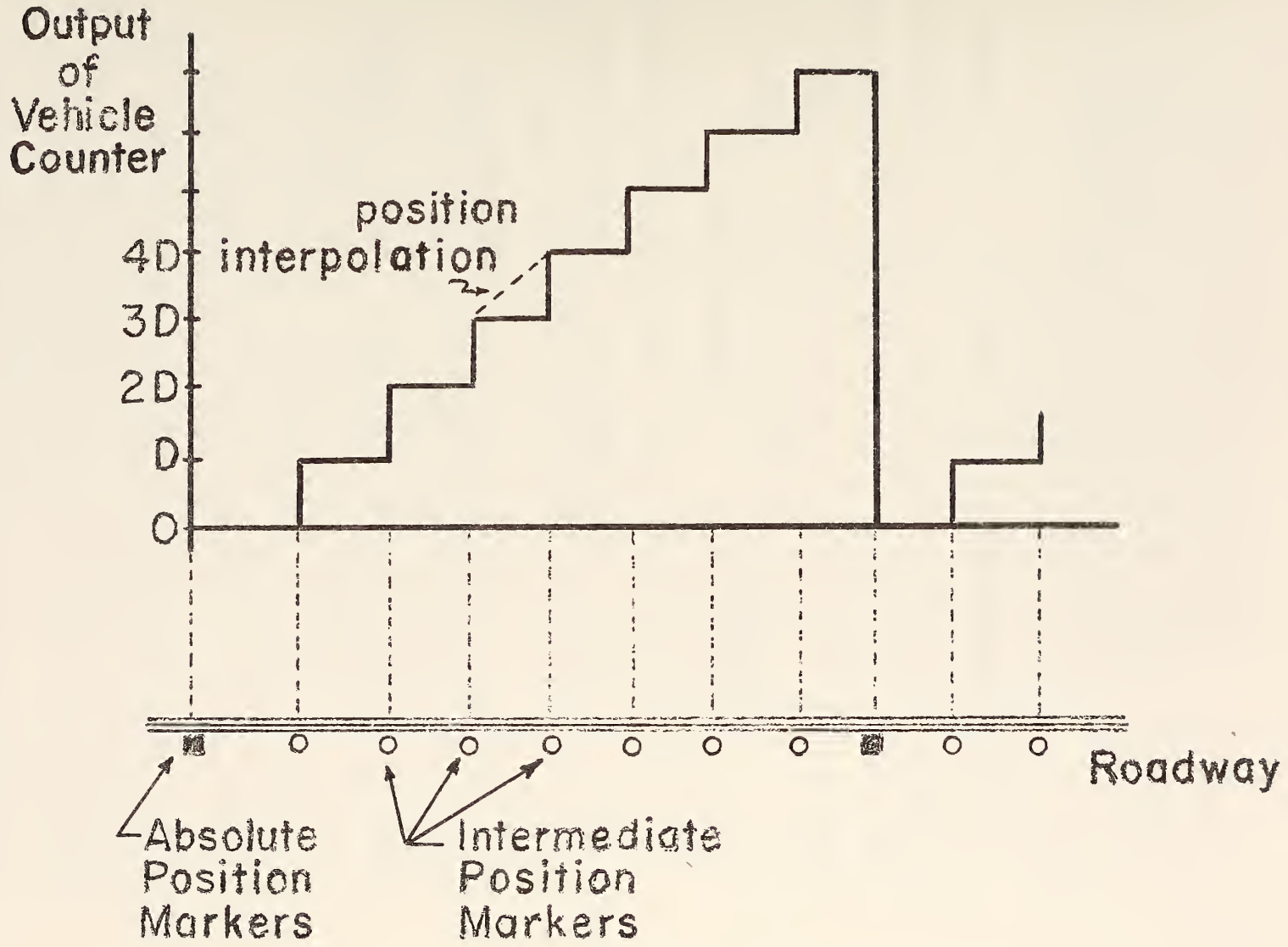

Fig. 22. A discrete-element information source with position interpolation.

located between the absolute markers. As a vehicle passed each intermediate marker, a vehicle-borne counter, containing position data, would be incremented, and when the vehicle passed over an absolute marker, this counter would be zeroed.

The crossed-wire configuration shown in Fig. 23 is employed to provide intermediate position markers.[2] Note that the magnetic flux, which results from the current flowing in this wire, reverses direction each half period (i.e., for each 0.61 m of longitudinal travel). These reversals can be used to accurately determine the position of each lateral wire (to within $\pm$ 0.16 cm) (18).

Position interpolation between intermediate position markers (see Fig. 22) could be accomplished by using unprocessed sensor outputs (e.g., a velocity signal from a tachometer); however, since such information is often contaminated with undesired errors (e.g., bias errors, calibration errors, noise, etc.), it is generally desirable to employ some effective means of processing so as to achieve improved interpolation or state estimation.

Two well-known approaches, Kalman filtering and adaptive filtering, were not considered here as these generally result in complex processors, which presently appear to be unnecessary for this application. Instead, a simpler approach, based on the concept of conditional feedback (25), wherein undesired signal errors are attenuated without affecting the desired quantities, is employed.

---

[2]This configuration was buried in 6.4 kilometers of test track at the Transportation Research Center of Ohio. Absolute markers (simple current loops) were also installed but were not used in this study.

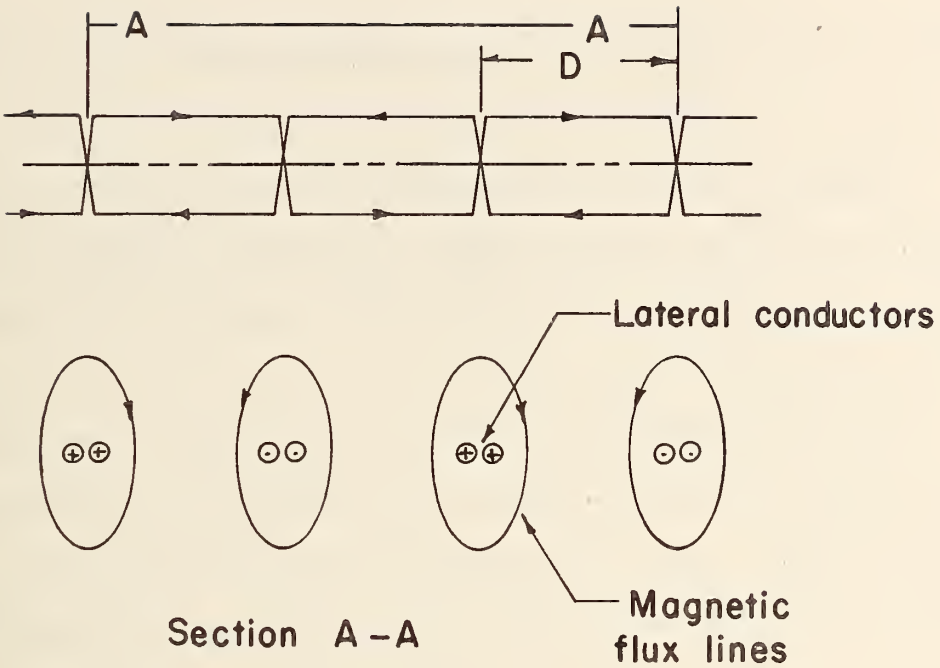

Fig. 23. A periodic crossed-wire configuration.

Using this approach, continuous estimates ($\hat{X}$, $\hat{V}$ and $\hat{A}$) of a vehicle's principal state variables are obtained by collectively processing the output signals of three vehicle-borne sensors:

1. A crossed-wire detector/counter to provide $X + e_X$.
2. A tachometer mounted on the driveshaft to provide $V + e_V$.
3. An accelerometer to provide $A + e_A$.

The e_X, e_V and e_A are errors in the measurement of position, velocity and acceleration, respectively. These six quantities have special properties, which are described below.

The desired quantities X, V and A are obviously related by the following equations:

$$A = pV = p^2X.$$

Thus, all of the sensors are used to measure longitudinal position -- in one form or another (i.e., X or one of its derivatives).

The measurement of $X + e_X$ is made at discrete instants and thus is available in sampled form. The sampling frequency is $\frac{\bar{V}}{D}$ where D is the nominal wire spacing and $\bar{V}$ is the average speed between adjacent wires.

The position measurement error e_X has a number of sources such as detector noise, motion-induced voltage, and inaccurate wire placement. Since these uncertainties do not result in long-term or accumulative errors, the mean of e_X is essentially zero.[3]

The signal e_V is composed of both slowly varying and high-frequency components, which result from tachometer miscalibration, wheel slippage, the detection process itself, and dynamic variations in tire-rolling radius. The latter appears to be the source of the most troublesome component of e_V.

The tachometer, which was used in this study, actually measures the angular speed of the drive shaft. If wheel-slip and calibration errors were assumed to be negligible, then this speed would be related to the vehicle's true speed by the following equation:

$$V = K_R \dot{\theta}_{DS} R_T$$

---

[3]The mean of e_X is actually dependent on V; however, for the speed range of interest, it is less than 0.2 cm and thus is assumed negligible.

where K_R = the rear-end gear ratio;

$\dot{\theta}_{DS}$ = the angular speed of the drive shaft;

R_T = the effective rolling radius of the rear wheels.

The tachometer circuit was designed on the assumption that R_T would be constant. However, in reality, pneumatic tires have finite deflection rates; thus, R_T varies with the instantaneous vertical force which is exerted on the rear wheels. These variations in R_T result in substantial e_V's -- especially at high speeds, where small percentages changes in R_T are observed as large, absolute velocity measurement errors.

The instantaneous vertical load on the rear wheels is proportional to an approximately linear combination of the compression of the vehicle's rear springs, and the rate of compression of its rear shock absorbers.[4] Thus, $e_V \doteq K_D pc + K_S c$, where K_D and K_S are constants, and c is the compression of the rear springs with respect to an equilibrium compression.

This analysis was followed by full-scale tests in which a velocity controller was employed to maintain the nominal speed of a test vehicle (an instrumented 1965 Plymouth sedan) at 30.5 m/sec. The low passed versions of the following signals were recorded:

1. The output of an accelerometer.
2. The velocity error signal, $V_c - V$, where V_c is the command velocity, and V was obtained from a tachometer mounted on the drive shaft.

---

[4]This would be true in the frequency range of interest (i.e., $f < 2Hz$). At higher frequencies, the inertia of the unsprung mass should be considered.

3. The output of a rate gyro mounted on the lever arm of a fifth wheel.

The latter was approximately proportional to the vertical velocity of the vehicle's sprung mass, and any random oscillations in this waveform could only have been excited by road surface undulations and irregularities.[5] Also, because the approximate time constant of the control system was 5 sec, any rapid oscillations in $V_c - V$ were not caused by the propulsion system.

Low-pass filtering was necessary as each of these signals contained a considerable amount of high-frequency noise. However, since identical low-pass filters $(\frac{10}{p + 10})$ were used on all three signals, a fair comparison can still be made.

Typical full-scale waveforms are shown in Fig. 24. Note that a strong correlation exists between these waveforms, and that the frequency of the waveforms' dominant component is roughly 11 rad/sec; this approximates the natural frequency of the vehicle's suspension system. At that frequency, the longitudinal velocity error signal lags the vertical velocity signal; this supports the previous claim that

$$e_V \doteq \left| \frac{K_D p + K_S}{p} \right| pc$$

where e_V is the dominant component of the velocity error signal and pc is the proportional to the vertical velocity measured by the gyro.

---

[5]The weight-transfer effects of the vehicle's tractive force was negligible since the throttle input was fairly constant.

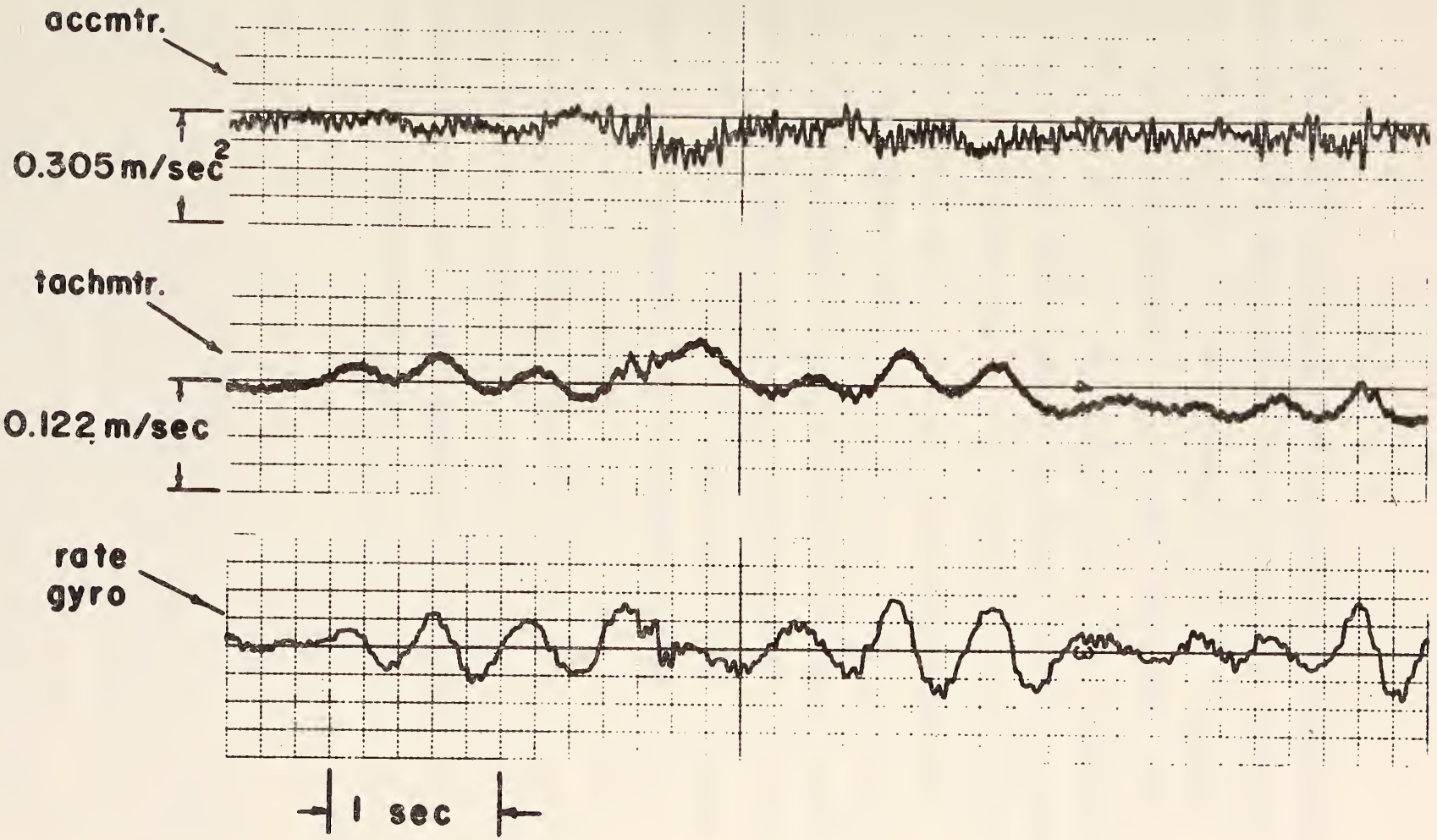

Fig. 24. A comparison of accelerometer and tachometer outputs with the vertical velocity of the sprung mass.

In short, these full-scale waveforms show that the tachometer output is measurably contaminated by the vertical motion of the sprung mass.

Because the dominant frequency components of e_V are relatively low, these could not be removed by filtering without seriously diminishing the value of the tachometer signal. The error e_V could be effectively eliminated if some means of measuring (or estimating) R_T were found, but this is left for a later study.

If the tachometer signal were used in the position controller described in Section C, V_i would contain, under high-speed conditions, random oscillations with peak-to-peak amplitudes on the order of a volt, and poor tracking and an uncomfortable ride would result. In addition, because the vertical load on the rear wheels is partly dependent on the longitudinal tractive force (via weight transfer), a limit-cycle condition could result if high-gain, velocity feedback were employed. In fact, this author strongly suspects that past limit-cycle problems (26) were caused, at least in part, by this component of e_V. For these reasons, the tachometer signal is not used in the state estimator circuit at speeds above 6.1 m/sec.

The accelerometer error signal e_A would also be composed of both slowly varying and high-frequency components, which result from gravitational forces and vehicle motions and/or vibrations.

The top waveform in Fig. 24 was obtained from the accelerometer through a low-pass filter $(\frac{10}{p + 10})$, which was employed to attenuate the high-frequency vibration noise. If this signal were integrated and compared to the tachometer signal, it would be noted that the

vehicle's vertical movements have a comparatively minimal effect on the accelerometer output.

Nevertheless, when tractive force is applied through the vehicle's tires, its pitch angle changes; this angular motion would affect the accelerometer in two ways. First, the gravitational component of e_A [6] would change, and second, if the longitudinal axis of the accelerometer did not intersect the vehicle's pitch axis[7], an angular acceleration about the pitch axis would be measured as a longitudinal one. Since these effects are largely deterministic, these could be included in the vehicle's longitudinal model. Here, it is assumed that the pitch dynamics are implicitly included in the functional model described in Section B. In the future, the pitch dynamics should be considered for explicit inclusion in the vehicle model.

These observations, concerning X, V, A, e_X, e_V and e_A, were utilized in the design, via the conditional feedback concept, of one possible state estimator, which is shown in Fig. 25. The estimator's inputs are $X + e_X$ and $A + e_A$, and its outputs are continuous estimates of position ($\hat{X}$), velocity ($\hat{V}$) and acceleration ($\hat{A}$).

---

[6] If the longitudinal axis of the accelerometer were perfectly level, the gravitational component of e_A would be zero. Slowly varying components of e_A, such as that due to changes in roadgrade, could easily be eliminated by a number of methods; unfortunately, this is not true for components resulting from abrupt pitching motions.

[7] This axis would probably not be, stationary with respect to the vehicle's body.

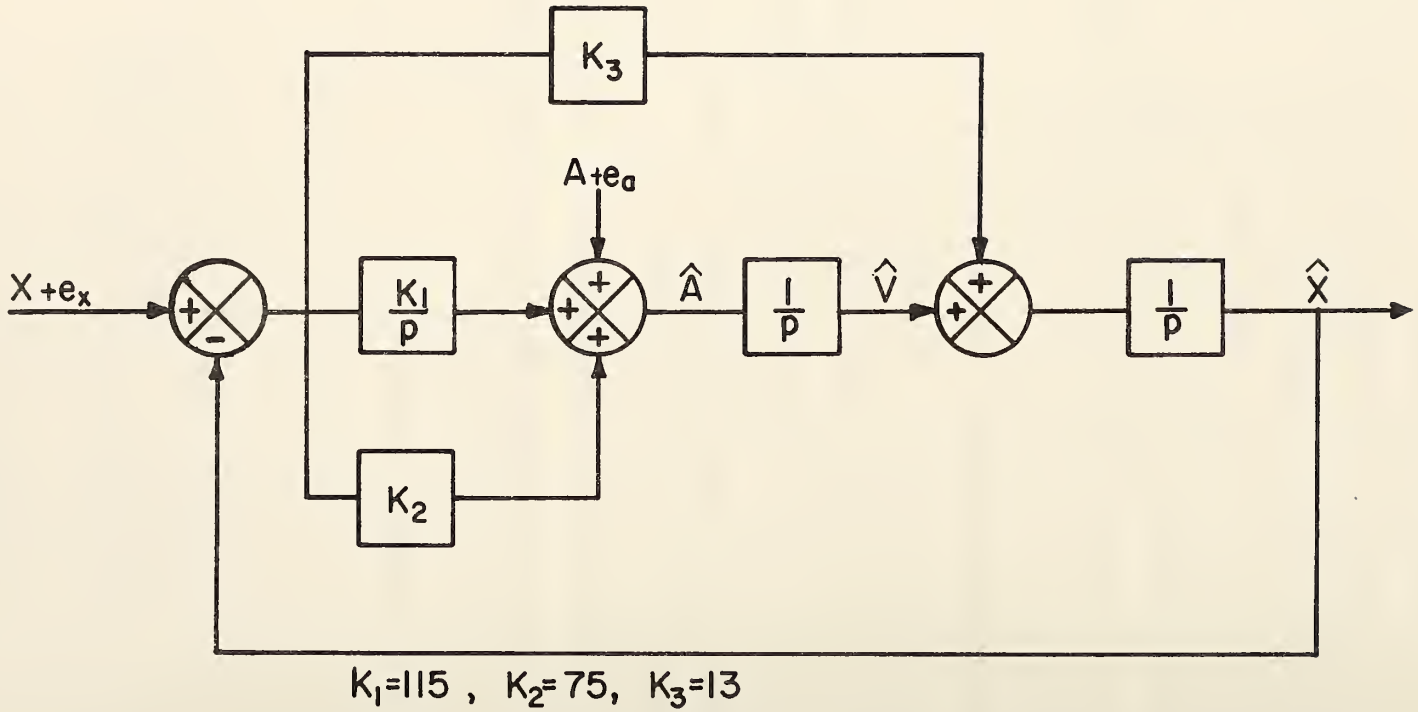

Fig. 25. One possible state estimator.

For the present $X + e_X$ is assumed to be continuous; the effects of sampling are discussed later.

These estimates are given by the following equations, which are readily derived from Fig. 25:

$$\hat{X} = X + \frac{K_3p^2 + K_2p + K_1}{\Delta} e_X + \frac{p}{\Delta} e_A ;$$

$$\hat{V} = V + \frac{K_2p^2 + K_1p}{\Delta} e_X + \frac{p^2 + K_3p}{\Delta} e_A ;$$

$$\hat{A} = A + \frac{K_2p^3 + K_1p^2}{\Delta} e_X + \frac{p^3 + K_3p^2}{\Delta} e_A ,$$

where $\Delta = p^3 + K_3p^2 + K_2p + K_1$.

Note that the desired quantities (X, V and A) are unaffected by the estimator, while the measurement errors are attenuated by either low-pass, high-pass, or band-pass functions.

The gains (K_1, K_2 and K_3) should be judiciously chosen to minimize effects of measurement errors and to insure stable behavior. For the specific measurement devices used here, the gain values shown in Fig. 25 result in low-noise and essentially unbiased[8] position and velocity estimates, and an unbiased

---

[8] In steady-state operation, the expected values of $\hat{X}$, $\hat{V}$ and $\hat{A}$ are X, V and A, respectively, and $X - \hat{X}$, $V - \hat{V}$ and $A - \hat{A}$ are bounded; i.e., they are not accumulative.

acceleration estimate.[9] Note that high-frequency components of e_A would be present in $\hat{A}$; thus, low-pass filtering of $\hat{A}$ should be included as part of the vehicle controller.

As noted previously, $X + e_X$ would be available in discrete form. A continuous position error $X + e_X - \hat{X}$ may be obtained by using a sample-and-hold device as shown in Fig. 26. The modified estimator would be stable for sufficiently large $(\frac{\overline{V}}{D})$'s (i.e., the additional phase lag introduced by the zero-order hold does not result in a phase margin $\leq 0°$). For example, if the gains were chosen as in Fig. 25, the estimator would be unstable for $\frac{\overline{V}}{D} \lesssim 5$ Hz. For small $\frac{\overline{V}}{D}$'s, some circuit modification would be necessary; one possibility is discussed shortly.

The circuit, shown in Fig. 27, is one physical realization of the theoretical state estimator of Fig. 25. The inputs are a wire-crossing pulse from the wire detector, $V + e_V$ and $A + e_A$, and the outputs are $\hat{A}$, $\hat{V}$ and $\hat{\hat{X}}$. The latter is an interpolation of the distance between adjacent laterally position wires; i.e., $\hat{X} = \hat{\hat{X}}$ + the stair-step output of the wire-counter.

For $\frac{\overline{V}}{D} > 10$ Hz (e.g., D = 0.61 m; V > 6.1 m/sec), the circuit operation would be nearly identical to that of the theoretical estimator shown in Fig. 25, except that D is subtracted from the

---

[9] K_1, K_2 and K_3 could have been chosen to be "optimum" in some statistical sense. However, this would require a detailed statistical description of the errors, which is difficult (if not impractical) to obtain. At present, it suffices to employ gains which are merely adequate.

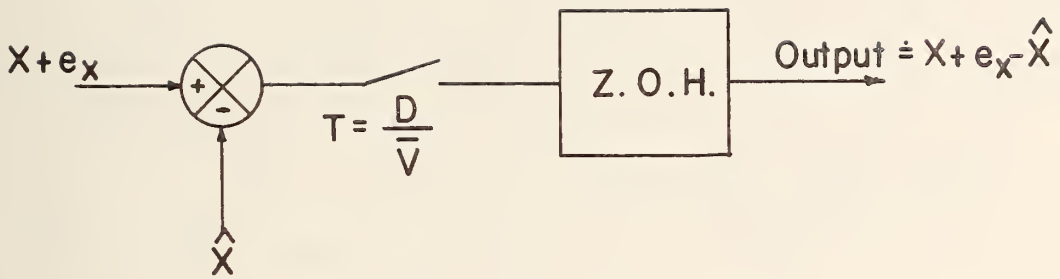

Fig. 26. The reconstruction of $X + e_X - \hat{X}$.

position output when a wire-crossing is detected. Then, $X + e_X - \hat{X}$ ($= D - \hat{\hat{X}}$) is sampled and held; after a negligible delay ($\doteq$ 50 μsec), Integrator A is also reset to $X + e_X - \hat{X}$.

For $\frac{V}{D} < 10$ Hz (e.g., D = 0.61 m; V < 6.1 m/sec), the estimator circuit is modified, via analog switches, to operate in another mode. The modified circuit is shown in Fig. 28, and the corresponding estimator equations are given below:

$$\hat{X} = X + \frac{1}{\Gamma} e_A + \frac{K_5 p + K_4}{p \Gamma} e_V ;$$

$$\hat{V} = V + \frac{p}{\Gamma} e_A + \frac{K_5 p + K_4}{\Gamma} e_V ;$$

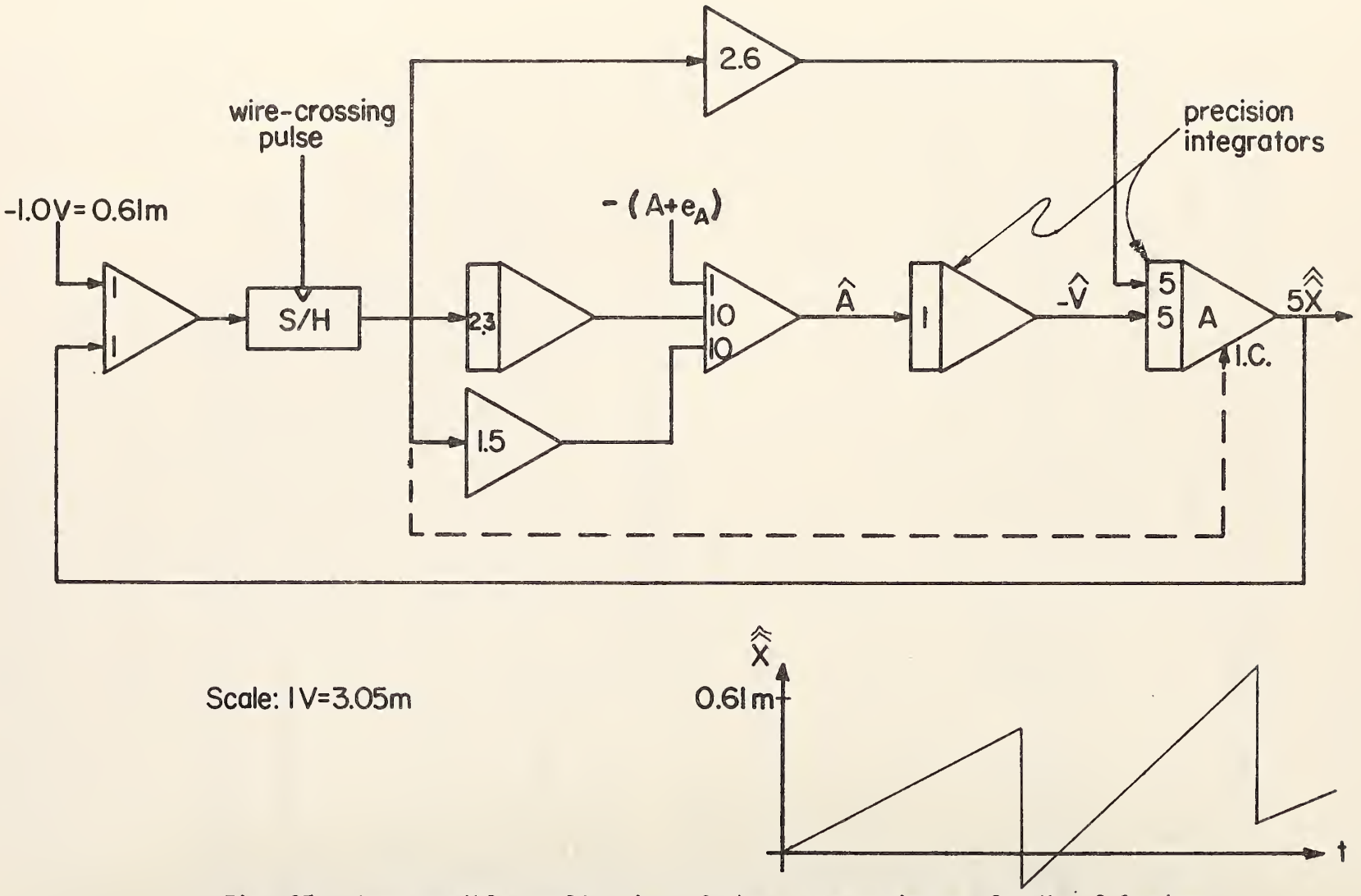

Fig. 27. One possible realization of the state estimator for V > 6.1 m/sec.

$$\hat{A} = A + \frac{p^2}{\Gamma} e_A + \frac{K_5 p^2 + K_4 p}{\Gamma} e_V ,$$

where $\Gamma = p^2 + K_5 p + K_4$; $K_4 = 100$, and $K_5 = 14$. In this mode, $\hat{V}(t)$ would not be unbiased, and $\hat{X}(t)$ ($\hat{\hat{X}}$ + the wire count) could contain small corrective steps at the instants of wire-crossings. If these steps were small ($\lesssim 0.015$ m), and vehicles were not required to operate at $0 < V < 6.1$ m/sec for prolonged time periods, this should not be a problem.

A detailed circuit diagram of the state estimator is given in Reference 24.

E. A Command Generator

The command variables (A_c, V_c and X_c) are related by the following differential equations:

$$p\, X_c = V_c$$

$$p\, V_c = A_c$$

The command acceleration A_c is the input to this system, and hence, X_c and V_c are acceleration-limited. Practical A_c's would be chosen such that the required $A(t)$ were well within the vehicle's acceleration capabilities. This method of command generation was selected to allow for good tracking (i.e., small position errors) and good ride comfort.

In an operational system, the command state (A_c, V_c and X_c) would be generated digitally and thus would be available at discrete times $t = k\, T_s$, where T_s is the sampling interval. By methods

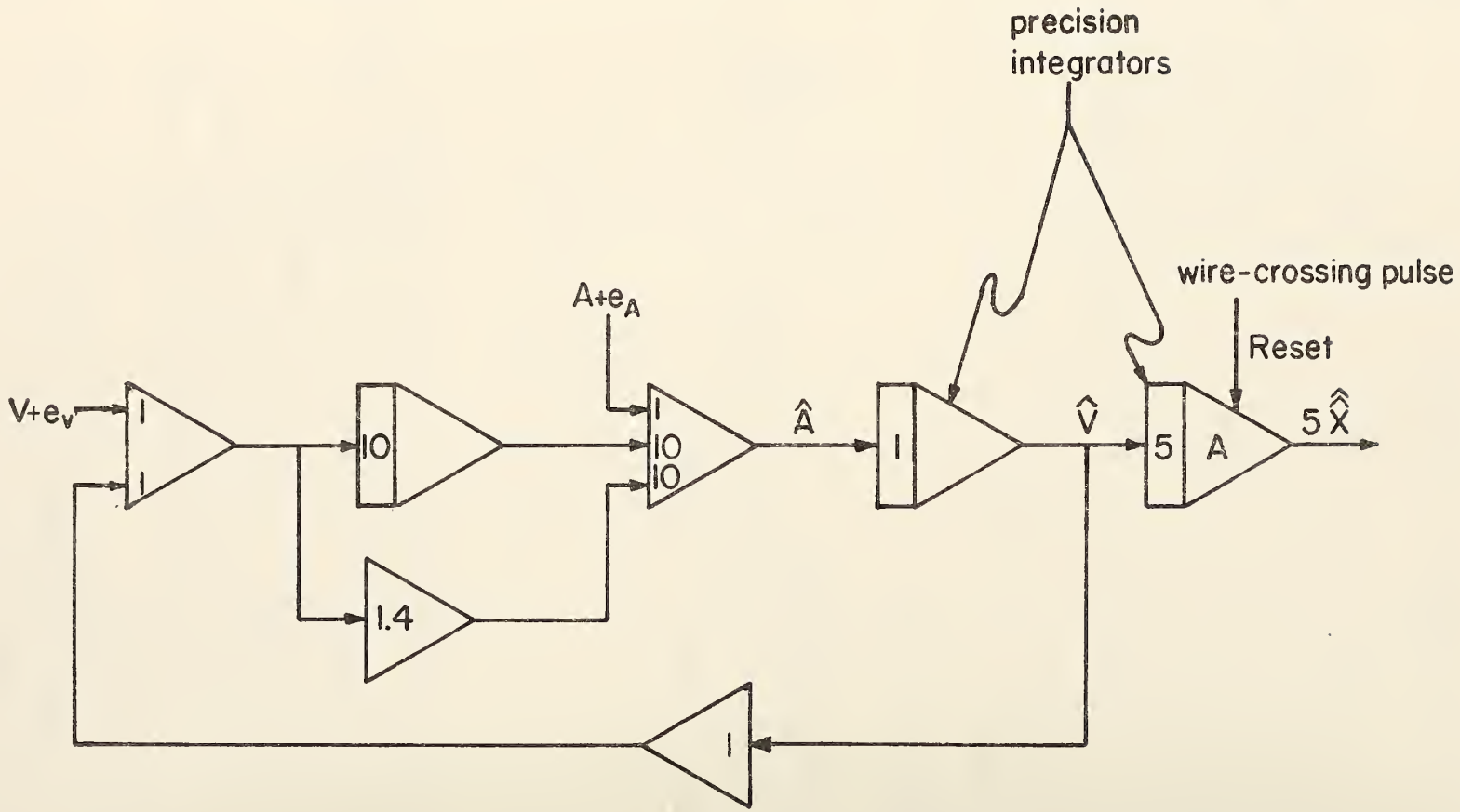

Fig. 28. One possible realization of the state estimator for V < 6.1 m/sec.

discussed in Chan, Chan, and Chan (27), the following discrete-time equivalents of the above equations could be obtained:

$$X_c\ ((k + 1)\ T_s) = X_c\ (k\ T_s) + V_c\ (k\ T_s)\ T_s + \frac{1}{2} A_c\ (k\ T_s)\ T_s^2$$

$$V_c\ ((k + 1)\ T_s) = V_c\ \ (k\ T_s) + A_c\ (k\ T_s)\ T_s$$

The accumulation process represented by these equations was implemented using special-purpose hardware. A block diagram of the resulting circuit is shown in Fig. 29; the specific operations executed by this machine are given below:

$$XC(27 - 0) \leftarrow XC(27 - 0) + 2\ VC(11-0) + AC(7 - 0);$$

$$VC(11 - 0) \leftarrow VC(11 - 0) + AC(7 - 0),$$

where XC(27 - 0), VC(11 - 0) and AC(7 - 0) are the binary representatations of X_c, V_c and A_c, respectively.

The weightings of the least significant bits (i.e., the quantization step-sizes) of AC(7 - 0), VC(11 - 0) and XC(27 - 0) are q_{AC}, $q_{AC}T_s$ and $\frac{1}{2}\ q_{AC}T_s^2$, respectively. By quantizing A_c, V_c and X_c in this manner and by restricting A_c to constant quantization levels between sampling instants, computational errors due to truncation and round-off are entirely avoided. In this study, q_{AC} and T_s were fixed at 0.238125 m/sec^2 and 0.1 sec, respectively.

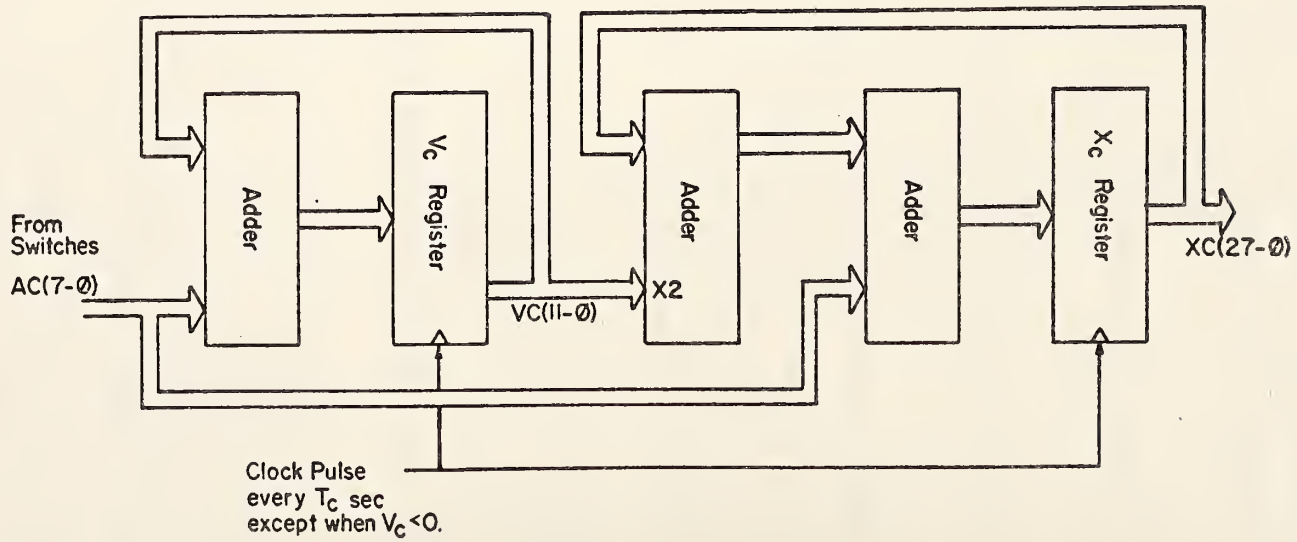

Fig. 29. A block diagram of the command generator.

AC(7 - 0) and VC(11 - 0) are transformed into the analog signals A_c and V_c, respectively, via digital-to-analog converters. Since these signals are accurate only at discrete times $t = kT_s$, $A_c(kT_s)$ and $V_c(kT_s)$ are sampled and held in the controller circuit (see Fig. 21).

One method of obtaining $X_c - \hat{X}$ is shown in Fig. 30. Here, the wire count (see Section D) is digitally subtracted from XC(27 - 0); the difference is transformed into an analog signal via another digital-to-analog converter.[10] The interpolating waveform $\hat{\hat{X}}$ (see Section D) is then subtracted, via an analog difference amplifier, from the output of the D/A converter to give $X_c - \hat{X}$. Since X_c is valid only at discrete times $t = kT_s$, $X_c(kT_s) - \hat{X}(t)$ is sampled and held in the controller circuit (see Fig. 21).

In addition to its primary functions, the command generator automatically disables the accumulation process when V_c becomes negative (i.e., VC(11) = 1). It also automatically disables positive A_c's when V_c becomes equal to or greater than 30.48 m/sec.

In a totally automated system, $A_c(t)$ would be obtained from a vehicle-based memory or directly from the sector-computer-to-vehicle communication link.[11] In this experimental study, A_c was manually selected from a set of switches on the vehicle's control panel;

---

[10] Since the input to the D/A converter consists of only 10 bits, $X_c - \hat{X}$ is truncated by the converter; however, the resulting quantization noise is negligible.

[11] The first alternative is favored here because it would ease communication bandwidth requirements.

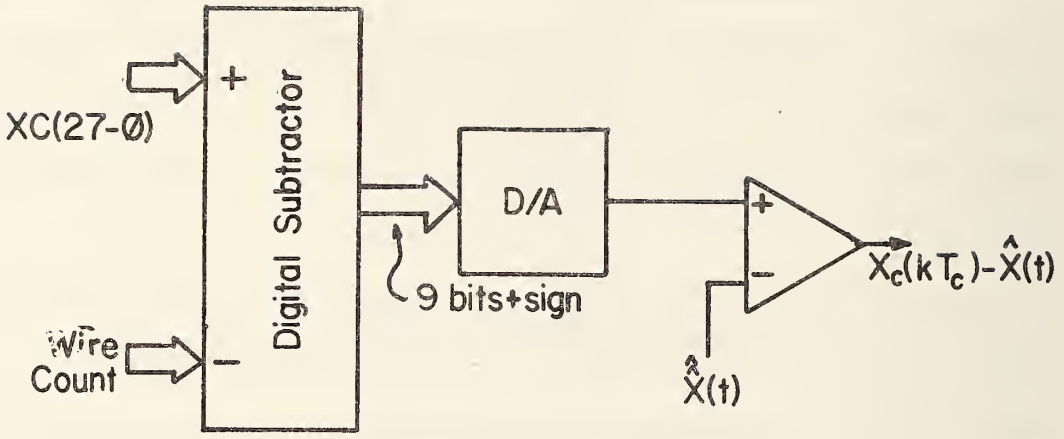

Fig. 30. One method of obtaining $X_c - \hat{X}$.

nevertheless, a command memory could be easily added to the circuit if it were to become necessary in subsequent investigations.

A detailed circuit diagram of the command generator is given in Appendix A.

F. Full-Scale Tests and Results

After the necessary circuits had been constructed and tested in the laboratory, full-scale tests were conducted on an instrumented test track using a specially equipped, 1965 Plymouth sedan. The control functions -- braking, acceleration and steering -- were accomplished using electrohydraulic actuators. An analog computer, consisting of 22 operational amplifiers, 15 potentiometers, and other

necessary components, was installed over the back seat; in these experiments, the computing elements were used only for data collection. Controller compensation, state estimation and command generation were accomplished via special circuits (see Sections C, D and E), which were separate from the computer. All collected data were recorded on a 6-channel, strip-chart recorder located next to the driving position.

A 6.4-kilometer loop of test track at the Transportation Research Center of Ohio was instrumented with the crossed-wire configuration shown in Fig. 23, and the lateral wires of this configuration were used as intermediate position markers. Simple current loops were also installed to serve as absolute position markers; however, these were not utilized in these tests. In addition, a lateral guidance wire was embedded in the center of the crossed-wire configuration, and was used, in conjunction with a lateral controller and sensor, to maintain the vehicle over the crossed wires.

The experimental procedure was as follows: At $t = 0$, a parabolic position command,

$$X_c = X_c(0) + V_c(0)\ t + 0.36\ t^2 \quad (m),$$

was initiated, and as the vehicle responded, $\hat{V}$, $X_c - \hat{X}$ and V_i were recorded. This was repeated several times at different speeds to verify that the responses were consistent.

Typical responses are shown in Fig. 31. Here, the discrete jump in $X_c - \hat{X}$ at time t_1 resulted from a poor choice of initial position. At time t_0, the vehicle's wire-crossing detector was

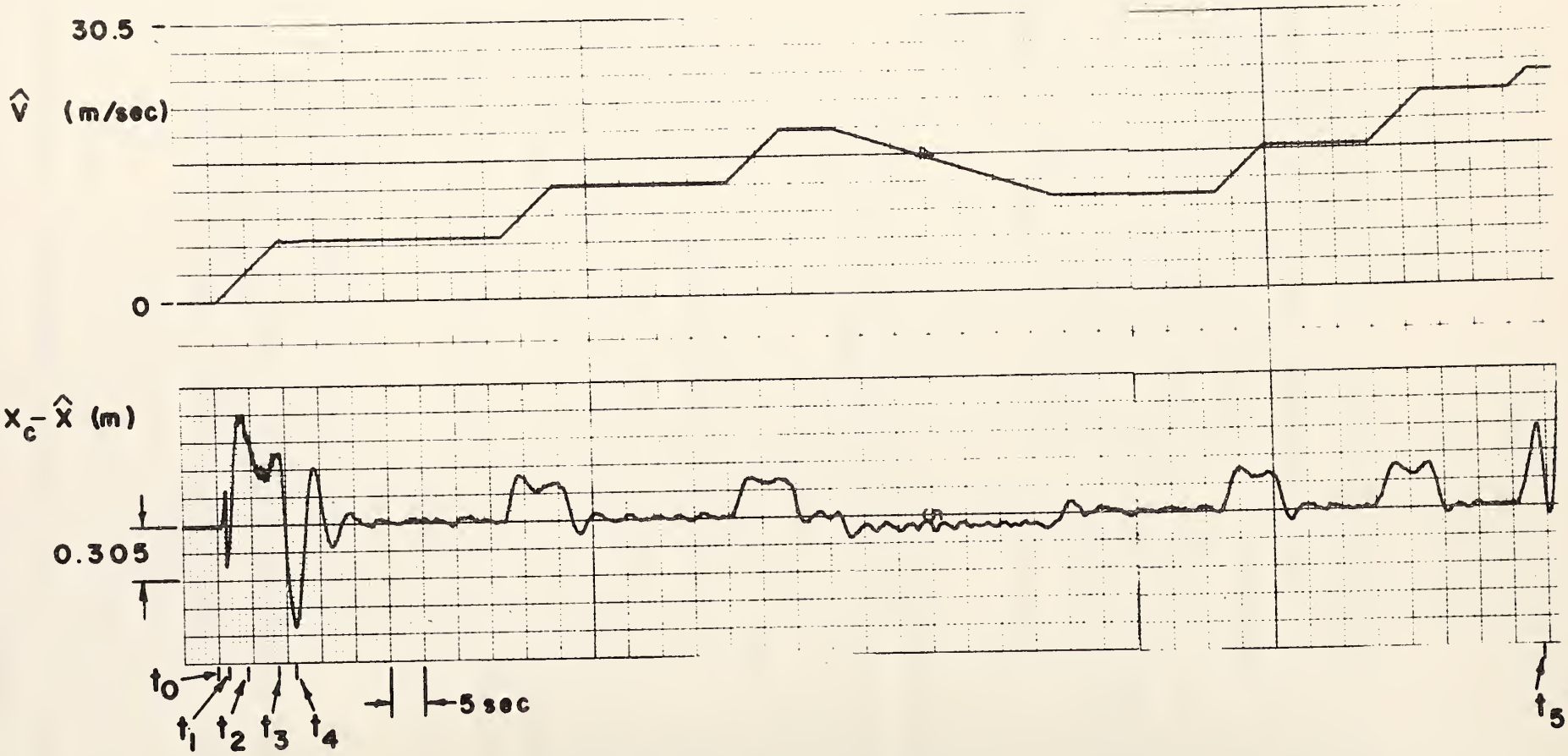

Fig. 31. A typical full-scale response.

placed somewhere between two lateral wires of the crossed-wire configuration, and as the vehicle accelerated, the $\hat{X}(t)$ shown in Fig. 32 was generated by the state estimator. The discrete jump at time t, could have been avoided if the wire detector were initially placed directly over a lateral wire. The subsequent overshoot in $X_c - \hat{X}$ at time t_2 resulted from the momentary braking caused by this jump.

The noise on $X_c - \hat{X}$ (i.e., the small discrete jumps in $\hat{X}$) at speeds between 0 and 6.1 m/sec resulted from a gain miscalibration in the tachometer circuit (see Section D). The jumps apparently triggered a limit-cycle condition, which resulted in an increase in $X_c - \hat{X}$ at time t_3. However, this condition disappeared after the mode-switching (at V_c = 6.1 m/sec) in the state estimator circuit was accomplished (i.e., after the tachometer signal was removed from the estimation process).

The large transient at time t_4 resulted primarily from the mode-switching process itself. This could be corrected by changing the arrangement of analog switches within the estimator circuit.

At speeds between 6.1 and 18.3 m/sec, the responses were generally satisfactory; however, at speeds above 18.3 m/sec, the responses were underdamped, especially when speed-up maneuvers were attempted. In fact, an unstable response (at time t_5) resulted when a speed-up maneuver (A_c = 0.73 m/sec^2) was initiated while the vehicle was traveling at 21 m/sec. However, these responses could be corrected by merely increasing $\frac{1}{k_p(A,V)}$ for these speeds and accelerations.

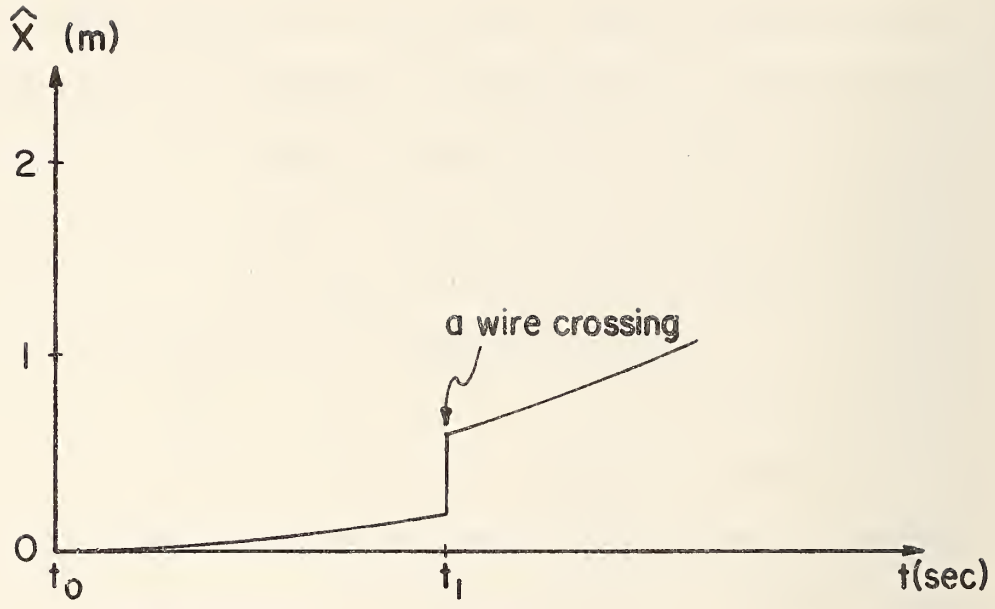

Fig. 32. An $\hat{X}(t)$ resulting from an improper initial position.

In spite of these apparent difficulties, the preliminary results obtained here are very promising since "tight", steady-state position tracking was achieved under most full-scale conditions. Also, all of the existing problems appear to be solvable through circuit modifications and a recalibration of the present model.

G. Directions for Future Work

Because of undesirable winter weather conditions, further full-scale testing was curtailed. As a result, much work remains to be done. One procedure for accomplishing the remaining tasks is described below: First, the state estimator circuit should be modified to avoid unnecessary transients during the mode-switching process.

Second, the tachometer circuit should be recalibrated so as to eliminate the small discrete jumps in $X_c - \hat{X}$, which occur during low-speed operation. This could be achieved by observing $X_c - \hat{X}$ under full-scale conditions and appropriately adjusting the gain of the tachometer circuit. Third, the estimation error signals (i.e., $X + e_X - \hat{X}$, $V + e_V - \hat{V}$ and $A + e_A - \hat{A}$) should be observed under different full-scale conditions (i.e., different speeds and accelerations). These signals should be essentially zero under all practical conditions; if these were not, some circuit adjustments (e.g., gain or bias trimming) may be necessary.

After the previous three tasks were completed, a new modeling study should be accomplished using the revised state estimator circuit. The following procedure is recommended: Full-scale data should be obtained by applying step commands directly to the throttle actuator input (V_i) (i.e., with no feedback loops), and $\frac{\alpha}{p + \alpha} \hat{A}$ should be recorded. Here, $\hat{A}$ would be available in the estimator circuit, and α would be chosen so as to obtain an adequately "clean" output signal.[12] Responses should be obtained for different speeds and step commands. Subsequently, the full-scale responses would be replicated on an analog computer. A system model would be excited with the same step commands, and the response would be matched with the corresponding full-scale response by appropriately adjusting the model's parameters. In this process, only the initial portion (i.e., the first second or two) of a response should be used for matching

---

[12] $\alpha = 10$ should be a good value.

purposes, as this part of the response would contain all pertinent transients. The model described in Section B could be used as a starting point; however, if higher-order effects (e.g., those due to the suspension dynamics) were noticeable, these should be explicitly included in the model structure (via additional poles and zeroes).

Finally, the existing controller circuit should be modified to accommodate the new propulsion system model and tested under full-scale conditions.

CHAPTER IV

AN INFORMATION SOURCE FOR LONGITUDINAL CONTROL-- FLAT, PERIODIC TRANSMISSION LINES

A. Introduction

Several approaches for providing automated vehicles with longitudinal state information via induction fields from transmission lines have been evaluated. Initially (13), a "moving" standing wave on a single line was employed, and a controlled vehicle was required to sense and track a unique null point of this wave. The minimum permitted spacing between vehicles was one-half wavelength and, to achieve a desired range of spacing, it was necessary to select line excitation frequencies in the range 2.5 MHz $\leq$ f $\leq$ 25 MHz. For such frequencies, the line properties are dependent on the environment, and this, together with line loss and a consequent inability to maintain sharp well-defined nulls (i.e., a well-defined signal for a vehicle to "track") over a practical extent of line, posed major difficulties in practically implementing this approach.

Next (15), two lines were excited from opposite ends at slightly different frequencies to create a linear, periodic, phase-difference waveform which could be moved at any desired speed. Each vehicle was commanded to follow a prescribed point of this waveform, and the minimum permitted spacing between vehicles was again half a wavelength. Thus, the allowed excitation frequencies were also in the range 2.5 MHz $\leq$ f $\leq$ 25 MHz and the line properties were frequency and

environmentally dependent. Line loss was not a serious problem; however, changing environmental conditions in the vicinity of the lines caused the propagation constant, and hence the period of the moving wave, to change drastically. Thus, unless elaborate means were taken to control the environment, precise control of the intervehicular spacing could not be achieved.

Subsequently (18), a technique utilizing circular, helically wound transmission lines was devised. Here, the phase-difference between the signals from two lines was sensed by each vehicle. This phase-difference was a linear function of the longitudinal coordinate and was spatially periodic with a period dependent not on the frequency or propagation constant of the lines but on their geometry--i.e., the pitch lengths. While this waveform could theoretically be used as a moving reference (since it could be made to move at any desired speed), the period could not be changed electronically. Thus, its use as a stationary reference to provide absolute position information appeared more attractive.

Since the information was frequency independent, the choice of frequency was completely arbitrary. However, frequencies in the range 1 KHz $\leq$ f $\leq$ 20 KHz were found to be desirable since the line loss was low and the voltage induced in signal-detecting coils was sufficiently high.

This method has decided advantages over the previous ones:

1) Low-frequency signals (1 KHz $\leq$ f $\leq$ 20 KHz) could be used;

2) The lines could be excited from the same ends[1] as opposed to opposite ends in the high-frequency, phase-difference techniques; and

3) The available signals are fixed by the geometry of the lines, and are independent of environmental conditions.

However, two disadvantages remain:

1) Helical lines are difficult to implement; and

2) Two lines are needed.

To circumvent these difficulties, a technique utilizing a periodic, "square wave" transmission line was developed. A signal is obtained only at the "crossovers" of this line, (i.e., every half wavelength), and there is a need to interpolate between crossovers so as to obtain a "continuous" position signal. This approach was selected for implementation at the TRCO skid pad, as was described in Chapter II.

In this Chapter, the results of laboratory tests of another technique are presented. This involves two transmission lines and the provision of continuous information to a vehicle, thereby eliminating the need for interpolation. Two "flattened helical lines" (strictly speaking--flat, periodic-transmission lines) are employed, and these should be relatively easy to construct and install due to their flat geometry.

---

[1] This results in both a simpler physical implementation and a reduction in crosstalk.

B. Theory of Operation

The function of a longitudinal information source is to provide each vehicle with a physical observable that will be a unique measure of the vehicle's state along the roadway. For practical reasons, a signal directly proportional to the longitudinal distance, z, would be desirable. Since any physical observable cannot increase indefinitely, the signal must be periodic. Thus, a position indication would be unique only within a period; but, by counting periods as well as measuring the interperiod distance, a unique indication would result.

Consequently, one property of the signal, H(z) would be

$$H(z) = H(z + P) \tag{4-1}$$

where P is the spatial period of the information. Any periodic, two-wire, transmission-line structure excited at low frequencies would produce a magnetic field distribution of this form. However, the field variation within a given period may not be linear in z. In general, a Fourier series expansion for the magnetic field, $H_1(z)$, can be written as

$$H_1(z) = \sum_{n=1}^{\infty} a_n \cos \left(\frac{2\pi n}{P} z\right) \tag{4-2}$$

where the a_n are dependent upon the traverse coordinates (x and y) and the current, I_1, on the line. Here, it is assumed that the line and its coordinate system is such that a cosine series can be used and that no average value of H_1 exists. These assumptions are valid if the lines have both half-wave and even symmetry and periodic crossovers.

If a second, identical two-wire line were placed on top of the first line but displaced along z by $\pm P/4$ and excited by currents I_2 which are equal in magnitude to I_1 but shifted in phase by $\pm 90°$, then the field, H_2, from this line would be

$$H_2(z) = \sum_{n=1}^{\infty} \pm j\, a_n \left[\pm \sin \left(\frac{2\pi n}{P} z\right)\right] \qquad (4\text{-}3)$$

If a vehicle were equipped with a magnetic field probe placed directly over the set of lines, it would detect the sum of H_1 and H_2. Further, if the lines were designed such that the first term in the Fourier expansion were dominant, then this sum, H, would be

$$H = a_1 \left(\cos \frac{2\pi}{P} z \pm j \sin \frac{2\pi}{P} z\right) \qquad (4\text{-}4)$$

or

$$H = a_1 e^{\pm j \frac{2\pi}{P} z} \qquad (4\text{-}5)$$

Thus, the phase of the detected signal would be linear and periodic in z.

This is also the field distribution of the circular helical-line structure (18), and hence, a four-wire, flat, periodic transmission line (hereafter referred to as a line pair since it is composed of two, two-wire lines) could replace it. Further, the techniques developed for use with the helical line should be usable with these flat lines.

In a full-scale situation, another line pair would be required to provide a phase reference.[2] If the spatial period of the first line pair were P_1 and that of the second (otherwise identical) line pair, P_2, then the phase difference as measured onboard a vehicle would be

$$\theta_d(z) = \frac{2\pi}{P_e} z \qquad (4\text{-}6)$$

where P_e, the effective period, is given by

$$\frac{1}{P_e} = \frac{1}{P_1} \pm \frac{1}{P_2} \qquad (4\text{-}7)$$

Eqn. (4-6) may be obtained from (4-5) as is demonstrated in Reference (18). Either the plus or minus sign is used, depending upon the method of excitation of each line, just as in the helical-line situation.

C. The Experimental Investigation

The flat, periodic transmission lines consist of two, two-wire lines, with each line laid flat and "twisted" so that periodic crossovers occur. The manner of twisting (i.e., the shape of the lines between crossovers) has not yet been specified; however, a desired shape is one which will result in a field distribution which has a sinusoidal magnitude variation in z. Then, the Fourier series for the field, Eqn. (4-2), will consist of only one term--as was assumed in the derivation of Eqn. (4-5).

---

[2] In this case, two detection coils would be required. One positioned over the first line pair and the other over the second. Appropriate processing of the detected signals in these coils yields $\theta_d(z)$ as given by Eqn. (4-6).

A theoretical approach to specifying the desired shape was unsuccessful; therefore, a detailed experimental investigation was necessary. This was divided into three parts: The determination of 1) a near-optimum (or optimum) shape; 2) a range of satisfactory widths; and 3) a range of satisfactory line spacings. For all of the tests, a frequency of 12 KHz was used so that an adequate field strength was obtainable at the detectors.[3]

a) The Shape of the Lines

The first pairs evaluated were sinusoidally periodic as shown in Fig. 33. A constant phase reference was used, and the phase versus z was measured with the probe positioned at x = 0 in the cross-sectional plane (i.e., at the midpoint of the lines), a probe height of y = 11.4 cm., and parameters of P = 2.4 m., d = 22.9 cm., and I_0 = 0.3 Amperes peak-to-peak (App), where $I_1 = I_0 \underline{/0°}$ and $I_2 = I_0 \underline{/90°}$.

Note from Fig. 34 that the sinusoidal shape was not suitable as the phase difference was highly nonlinear in z. Subsequently, the triangular and square wave configurations, which are shown in Fig. 35, were evaluated. (In the discussions to follow, the line parameters and the cross-sectional coordinates will be shown on the figures, and only those factors pertinent to the topic under discussion will be referred to in the text.)

---

[3] In a full-scale situation, the choice of frequency would be a trade-off between line loss and the strength of the detected signal. For extremely long lines, the frequency should be low enough to maintain an appreciable current all along the line and high enough to induce an adequate voltage in the detectors.

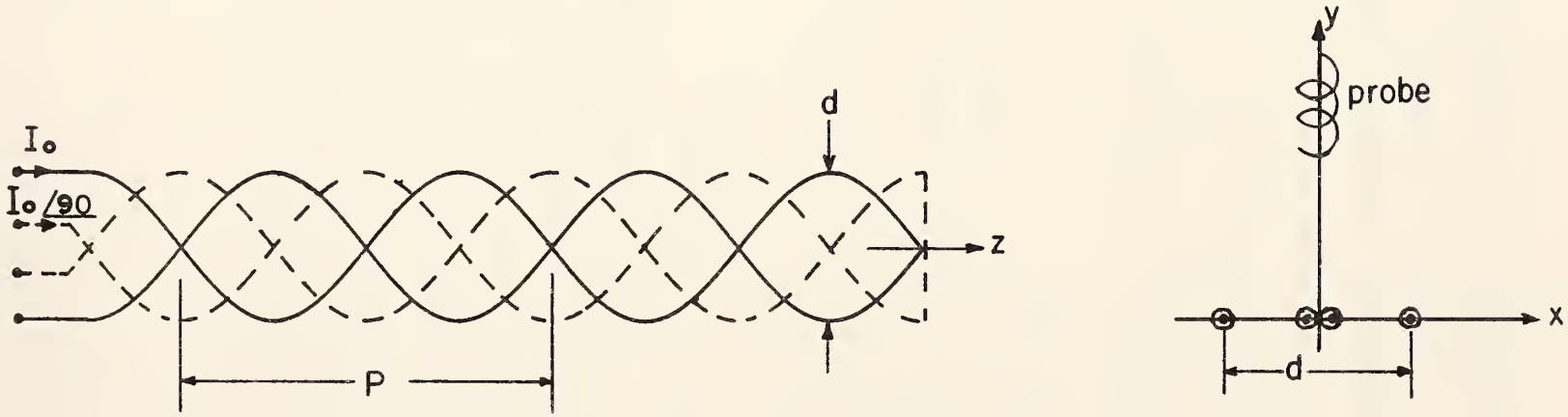

Fig. 33. Geometry and coordinate system for the sinusoidally shaped line.

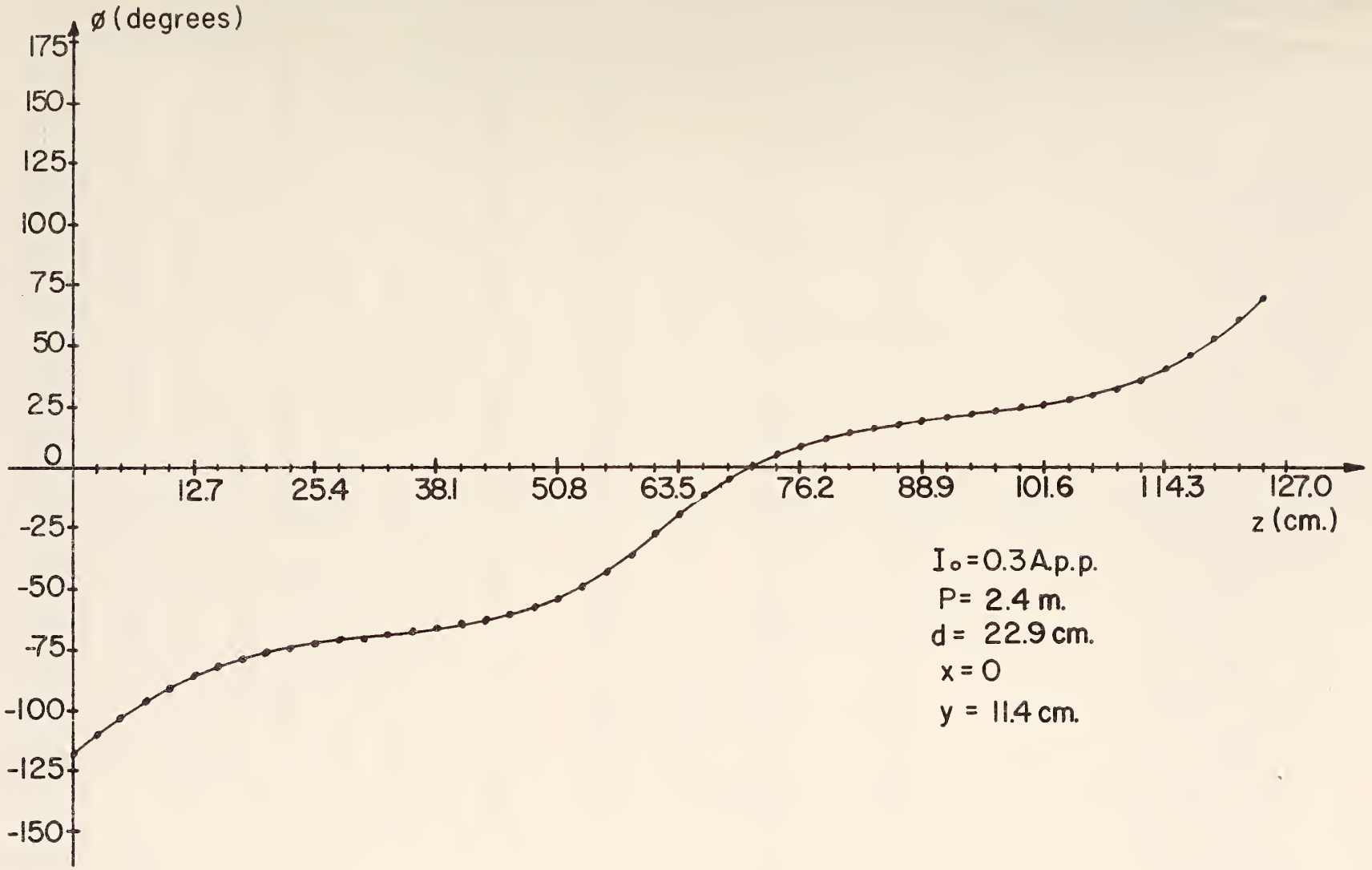

Fig. 34. Longitudinal phase characteristics for the sinusoidally shaped line.

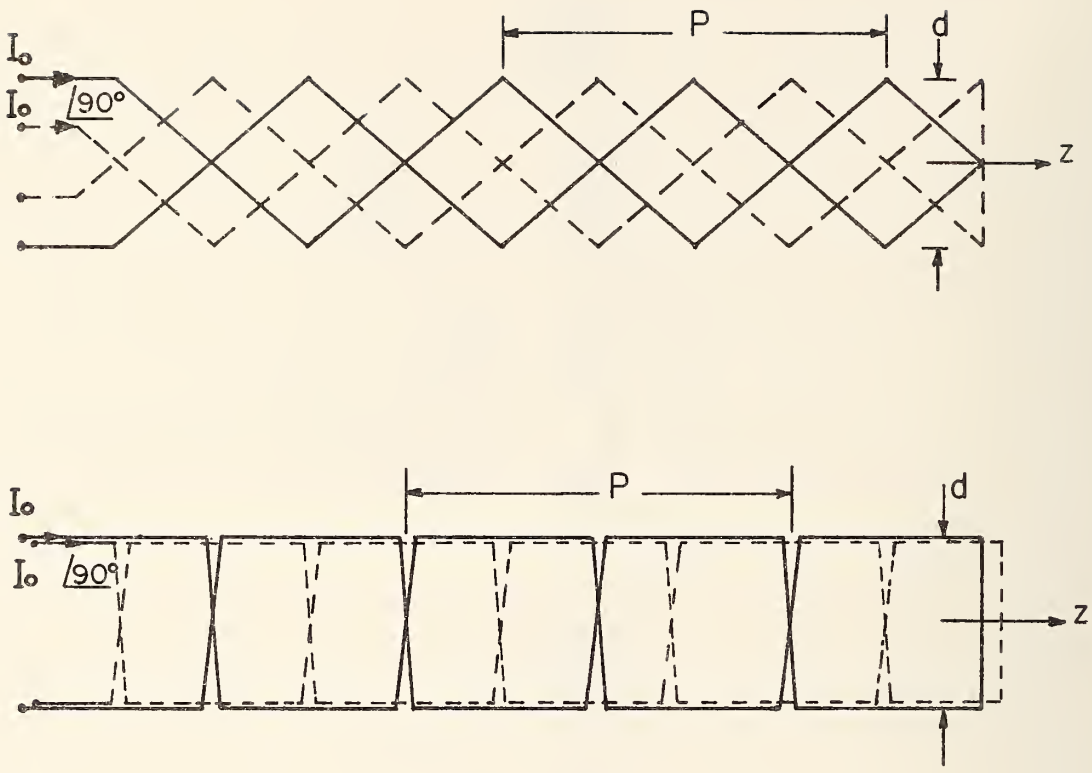

Fig. 35. Geometry for the triangular and square shaped lines.

The results for the square-shaped lines for three probe heights (y = 11.4 cm., 24.1 cm. and 44.5 cm.) are shown in Figs. 36, 37, and 38. It is evident that as y increases, the phase curves become more linear. This trend was also observed for the triangular and sinusoidal shapes. Thus, it appeared that any periodic flat line with crossovers would yield the required linear phase characteristics provided the probe height was sufficiently large. However, two other factors must be considered. First, at large heights noise can be detrimental since the signal strength would be greatly decreased. Second, the probe will not remain at a fixed height due to vehicle bounce. Hence, it is desirable

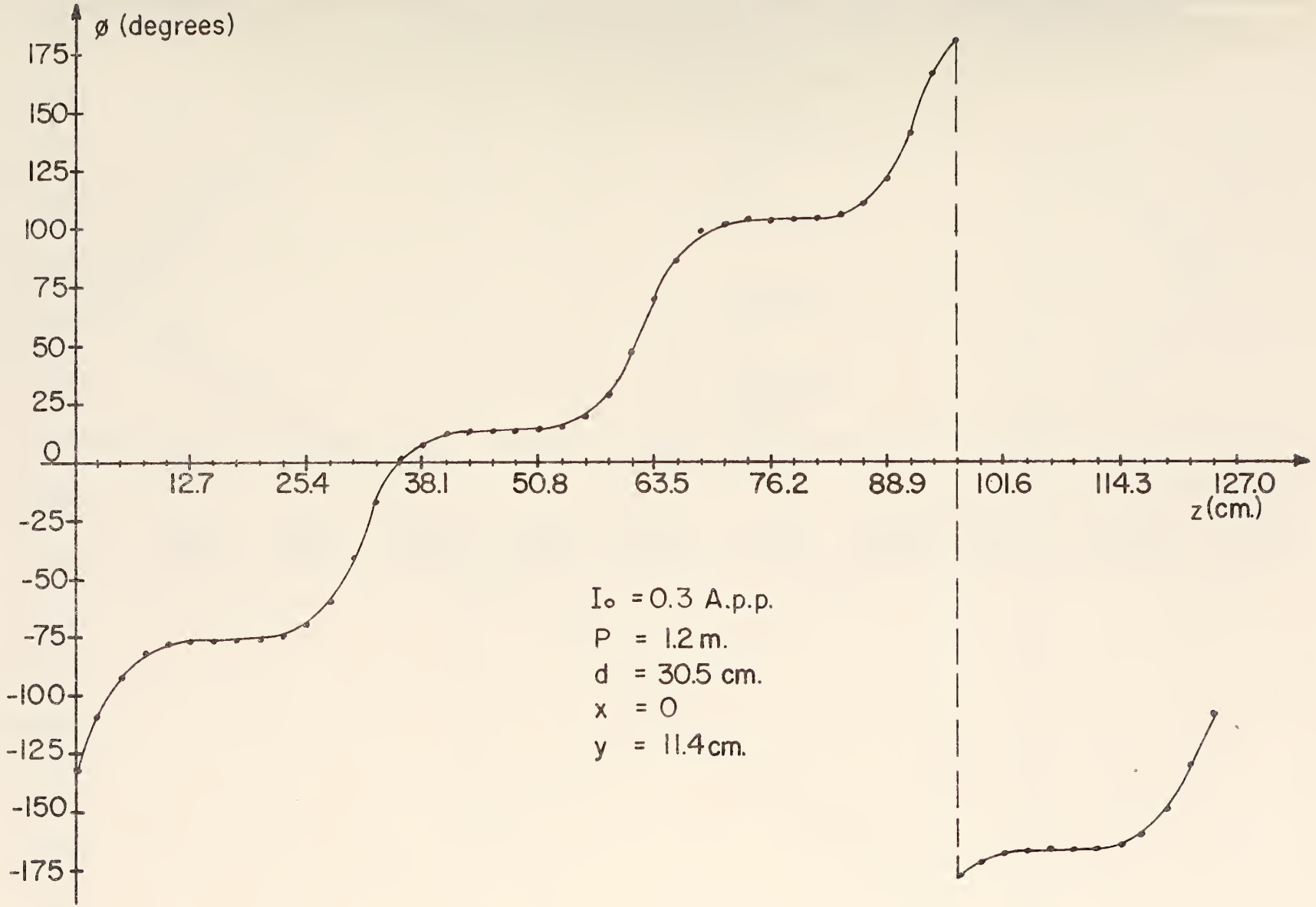

Fig. 36. Longitudinal phase characteristics for the square-shaped line --- low probe height.

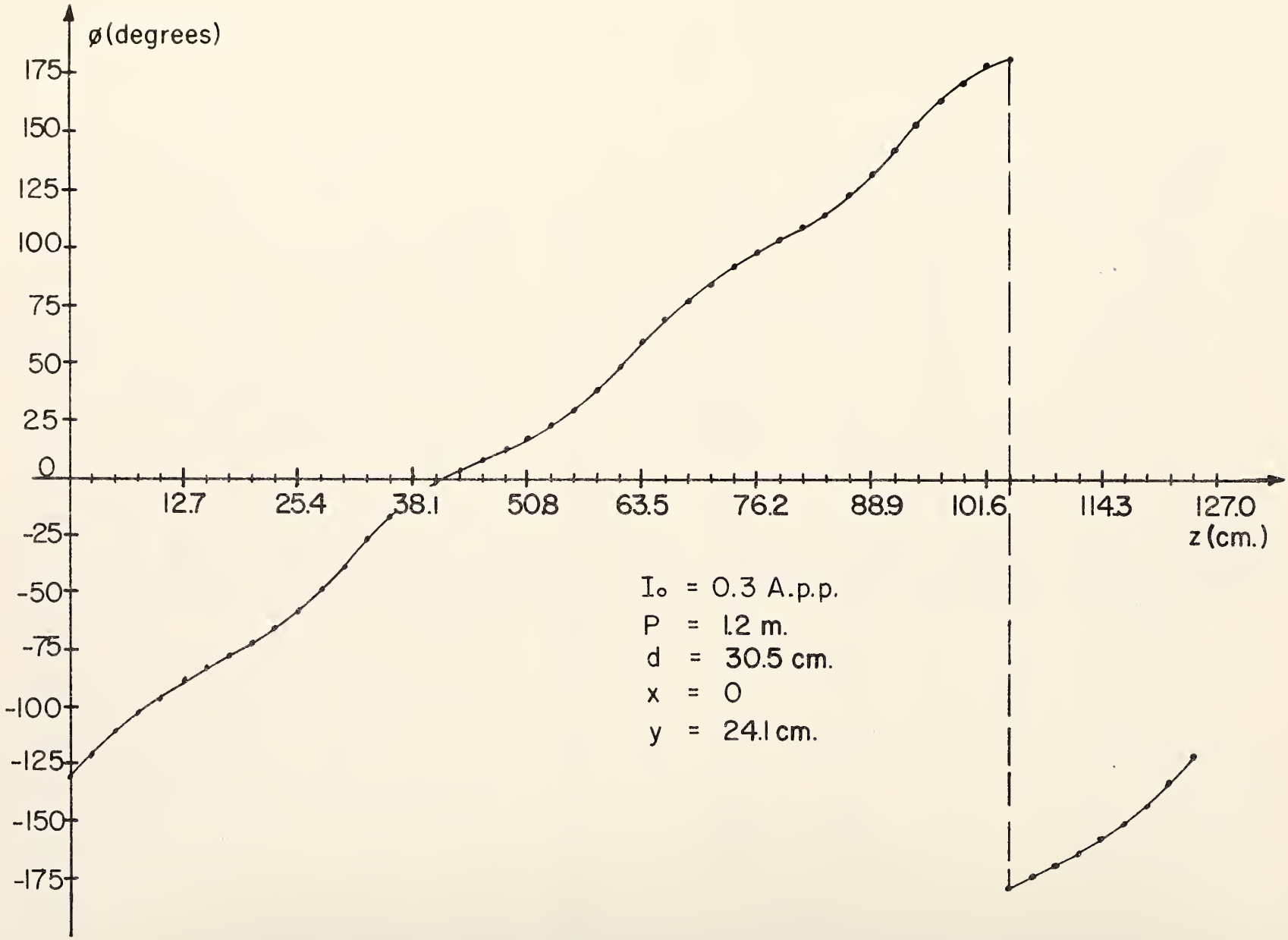

Fig. 37. Longitudinal phase characteristics for the square-shaped line --- medium probe height.

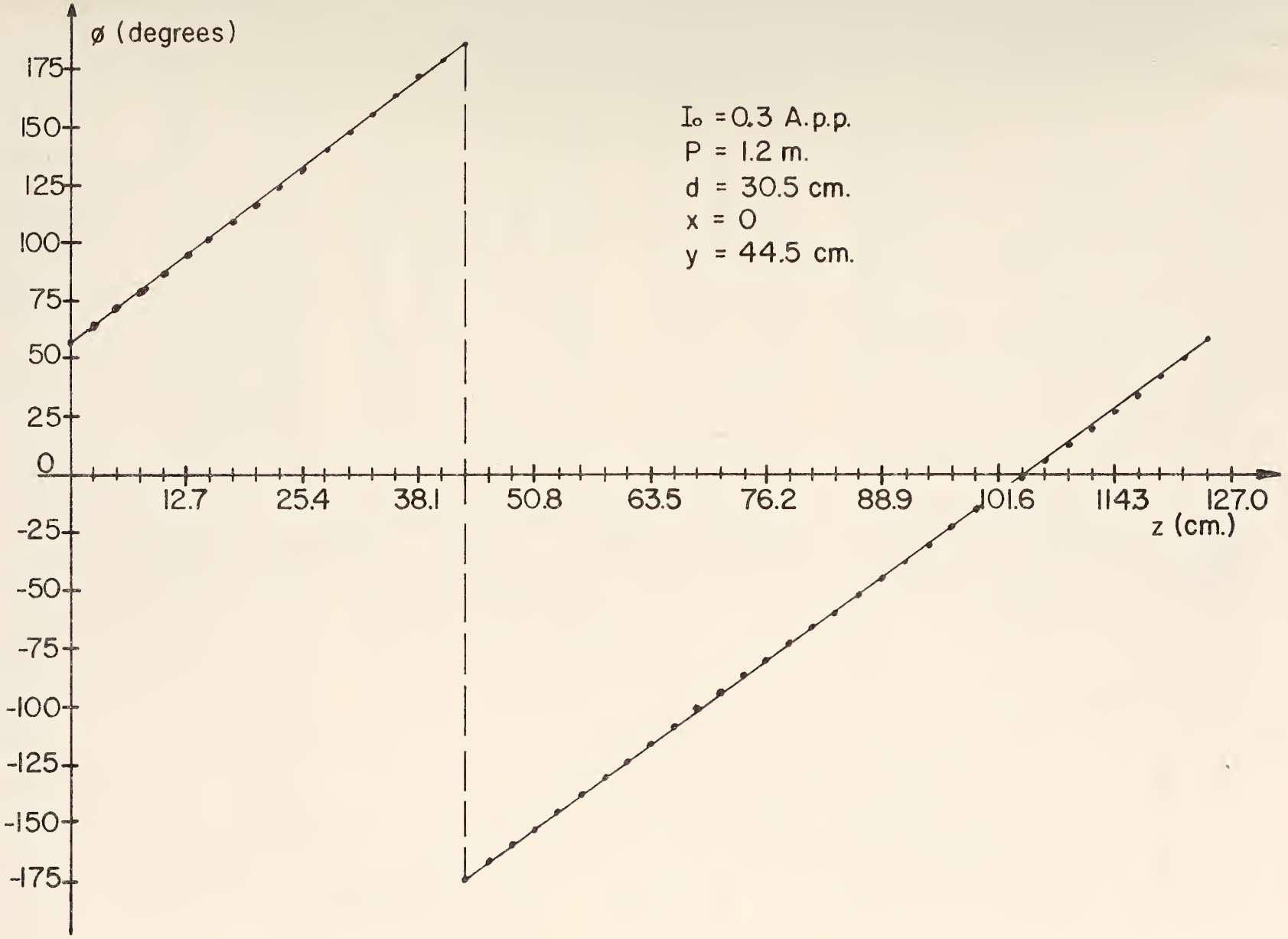

Fig. 38. Longitudinal phase characteristics for the square-shaped line --- large probe height.

to choose that shape which will have a linear phase curve over the expected range of probe heights.

In this respect, the triangular shaped lines were the best of those tested. This is shown in Figs. 39 and 40 where phase measurements for two extreme probing distances (y = 14 cm. and y = 41.8 cm.) are presented. The linearity is obviously better for the larger distance (Fig. 40) but it is very acceptable for the lower. In view of this result, it was decided to henceforth consider only triangular lines.

b) The Width of the Line

From the point of view of construction and installation, it seems desirable to choose line pairs of narrow width. The effects of reducing width were evaluated by tests on a narrow (d = 7.6 cm.) line pair with the results shown in Figs. 41 and 42.

No appreciable change occurred in the linearity of the phase characteristic with the probe at y = 39.4 cm. A slight non-linearity occurred at y = 11.4 cm; however, this was deemed acceptable. It was noted that the signal strength was less for the narrower width. This was expected since if the width goes to zero, there would be no detectable field.

Thus, one effect of reducing line width is to reduce the signal strength. A second effect involves vehicle lateral motion. In practice, a vehicle moves laterally, and the probe would not remain at the center (x = 0) of the line pair.

For small x, the phase characteristic is approximately the same as that for x = 0; however, for x sufficiently large (a distance beyond

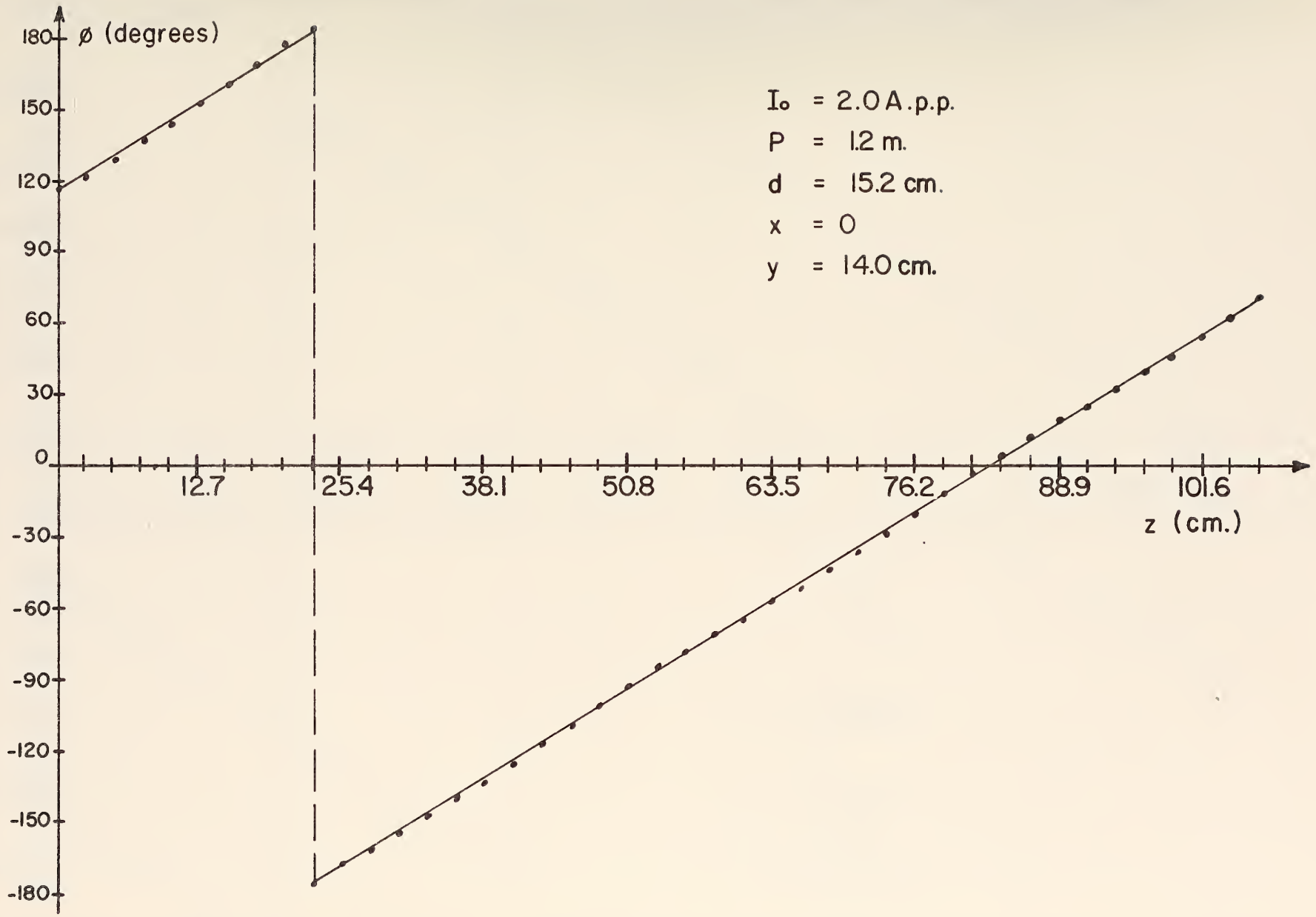

Fig. 39. Longitudinal phase characteristics for the triangular-shaped line -- low probe height.

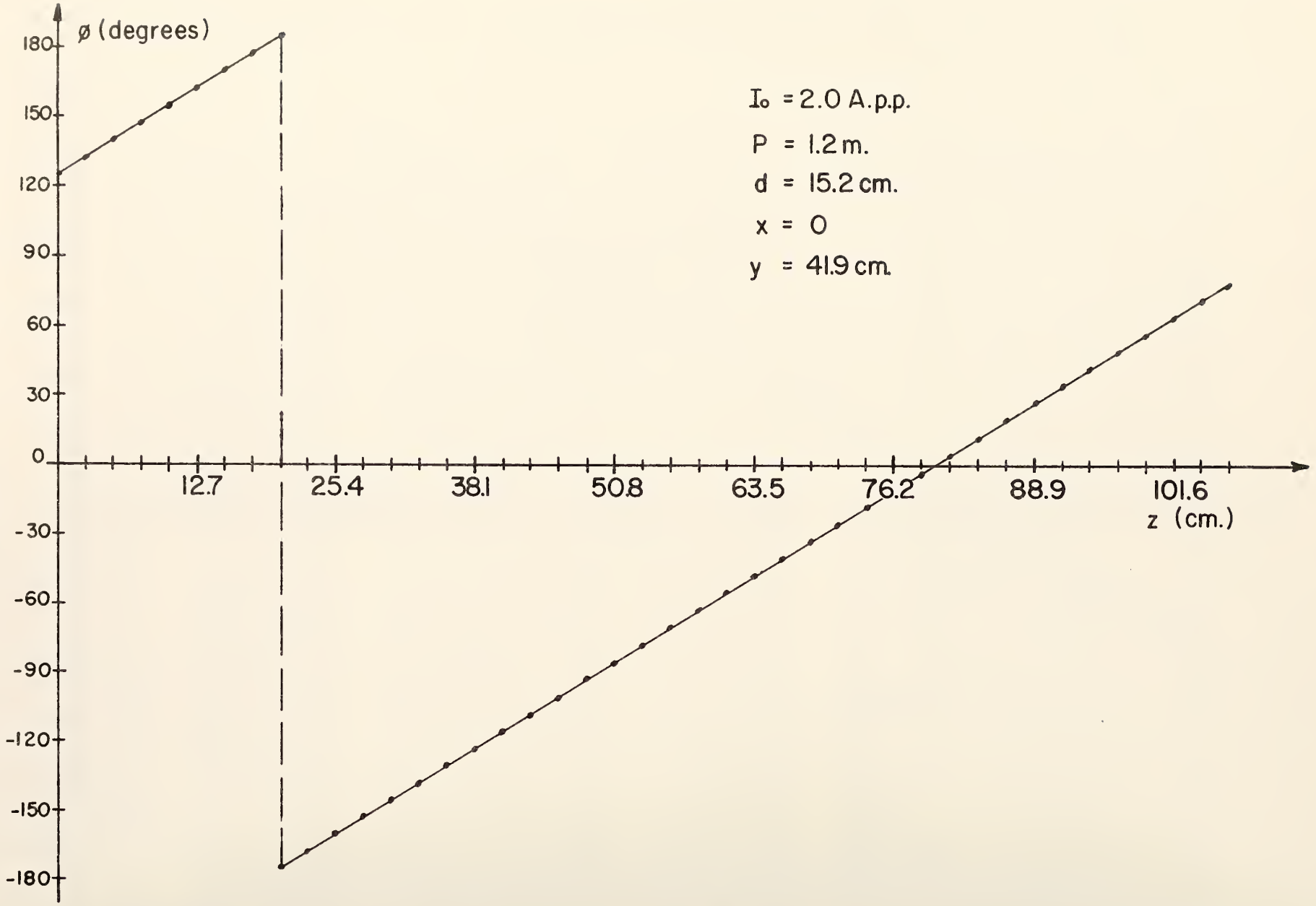

Fig. 40. Longitudinal phase characteristic for the triangular-shaped line -- large probe height.

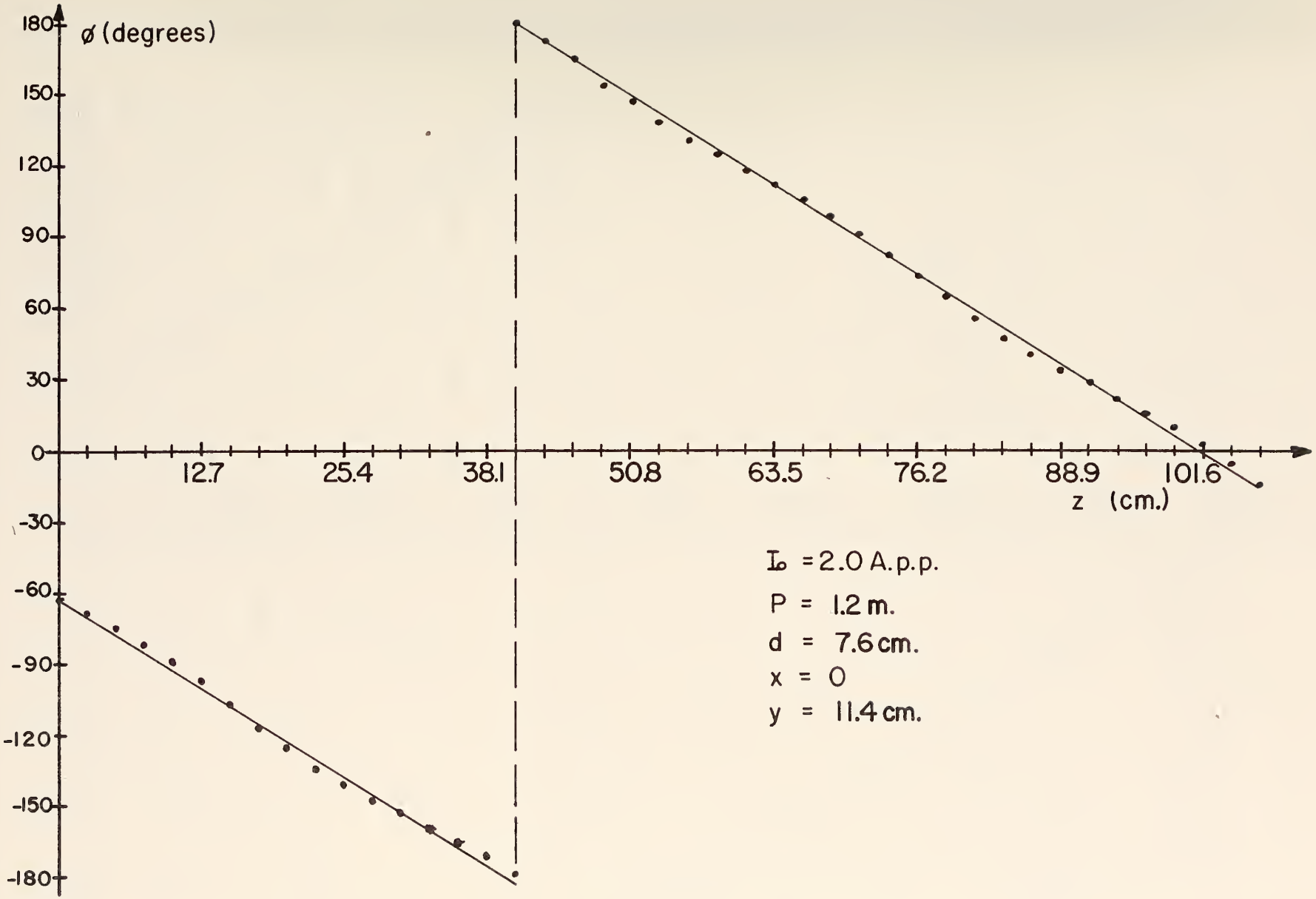

Fig. 41. Longitudinal phase characteristic for the triangular-shaped line -- narrow line with a low probe height.

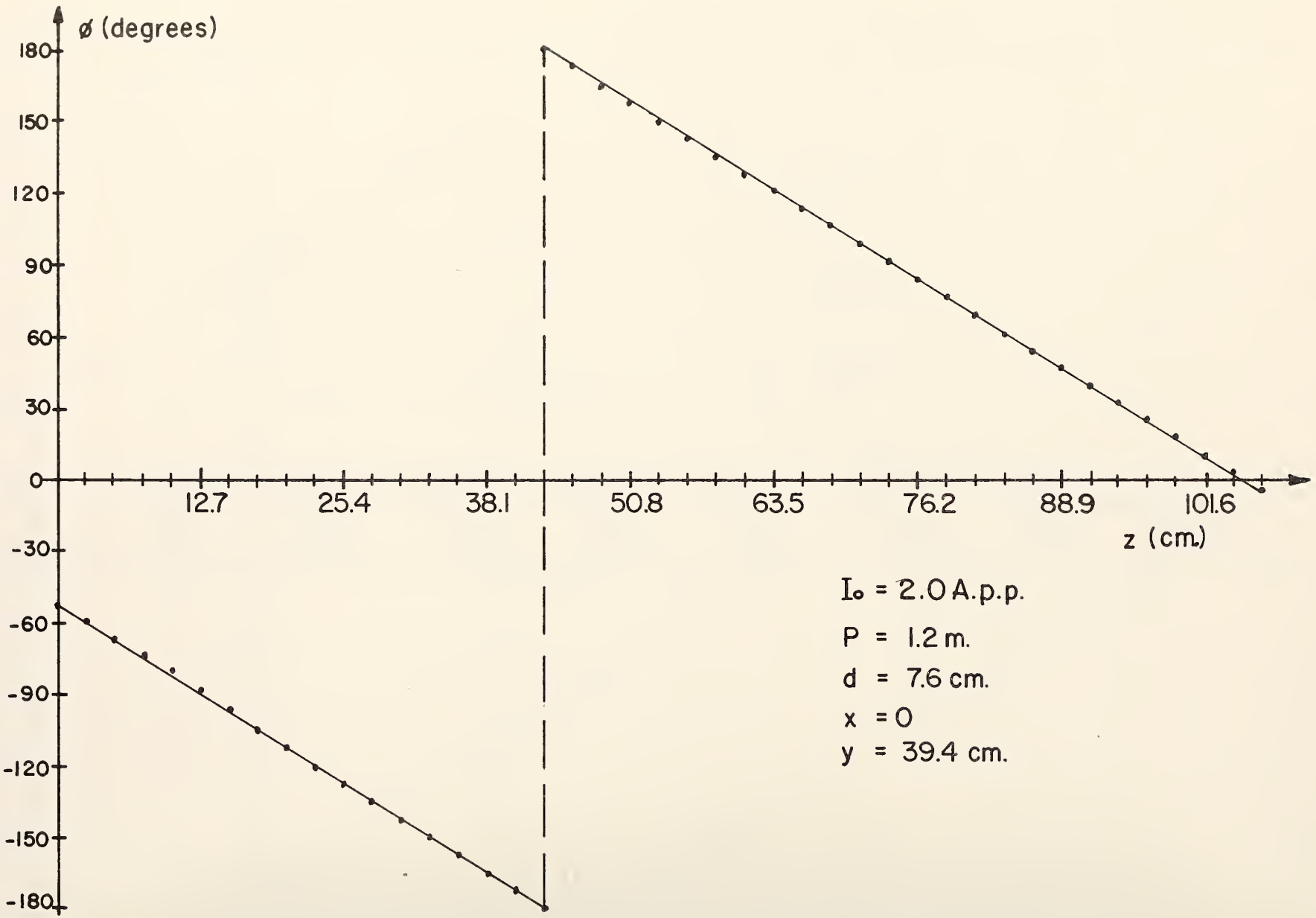

Fig. 42. Longitudinal phase characteristics for the triangular-shaped line -- narrow line with a large probe height.

the width of the line), the phase characteristic differs by as much as 180°. As changes in phase would be interpreted as longitudinal position deviations, they must be minimal.

A series of tests were conducted to determine the allowable range of lateral variation, Δx, and the allowable range of vertical deviation, $y_{min} \leq y \leq y_{max}$, of the probe for an acceptable maximum phase error $\Delta\phi$. Since these ranges are related to the width of the line, the initial measurements were made with 3 lines of width, 22.9 cm., 15.2 cm., and 7.6 cm., respectively. The phase was measured in a cross-sectional plane as the probe was varied from x = -15.2 cm. to +15.2 cm. and for probe heights y = 16.5, 21.6, 26.7, 31.8, and 41.9 cm. These choices encompass the range of expected vehicle deviations. The data are shown in Figs. 43, 44, and 45, and the results are summarized in Table 1. Here, $\Delta\phi$ was computed assuming that the desired phase is that measured at x = 0 and y = 26.7 cm. -- a reasonable choice for the undisturbed probe position.

The least phase change results when the widest line is used. Also, as the height is increased, the phase change for lateral variations is lessened. All phase errors appear to be quite acceptable -- in fact, they are less than those encountered with the helical lines -- but, there is a trade-off between the line width and the allowed vehicle deviations. If the latter is decreased then the line width can also be decreased for a prespecified maximum phase error. Thus, once the Δx, y_{max}, y_{min}, and $\Delta\phi$ are specified, a line width can be chosen.

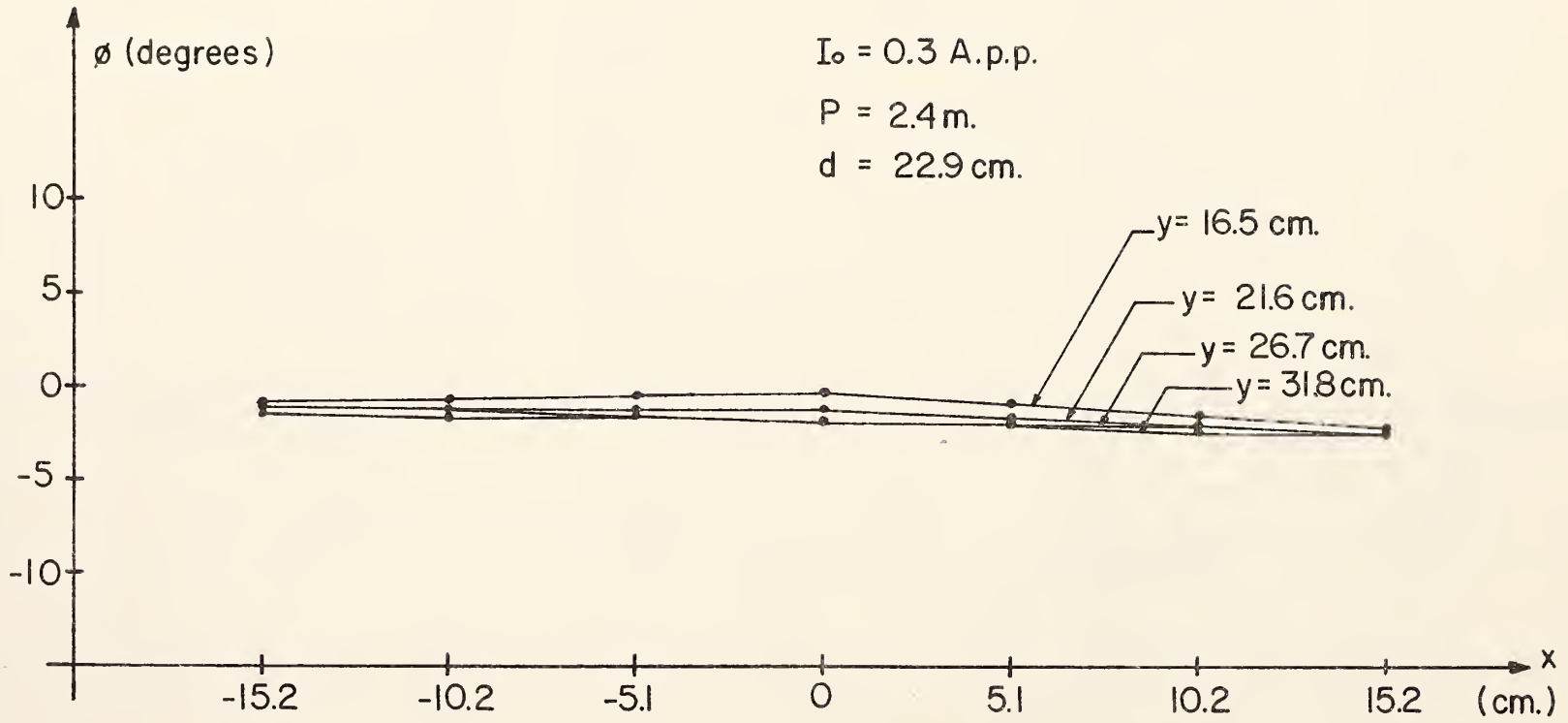

Fig. 43. Transverse phase characteristics of a relatively wide, triangular line as a function of the lateral (x) and vertical (y) probe position.

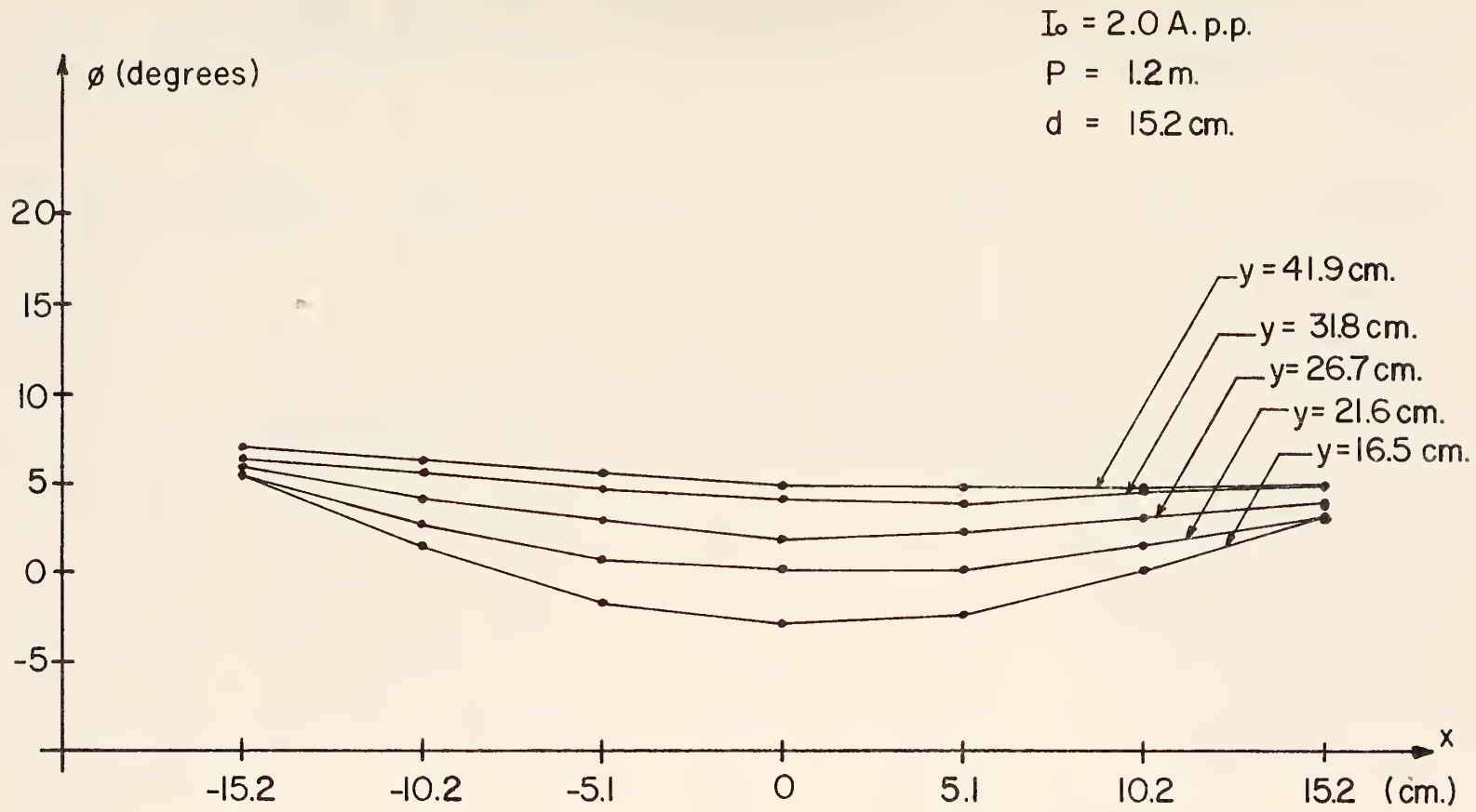

Fig. 44. Transverse phase characteristics of a medium width, triangular line as a function of the lateral (x) and vertical (y) probe position.

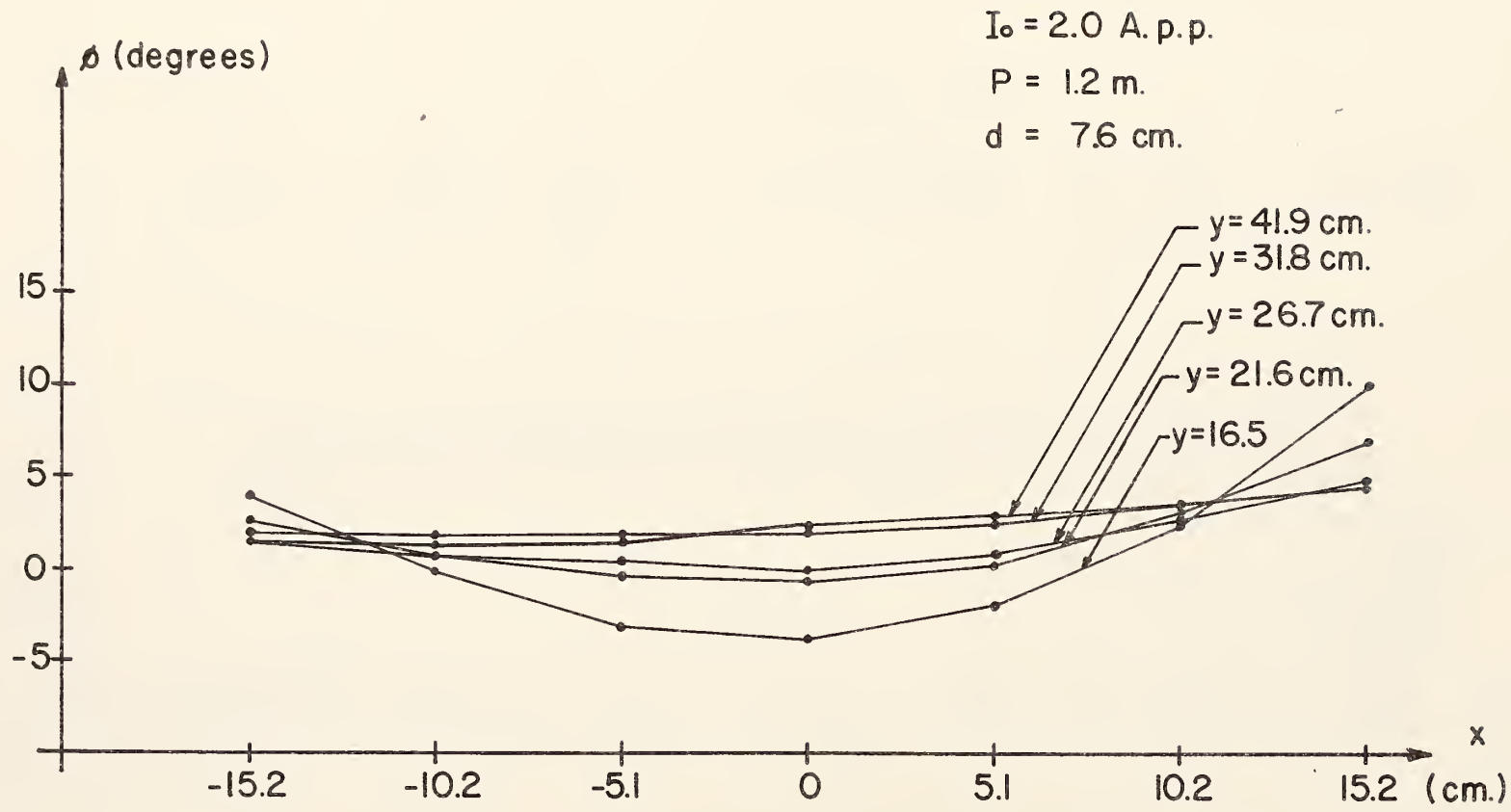

Fig. 45. Transverse phase characteristics of a relatively narrow, triangular line as a function of the lateral (x) and vertical (y) probe position.

TABLE 1

MAXIMUM PHASE ERROR FOR TRIANGULAR-SHAPED LINES OF VARIOUS WIDTHS

Line Width (cm)	Δx (cm)	y_{min} (cm)	y_{max} (cm)	$\Delta\phi$ (degrees)
22.9	$\pm$13.0	16.5	31.8	+1.0 -1.5
15.2	$\pm$13.0	16.5	41.9	$\pm$5.0
7.6	$\pm$13.0	16.5	41.9	+6.5 -4.0

c) The Spacing Between Lines

The results presented might be misleading since phase-errors are given for only one line pair. In a full-scale implementation, two line pairs would be used (since one is needed for the reference) and, from the experience gained with the helical lines, cross coupling between each line pair and the opposite probe could result. This would cause additional phase errors.

This cross coupling is a function of the spacing, s, between the two lines -- the wider the spacing the less the cross coupling. Thus, a series of tests using two 7.6 cm. wide line pairs were conducted with various spacings (s = 38.1, 60.9, and 76.2 cm.). These lines were chosen since it is desired to keep the width to a minimum. If 15.2 cm. or 22.9 cm. line pairs were used, even smaller phase errors would probably result.

First, the effect of the presence of a second line pair on the linearity of the phase characteristics was examined. The phase-difference, θ_d, versus z was measured for the three selected line

spacings, with the results shown in Figs. 46, 47, and 48. No appreciable increase in the non-linearity occurred due to the presence of the second line pair.

Next, the phase error resulting from lateral and vertical motion of the probes was measured for the same three line spacings. The results are shown in Figs. 49, 50, and 51, and the results are summarized in Table 2. For an allowed lateral deviation of $\Delta x = \pm 13.0$ cm., the largest error ($\Delta\theta_d$ = +11.0°, -2.5°) resulted for the smallest line spacing (s = 38.1 cm.). For the two larger spacings, the error was nearly the same ($\Delta\theta_d$ = +1.0°, -3.0°, and +1.5°, -4.5°) and was smaller than that for the smallest spacing. However, if Δx were limited to ± 10 cm. the resultant phase errors would decrease to much more acceptable values for all spacings. If Δx could not be reduced, then the lower phase errors could be achieved by using slightly wider lines. Again note the trade-off which exists between line spacing, line width, and the maximum allowed vehicle deviation and the maximum phase error. The latter two must be specified before the line width and spacing can be selected.

D. Summary

It appears that a system composed of two, flat transmission lines could be effectively used as an information source for an automated highway system. For given specifications on the maximum allowable vehicle deviations in the lateral and vertical directions, and the maximum allowable uncertainty in the longitudinal state

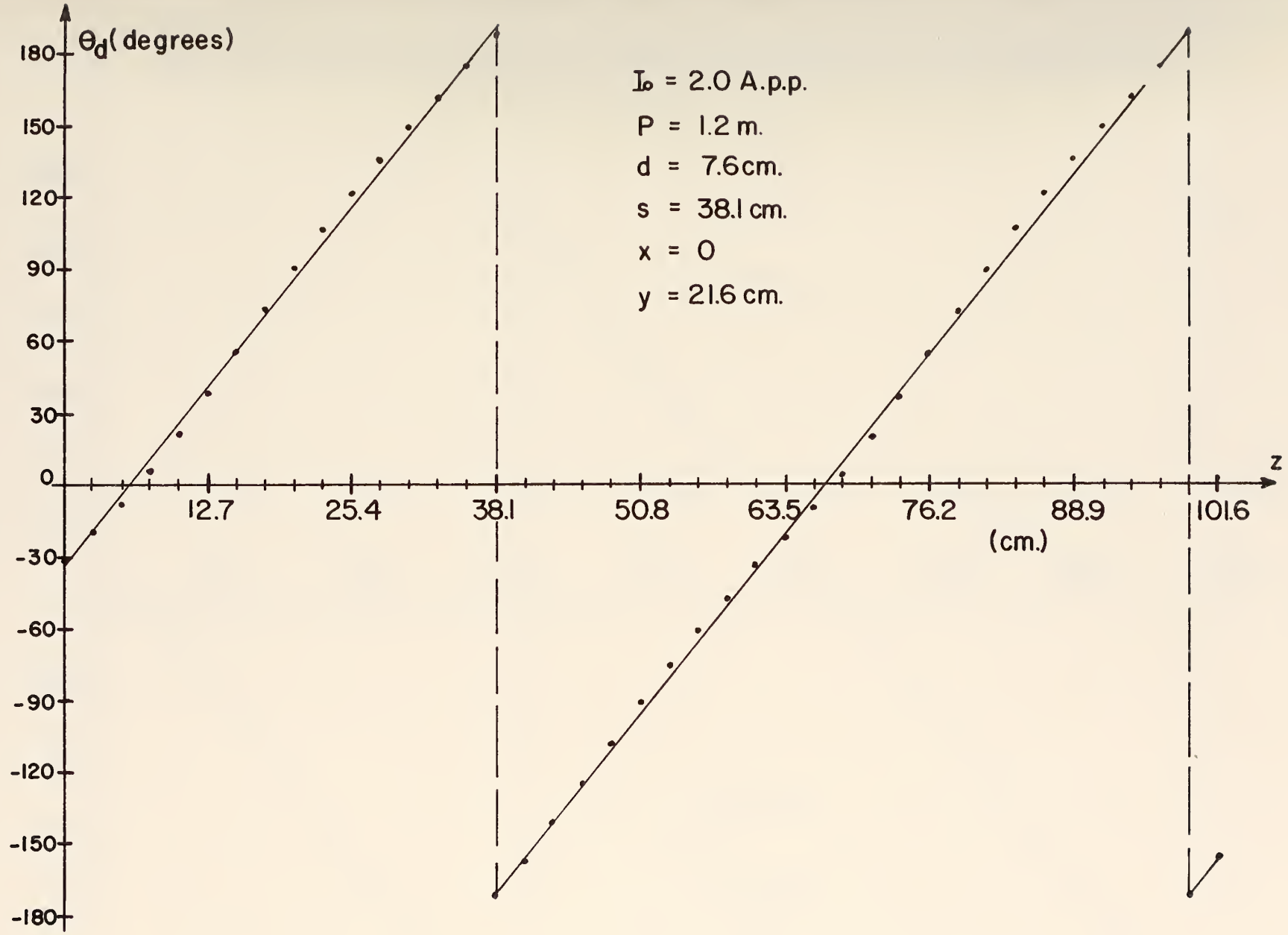

Fig. 46. Longitudinal phase characteristics of a pair of narrow triangular lines -- narrow-line spacing.

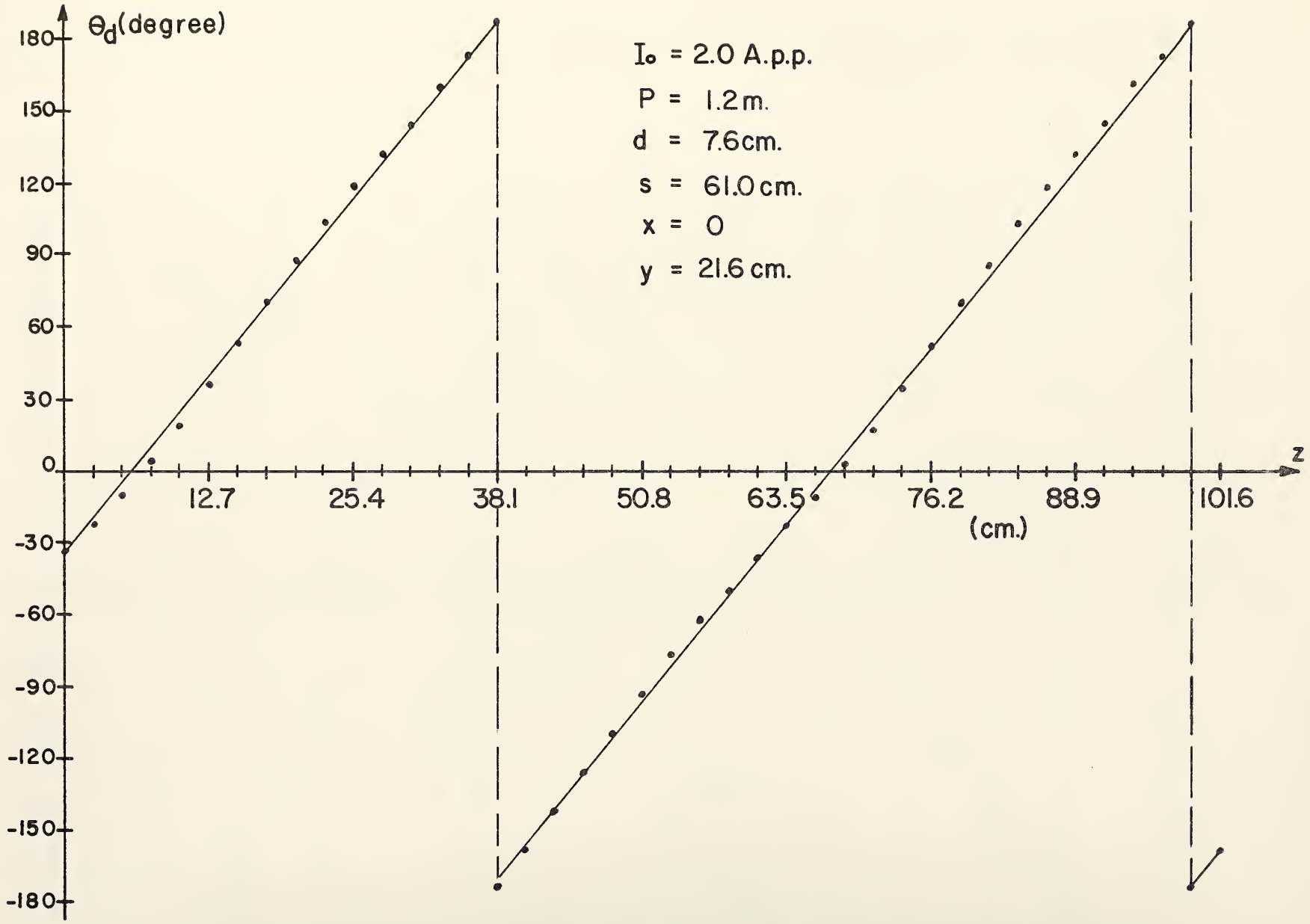

Fig. 47a. Longitudinal phase characteristics of a pair of narrow triangular lines (medium probe height -- medium line spacing).

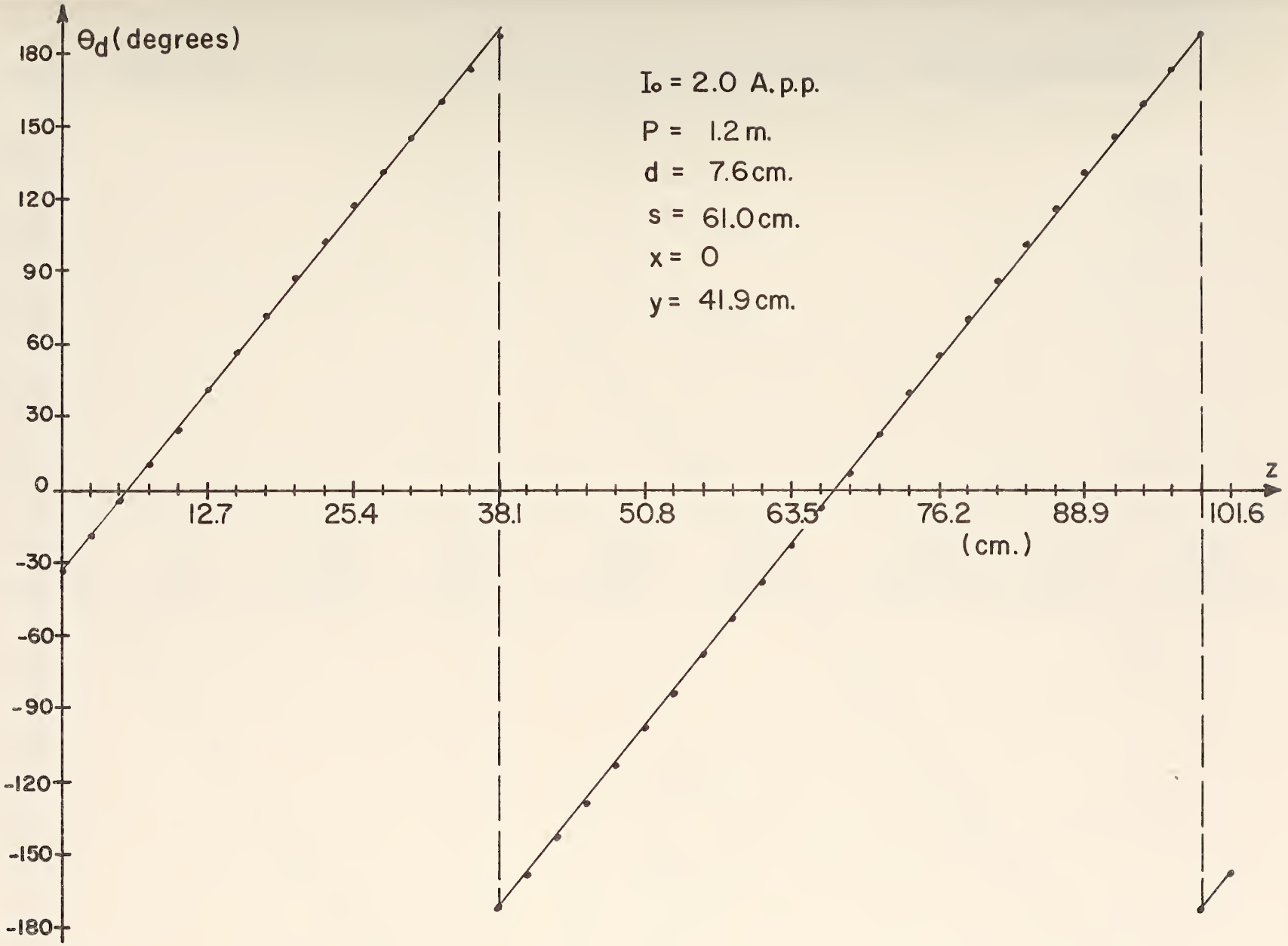

Fig. 47b. Longitudinal phase characteristics of a pair of narrow triangular lines (large probe height -- medium line spacing).

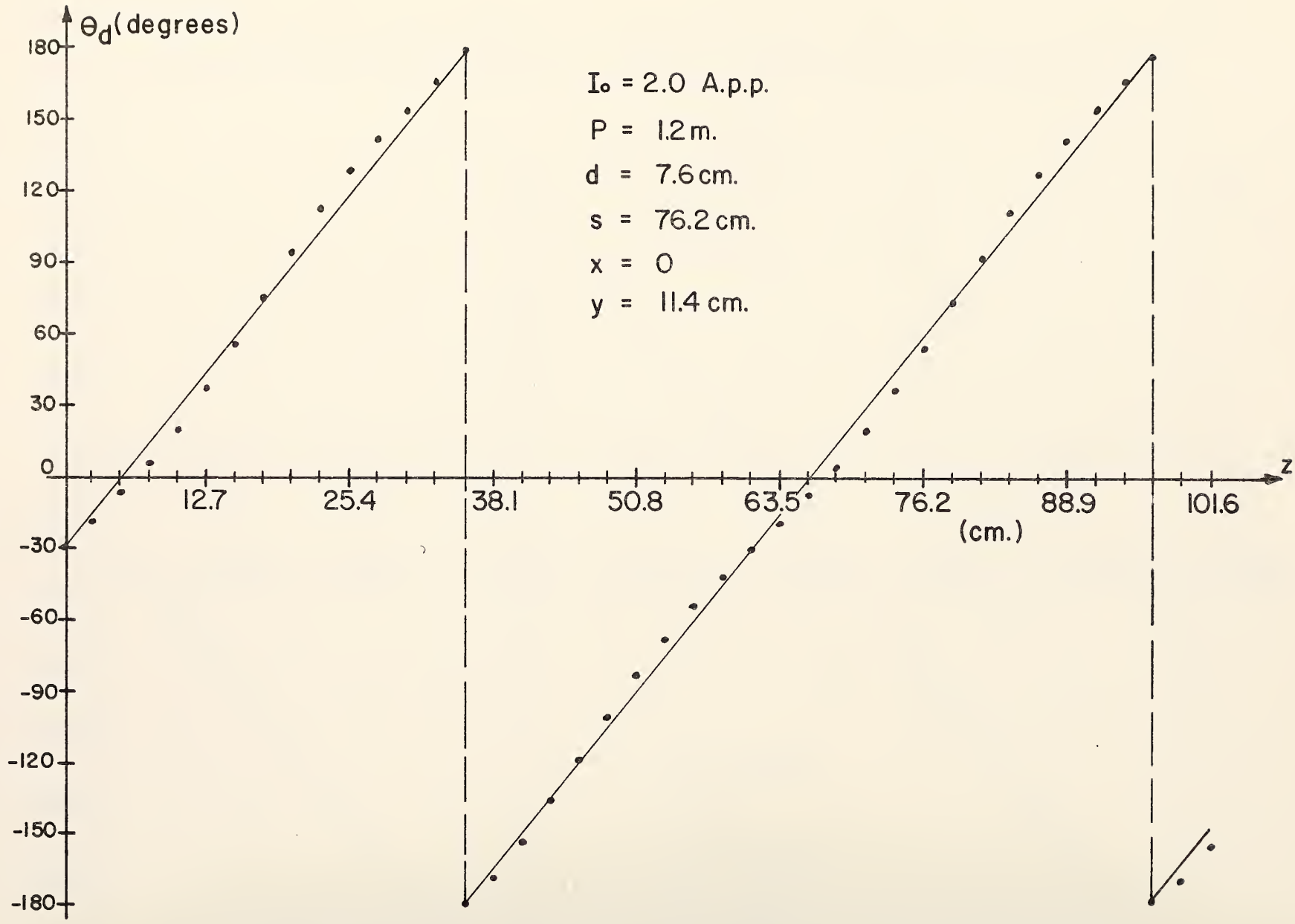

Fig. 48a. Longitudinal phase characteristics of a pair of narrow triangular lines (low probe height -- large line spacing).

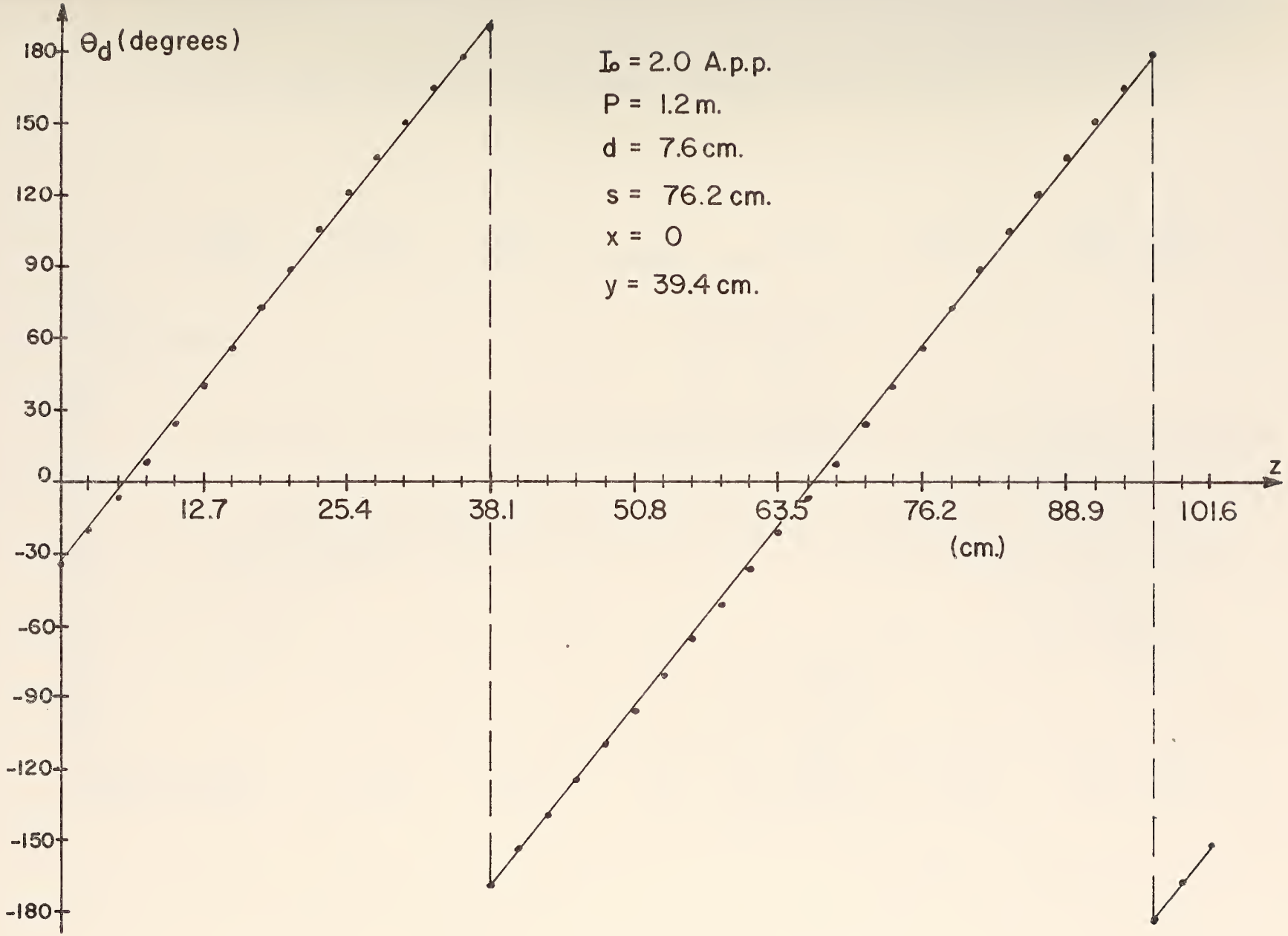

Fig. 48b. Longitudinal phase characteristics of a pair of narrow triangular lines (medium probe height -- large line spacing).

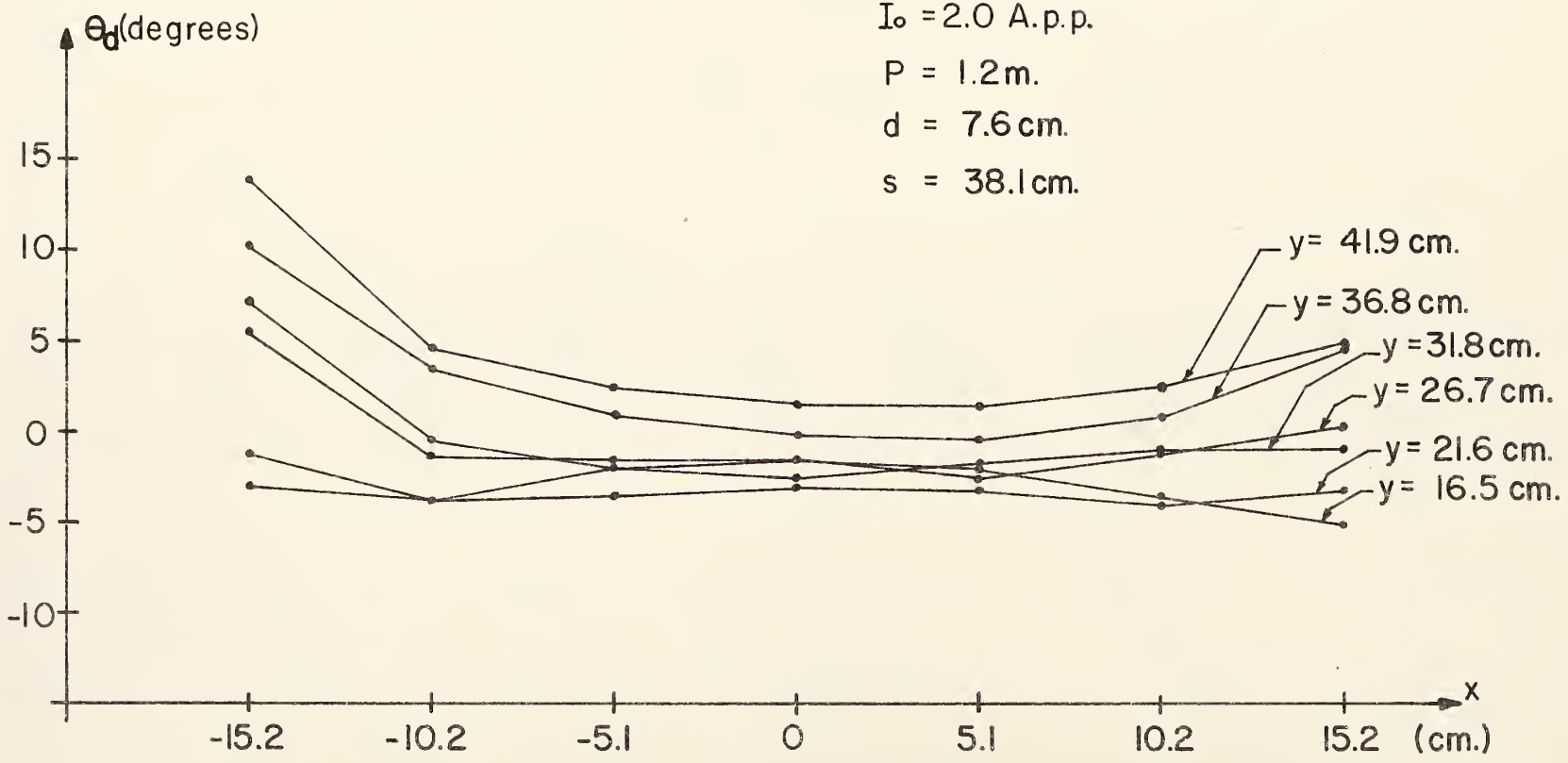

Fig. 49. Transverse phase characteristics of a pair of narrow triangular lines -- narrow spacing.

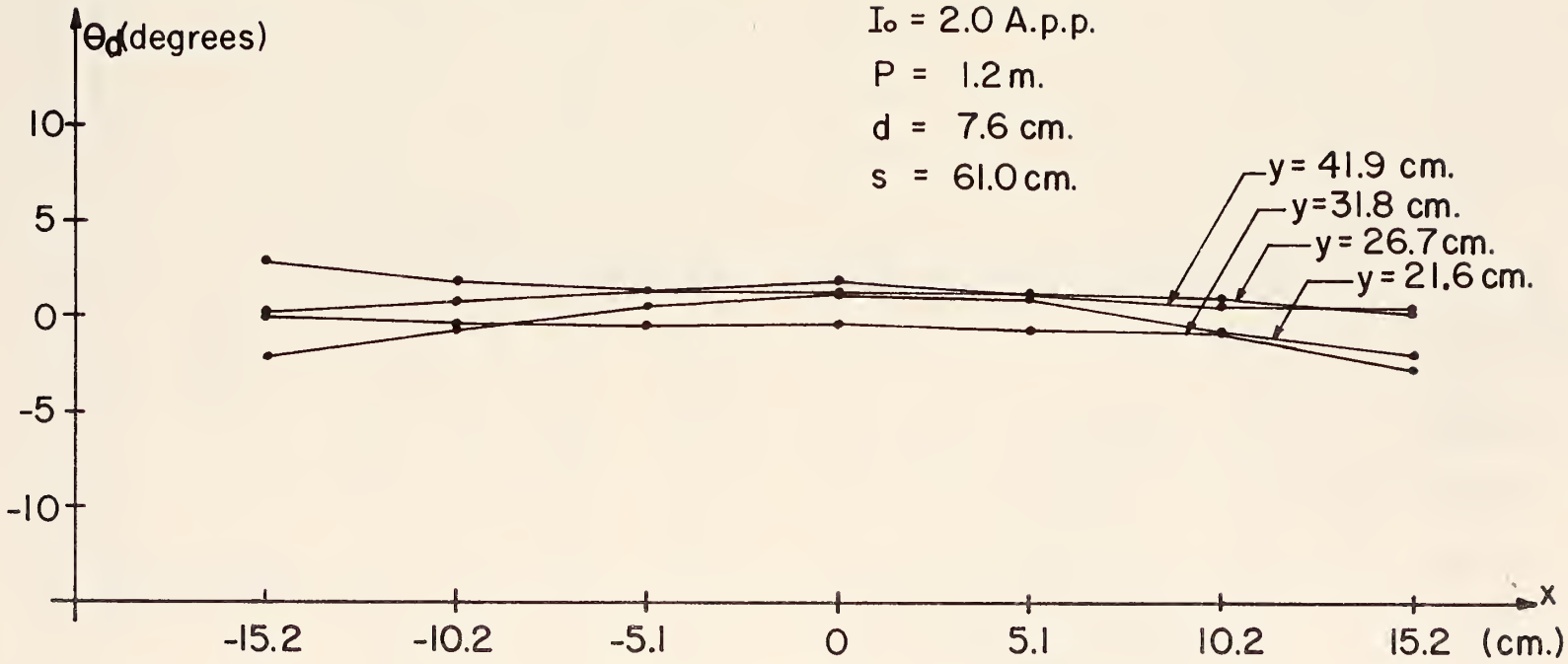

Fig. 50. Transverse phase characteristics of a pair of narrow triangular lines -- medium spacing.

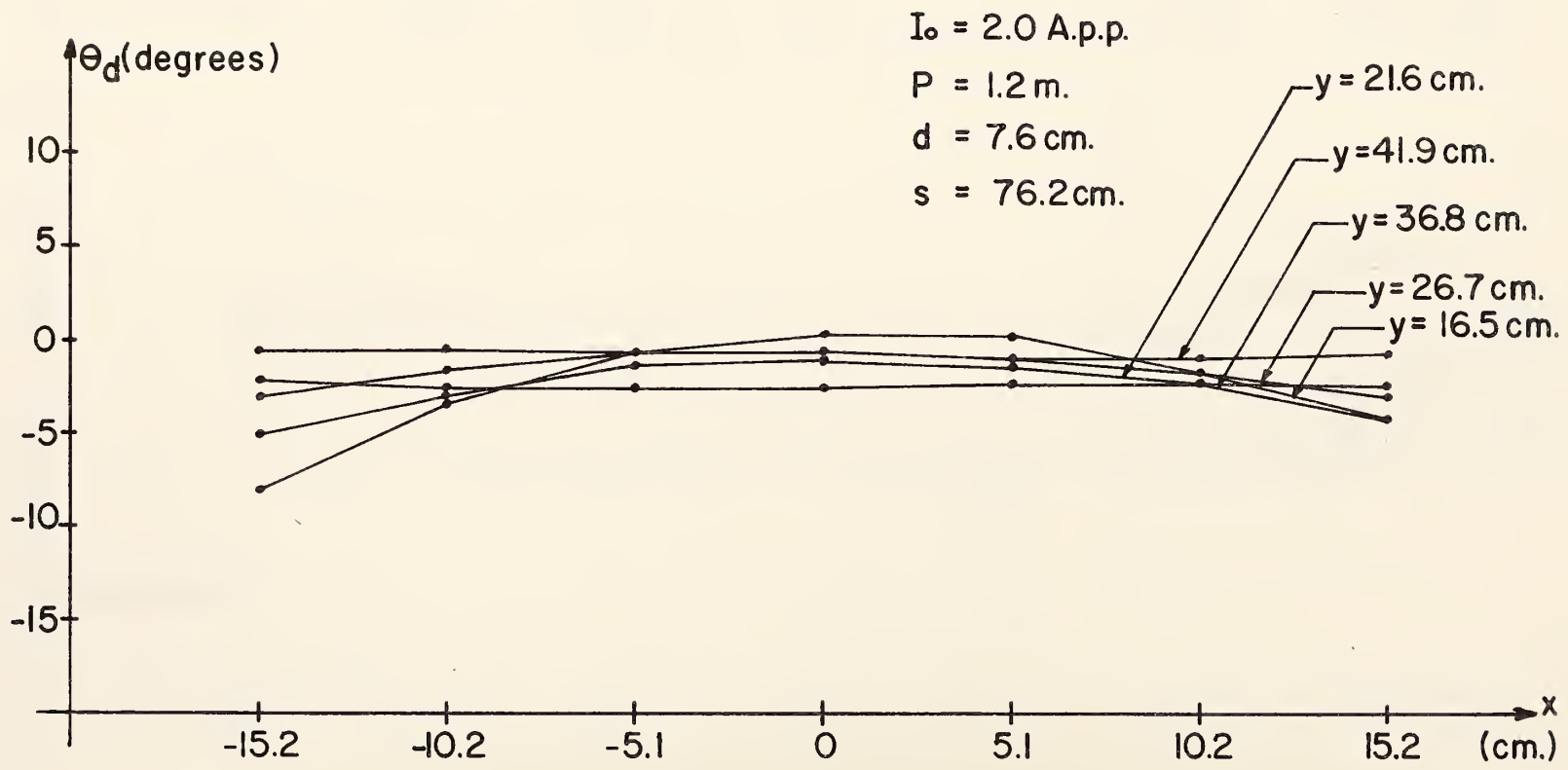

Fig. 51. Transverse phase characteristics of a pair of narrow triangular lines -- large spacing.

TABLE 2

MAXIMUM PHASE ERROR FOR A PAIR OF TWO-WIRE LINES OF VARIOUS SPACINGS

$d = 7.6$ cm. $\quad y_{min} = 16.5$ cm. $\quad y_{max} = 41.9$ cm.

Spacing (cm.)	Δx (cm.)	$\Delta\theta_d$ (degrees)
38.1	$\pm$13.0	+ 11.0 - 2.5
	$\pm$10.00	+ 5.0 - 2.0
61.0	$\pm$13.0	+ 1.0 - 3.0
	$\pm$10.0	+ 0.5 - 2.0
76.2	$\pm$13.0	+ 1.5 - 4.5
	$\pm$10.0	+ 1.5 - 2.0

information, the parameters of the transmission lines (P_e, d) and their spacing, s, can be chosen.

For example, suppose the maximum allowable position uncertainty were $\Delta z = \pm 0.33$ cm. and the vehicle could be constrained to $\Delta x = \pm 10$ cm. and between $y_{min} = 16.5$ cm. and $y_{max} = 41.9$ cm. The position uncertainty specification governs the relationship between $\Delta\theta_d$ and P_e. That is,

$$\Delta z = \frac{\Delta\theta_d}{360} P_e$$

Thus for $P_e = 60$ cm., $\Delta\theta_d = \pm 2°$, it can be inferred from the experimental data that a maximum phase error of $\pm 2°$ could be achieved with a line spacing of at least 60 cm. and a line width of approximately

8 cm. Other combinations of d and s might yield the same $\Delta\theta_d$. However, since the relationship between the three is only known empirically, further tests would have to be made for other combinations of d and s. In general, however, as d and s increase, $\Delta\theta_d$ should decrease. For implementation purposes, it is desirable to keep both d and s as small as possible.

The above tests were conducted both with and without reinforcing steel mesh present, and no great difference between the two cases was observed. From previous experience with guidance fields, as provided by a single wire for steering, no observed laboratory effects does not necessarily imply no full-scale effects. However, due to the "twisted-pair" geometry of the helical lines, it is expected that any full-scale effect (if present) would be less than that observed for the steering lines.

CHAPTER V

A HEADWAY SAFETY POLICY FOR AUTOMATED HIGHWAY OPERATIONS

A. Introduction

Four general approaches can be employed to obtain the high lane capacities necessary for viable automated highway operations:

a) Entrainment--individual vehicles would be mechanically coupled into long trains.

b) Platooning--vehicles would be formed into platoons with small distances (e.g., 1 m) between vehicles within the platoon and large distances (e.g., 100 m) between platoons.

c) Multi-vehicle pallets with individual pallets uniformly spaced (e.g., at 100 m intervals).

d) Individual vehicles uniformly spaced at relatively small distances (e.g., 30 m).

In each approach, the achievable capacities are closely related to system safety via a headway policy; e.g., a specification of the minimum permitted headway (as a function of speed) for mainline operations. In the entraining and platooning approaches, this would pertain to headways between groups of vehicles and, in the other two cases, to headways between individual vehicles.

There are three primary aspects to a headway policy.

a) The specification of those abnormal situations in which a collision can be avoided;

b) The specification of the probability of a collision occurring (i.e., the probability of abnormal situations beyond those included in (a)); and

c) The severity and "cost" of each collision.

In this chapter, the first of these is examined in the context of a dual-mode system for intercity application (i.e., an automated highway system) wherein uniformly spaced, individual vehicles would be employed. The second could be achieved if an appropriate system-level model were available. As its development would require a detailed knowledge of both system components and system operations, this task cannot be successfully completed at this time. The third aspect can be evaluated for various accident situations by employing a cost-function approach as is done in Appendix D.

In past studies (e.g., (28) to (32)), the emphasis was on the specification of a policy which would result in acceptably "safe" operations. One very safe policy is associated with the "brickwall" stopping criterion, wherein the minimum permitted distance between two vehicles, traveling in a single lane at mainline speed, is chosen so that if the lead vehicle were to instantly stop (e.g., hit an immovable brickwall), the following vehicle could be stopped without a collision occurring. The choice of this criterion would probably result in a very small number of vehicular collisions; however, the operational price is a small maximum lane capacity--some 1300 to 1500 vehicles/lane/hour for traffic moving at 26.8 m/s (60 mph). This criterion is more conservative than sometimes practiced by today's motorists; thus, its adoption could

result in a decline in capacity under high-density traffic conditions.

A non-brickwall criterion may be expressed in several ways; however, in all cases, the basic intent is to avert collisions due to "reasonable" lead-car decelerations. If, in practice, the lead vehicle were to exceed the deceleration specified in the policy, a collision could occur. Some of the reported efforts have been focused on the specification and/or evaluation of policies based on this intent.

One aspect that has been generally ignored is the interaction between the required capabilities of a vehicle's automatic control system (especially in the longitudinal mode) and the selected headway policy. Here, this interaction is included together with a detailed evaluation of a policy for achieving high capacity ($\geq$ 3,600 vehicles/lane/hour) over a range of typical highway speeds--13.5 to 30 m/s (30.2 to 67.2 mph). These conditions are those which are generally felt to be essential for successful operation of a dual-mode system intended for automated highway (inter-city) use.

B. Policy Development

Consider a platoon of identical vehicles moving along a single-lane guideway at a nominal speed of V_s. The control exercised could be either of the point-following type, where (except possibly in an emergency situation) the control applied to a vehicle is dependent on its state with respect to its absolute desired state (i.e., desired position and speed), or of the car-following type wherein the control applied is dependent on a vehicle's state with respect to the nearest lead vehicle.[1]

[1] More complex types of car following, wherein the control applied to a vehicle is dependent on that vehicle's relative state to is $n(n \geq 1)$ nearest forward neighbors and its $m(m > 0)$ nearest backward neighbors, can be formulated. However, the benefits to be gained appear somewhat marginal when compared to the added complexity associated with this approach.

Here, equations will be developed for the former, and modified for applicability to the latter.

a) Point-Following Control

A worst-case situation is defined as one wherein the lead vehicle when it is in a worst-permissible normal state, suddenly decelerates at a rate of A_l m/s^2. After a communiation delay of no more than t_c sec., a computer at wayside is notified of the change in this vehicle's state; subsequently, after a second delay t_p due to computer processing and retransmission time, the following vehicles are commanded to brake. The greatest likelihood of a collision is between the lead and second vehicles, and thus only their behavior is considered further.

The initial state of the lead vehicle is such that it crosses three emergency-initiating threshold simultaneously:

i) A deceleration threshold, $A_T < A_l$;

ii) A velocity-deviation threshold $(-\Delta V_T)$; and

iii) A position-deviation threshold $(-\Delta X_T)$.[2]

The stopping distance for this vehicle is easily derived as

$$S_l = \frac{(V_s - \Delta V_T)^2}{2A_l} \qquad (5\text{-}1)$$

If the state deviations of the following vehicle is specified as $(+\Delta X_T, +\Delta V_T)$ at $t = 0$, then the initial separation $d(0)$ between it and the lead vehicle is

$$d(0) = V_s H_t - 2\Delta X_T - L \qquad (5\text{-}2)$$

---

[2] A crossing of any one of these thresholds would result in emergency operation being initiated by the sector computer. It is unlikely that a vehicle would cross all three simultaneously; thus, the development here is slightly conservative.

where L = vehicle length and H_t is the desired minimum headway in seconds.

The following vehicle receives a deceleration command at t = $t_c + t_p$, and subsequently decelerates at a rate A_2 m/s^2 as is shown in Fig. 52. Note the presence of a braking reaction delay (τ), a finite jerk rate (J_m), and the selected deceleration A_2.

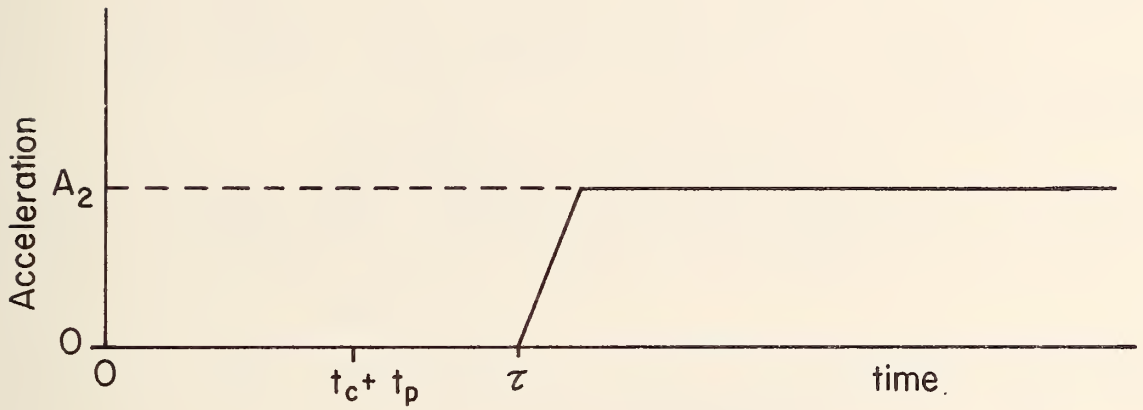

Fig. 52. Deceleration trajectory of the following vehicle.

A slightly conservative bound on the distance (S_2) traveled from t = 0 until this vehicle stops is

$$S_2 = (V_s + \Delta V_T)(t_c + t_p + \tau + \frac{A_2}{J_m}) - \frac{1}{6}\frac{A_2^3}{J_m^2}$$

$$+ \frac{(V_s + \Delta V_T - \frac{1}{2}\frac{A_2^2}{J_m})^2}{2A_2} \qquad (5\text{-}3)$$

To prevent a collision between the lead and second vehicles, it is necessary that

$$d(0) \geq S_2 - S_1. \tag{5-4}$$

Upon substituting Eqs. (5-1) to (5-3) into (5-4) and rearranging, there results

$$V_s H_t \geq L + 2\Delta X_T + (V_s + \Delta V_T)(t_c + t_p + \tau + \frac{A_2}{J_m}) - \frac{1}{6}\frac{A_2^3}{J_m^2} + \frac{(V_s + \Delta V_t - \frac{1}{2}\frac{A_2^2}{J_m})^2}{2A_2} - \frac{(V_s - \Delta V_T)^2}{2A_1}. \tag{5-5}$$

b) Car-Following Control

In this type of control, emergency operations would be initiated by the detection of an abnormal condition (e.g., an excessive relative velocity) between two successive vehicles separated by a sufficiently small distance. Let the failed vehicle be the platoon leader, and assume that it and the nearest following vehicle are in the worst-permissible relative state when the former is commanded to decelerate at t = 0. Then Eq. (5-5) may be employed provided $t_c + t_p$ is replaced by T_s where the latter is the time from t = 0 until the following vehicle is commanded to decelerate. The condition for no collision is then

$$V_s H_t \geq L + 2\Delta X_T + (V_s + \Delta V_T)(T_s + \tau + \frac{A_2}{J_m}) - \frac{1}{6}\frac{A_2^3}{J_m^2}$$

$$+ \frac{(V_s + \Delta V_T - \frac{1}{2}\frac{A_2^2}{J_m})^2}{2A_2} - \frac{(V_s - \Delta V_T)^2}{2A_1} \qquad (5\text{-}6)$$

The magnitude of T_s is dependent on the mechanism by which emergency operations are initiated in the following vehicle. This could be done in at least three ways:

i) The detection of a beyond-threshold relative velocity between it and the failed vehicle;

ii) The reception of an emergency transmission from this vehicle; or

iii) The reception of an "indirect" emergency transmission (e.g., from a wayside computer).

Note from Eq. (5-5) or (5-6) that H_t is dependent on V_s; thus, the maximum capacity C, which is given by

$$C = \frac{3600}{H_t} \text{ (veh/lane/hr)} \qquad (5\text{-}7)$$

is also dependent on V_s. It is important to note that the capacities obtained from this equation would only be achievable on a long, linear (or nearly so) section of highway on which there were no complex traffic interaction points (e.g., intersections). When traffic streams interact, the maximum achievable capacity would be less than that predicted by Eq. (5-7) (e.g., see the study by Rule (33).

C. Analysis

a) Parameter Ranges

There are seven quantities in Eqs. (5-5) and (5-6) which affect the minimum permissible headway.[3] The expected value or range of values for each of these can be readily specified considering such factors as the expected characteristics of future vehicles, the accuracy with which various state variables can be measured, and assumed achievable values of vehicle decelerations and deceleration rates.

In view of the trend toward smaller, fuel-efficient vehicles, and the possibility that automated highways may be electrified (and relatively small electric vehicles employed thereon), L was selected as 3.67 m (12 ft.). H_t, and therefore C, is relatively insensitive to $J_m > 30.5$ m/s^3, and J_m was selected as 76.2 m/s^3 under the suppositions that this rate would be readily achievable in future vehicles and all vehicle occupants would be belt/harness constrained in their seats.

The quantity ΔX_t is comprised of two components--one associated with the accuracy with which a vehicle's position could be measured and a second with vehicle-position deviations under various maneuvering and disturbance conditions. In practice, $\Delta X_t \leq .3048$ m ($\leq$ 1 ft.) appears to be achievable (34) and thus ΔX_t was conserva-

---

[3] In Eq. (5-5), $(t_c + t_p + \tau)$ is considered as a single delay term T as is $(T_s + \tau)$ in Eq. (5-6).

tively selected as 0.3048 m. (In the next section, it is demonstrated that C is relatively insensitive to changes in L, J_m, and ΔX_T, thus providing further justification for fixing these quantities.)

The quantity ΔV_T is the sum of

i) ΔV_m, the accuracy to which instantaneous velocity can be measured; and

ii) ΔV_c, the maximum deviation in instantaneous velocity expected under normal operating conditions.

At present, the most accurate reported technique for obtaining ΔV_m has an accuracy of some ±0.1524 m/s (0.5 f/s) (18). The measurement involved includes a measurement time of some 0.05 - 0.1s, and thus an effective delay is present. For a good vehicle controller,

$$\left|\Delta V_c\ (t)\right| < 0.1524 \text{ m/s} \qquad (5\text{-}8)$$

should be achievable; thus, a "present" lower limit on ΔV_T would be 0.3048 m/s. A reasonable range for evaluation would be 0 - 0.762 m/s.

Various industrial concerns have reported that a lower limit on τ is some 0.100s; thus, this value was taken as a lower limit on the total delay time. The upper limit was selected as 0.6s as larger values would make the required capacity exceedingly difficult to obtain for any realistic choices of the other parameters.

The range of possible lead vehicle decelerations is from 0 to ∞ m/s^2; however, if that vehicle were not involved in a front-end collision (e.g., as with a bridge abutment), a reasonable range

to consider would be 3.92 - 7.85 m/s^2 (0.4 to 0.8 g). The highest value corresponds to vehicle braking at maximum efficiency on high-traction, dry concrete.[4] The range of following-vehicle decelerations was selected to be the same as for the lead vehicle.

The parameter choices and ranges specified here are summarized in Table 3.

b) Sensitivity Analysis

The effect of each parameter in Eqs. (5-5) and (5-6) was established via a sensitivity analysis. The change (ΔH_t) in H_t, for changes in a given parameter were obtained, and the resulting change in maximum capacity was computed via

$$C = \frac{3600}{H_t + \Delta H_t} - \frac{3600}{H_t} \qquad (5\text{-}9)$$

Typical results, which were obtained for one expected operating condition, are presented in Table 4, together with the definition of that condition.

First note that C is relatively insensitive to changes in L, J_m, and ΔX_t unless, of course, these changes are large; e.g., an increase of 6 ft. in vehicle length. Next, note that C is quite sensitive to even modest changes in T, ΔV_T, A_1, and A_2. As these observations are also valid for evaluations at other expected

[4] It could also correspond to a variety of abnormal situations, e.g., a vehicle being braked via a dragging axle.

TABLE 3

SELECTED RANGES OF PARAMETER VALUES

Symbol	Definition	Range	Comments
V_s	Stream speed	0 to 30.4 m/s	Range of expected operations.
L	Vehicle length	3.67 m	Assumed length for a future, fuel-efficient vehicle.
T	Total reaction delay	0.1 to 0.6s	
J_m	Maximum jerk	76.2 m/s^3	Jerk limit of vehicle for constrained, seated occupants.
A_1	Lead-car deceleration	3.92 to 7.85 m/s^2 (0.4 to 0.8 g)	
A_2	Following-car deceleration	3.92 to 7.85 m/s^2 (0.4 to 0.8 g)	
ΔV_T	Maximum permitted velocity deviation	0 to 0.762 m/s (0 to 2.5 f/s)	Due to controller dynamics, disturbances (e.g., wind forces) and measurement errors.
ΔX_T	Maximum permitted position deviation	$\leq$ 0.3048 m (1 ft.)	Due to controller dynamics, disturbances (e.g., wind forces) and measurement errors.

TABLE 4

RESULTS OF SENSITIVITY ANALYSIS

Sensitivity Parameter	Value	Typical Variation	ΔH_t	ΔC
$\frac{\delta H_t}{\delta L}$	0.011	±0.3048 m	0.011	±40
$\frac{\delta H_t}{\delta T}$	1.011	±0.1s	0.1011	±330
$\frac{\delta H_t}{\delta \Delta V_T}$	0.093	±0.3048 m/s	0.093	±307
$\frac{\delta H_t}{\delta \Delta X_T}$	0.022	±0.1524 m	0.011	±39
$\frac{\delta H_t}{\delta J_m}$	-0.0003	±15.2 m/s^3	-0.0152	∓54
$\frac{\delta H_t}{\delta A_1}$	0.0663	±0.981 m/s^2	0.2135	±633
$\frac{\delta H_t}{\delta A_2}$	-0.1213	±0.981 m/s^2	-0.3906	∓1011

Evaluation Conditions

V_s = 27.4 m/s
T = 0.20s
H_t = 1.0s

A_1 = 7.85 m/s^2 (0.8 g)
A_2 = 5.89 m/s^2 (0.6 g)
J_m = 76.2 m/s^3

ΔV_T = 0.3048 m/s
ΔX_T = 0.3048 m
L = 3.67 m

operating conditions, the first three quantities were fixed, per the previous discussion, and C was evaluated as a function of the other four.

The marked influence of T is shown in Fig.53 where C vs. V_s is presented with T as a parameter (here, A_1 = 0.8 g, A_2 = 0.6 g, and ΔV_T = .3048 m/s). Note that a peak capacity of some 3850 veh/lane/hr was obtained for T = 0.2s, whereas this capacity decreased to 2675 veh/lane/hr for T = 0.6s. This same relationship is also obtained for other typical parameter combinations; therefore, as other investigators have stated, T must be reduced to as small a value as is practical--probably some .3 to .4s.

The effect of ΔV_T on capacity is shown in Fig.54, where C vs. V_s is presented with ΔV_T as a parameter with A_1 = 0.8 g, A_2 = 0.6 g, and T = .3s. Clearly, ΔV_T must be small, and given both the accuracy with which ΔV_m can be obtained and expected controller performance, a practical choice would be in the range

$$0.3048 < \Delta V_T < 0.6096 \text{ m/s} . \qquad (5\text{-}10)$$

The effects of varying A_2 with A_1 fixed (A_1 = 0.8 g) are shown in Fig. 55. Clearly, if A_2 is markedly smaller than A_1, the desired capacity is not safely achievable. Other similar plots, for different values of A_1, resulted in the same finding. A typical result for A_2 fixed (0.6 g) and A_1 variable is shown in Fig.56. For A_1 markedly larger than A_2 (e.g., 0.8 g vs. 0.6 g), the desired minimum capacity is not achieved at any speed; however, as A_1 approaches A_2, substantial increases in capacity are obtained. If

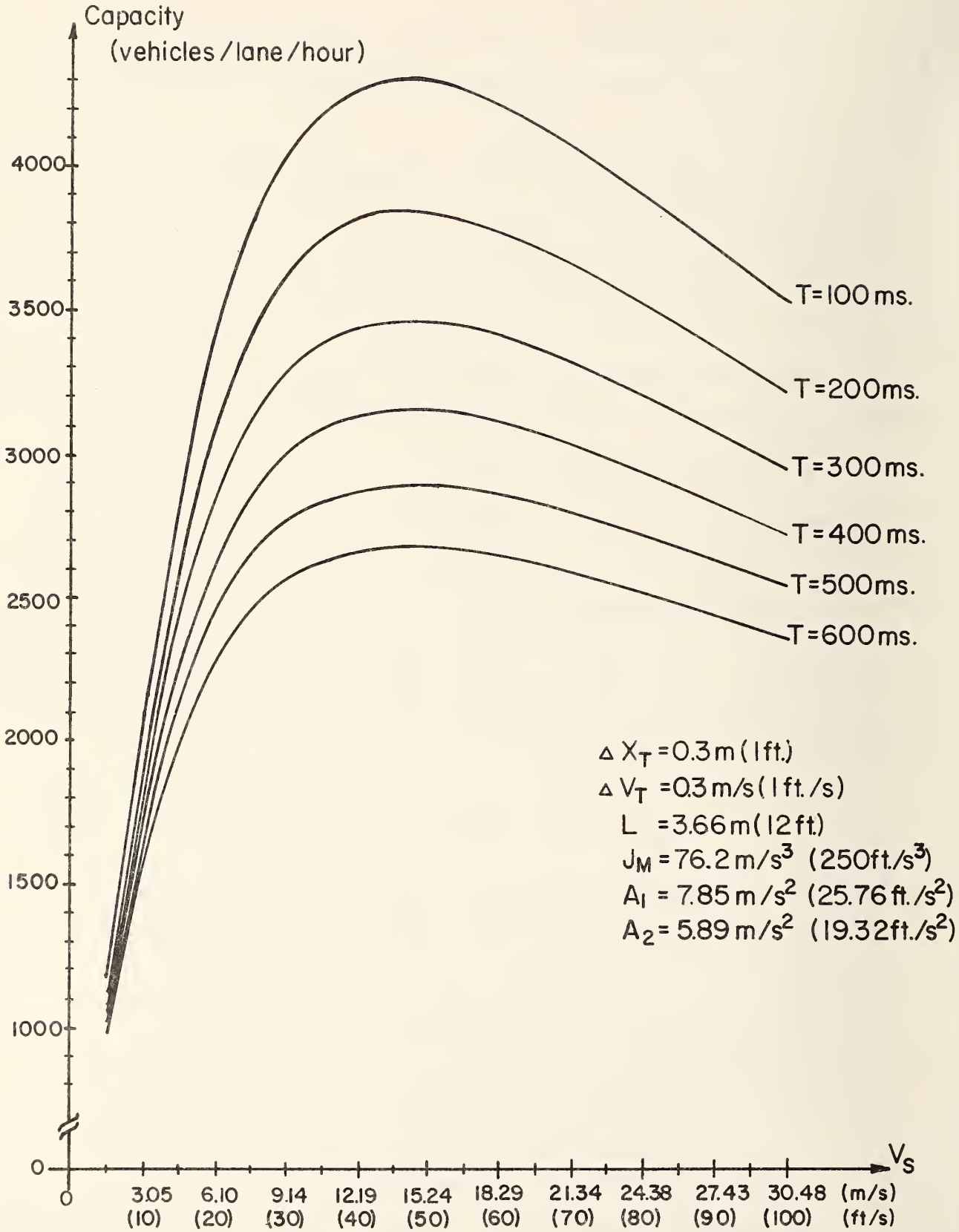

Fig. 53. Maximum capacity versus speed with T as a parameter.

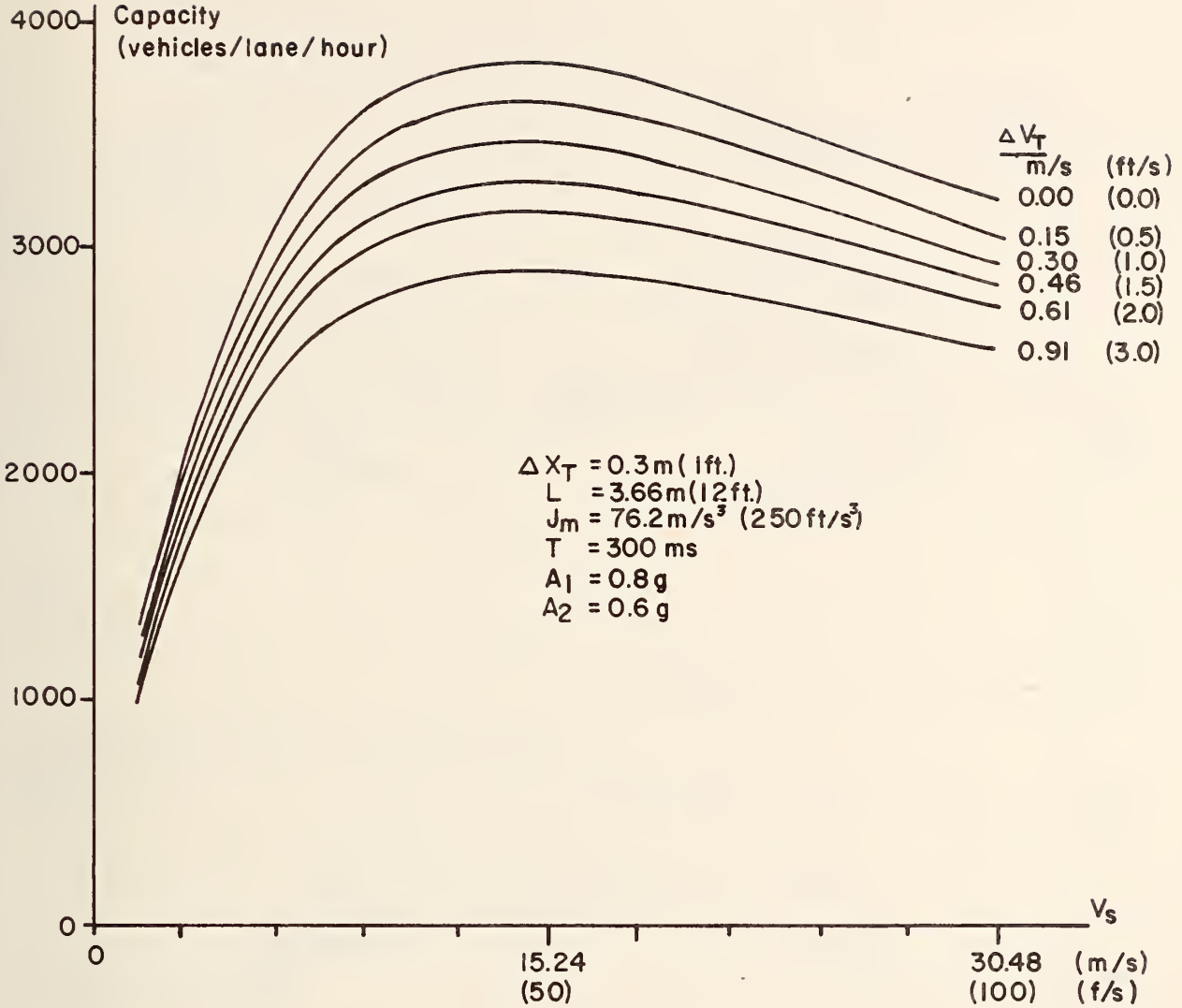

Fig. 54 Maximum capacity versus speed with ΔV_T as a parameter

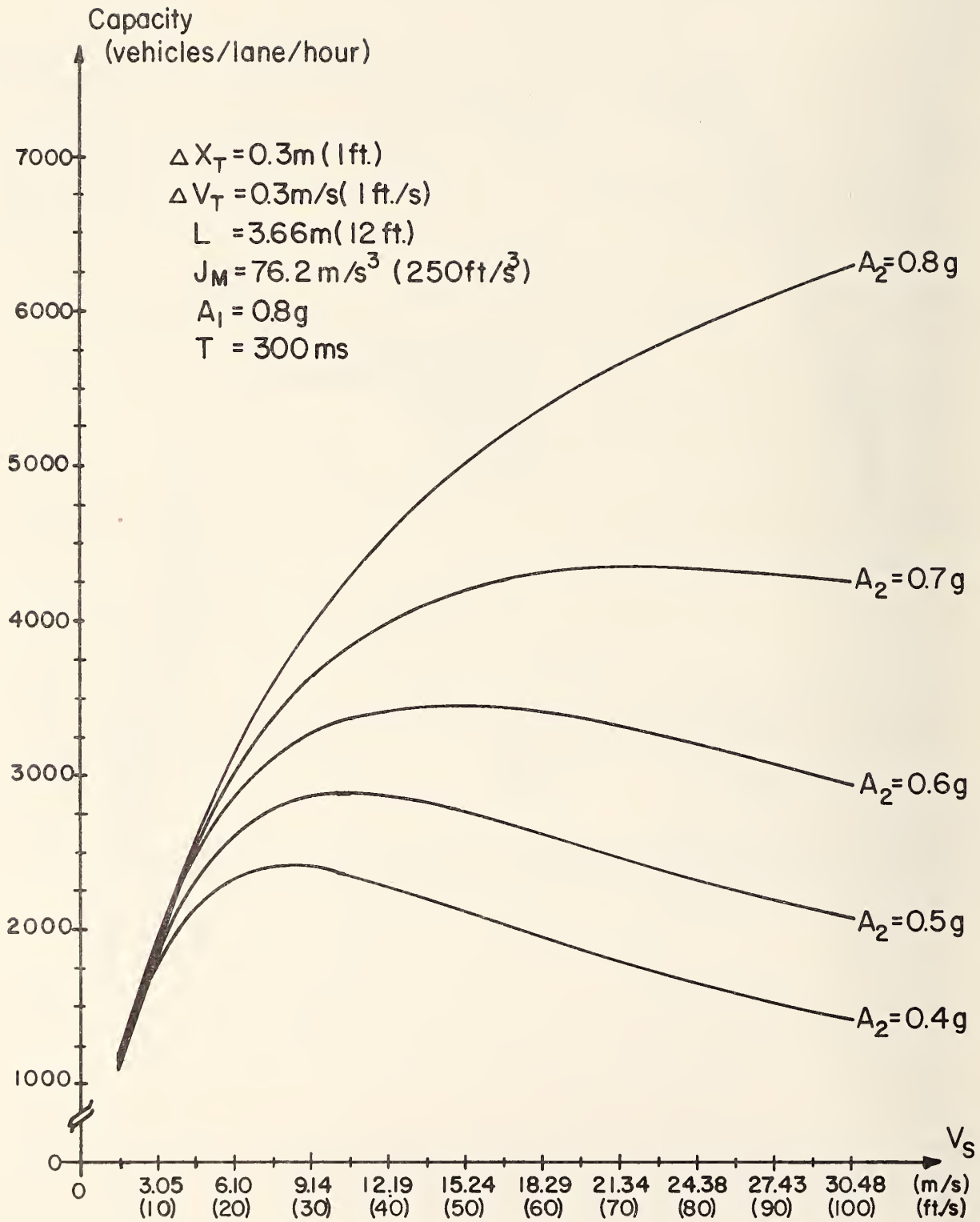

Fig. 55 Maximum capacity versus speed with A_1 fixed and A_2 variable

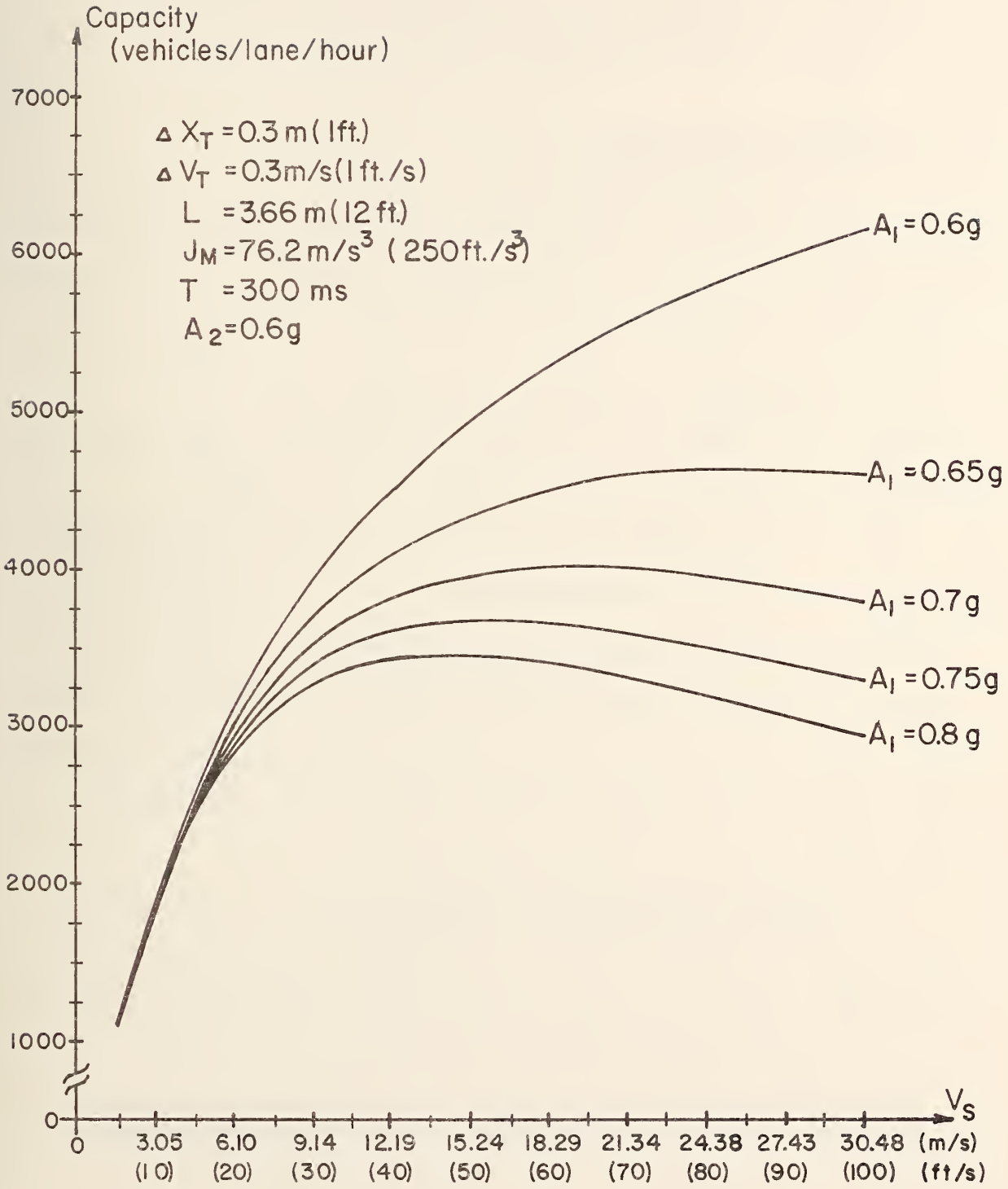

Fig. 56 Maximum capacity versus speed with A_2 fixed and A_1 variable

$A_1 = A_2$, a capacity in excess of some 3600 veh/lane/hr is achieved for all speeds above 7.6 m/s. This same trend was present in other parameter sets; thus, $A_1 - A_2$ is more critical quantity than either of the accelerations considered individually.

D. Parameter Specification

A set of parameters selected for an operational system must satisfy Eq. (5-5) (or (5-6)) over the speed range of interest of A_1 being selected as large as is consistent with this restriction. If, of course, lead-car deceleration were to exceed A_1 (i.e., $a_1(t) > A_1$), then the policy condition (Eq. (5-5)) would be violated and collisions could result. The larger the choice of A_1, the less likely this will happen.

Three general approaches toward selecting parameters may be employed. The first is to choose minimal values for ΔV_T and T on the basis of what could be achieved via ongoing or planned development efforts,[5] to choose a reasonable lower limit for A_2 (which would rarely be violated), and then select A_1 so that Eq. (5-5) is satisfied over the speed range of interest (equivalently, the capacity-versus-speed relationship must be satisfied over this range).

This approach was employed in selecting the first five parameter sets listed in Table 5. The first of these (see Fig. 57) corresponds to a small choice for T, a choice for A_2 small enough to be realized

---

[5] One reason for desiring a larger ΔV_T is to reduce the probability of a "false alarm" (i.e., an emergency indication when no emergency exists).

TABLE 5

EIGHT SELECTED PARAMETER SETS

Set	ΔV_T (m/s)	T (s)	A_1 (g)	A_2 (g)
1	0.3048	0.30	0.44	0.40
2	0.3048	0.30	0.60	0.50
3	0.3048	0.40	0.69	0.60
4	0.3048	0.30	0.72	0.60
5	0.1624	0.30	0.74	0.60
6	0.3048	0.525	0.70	($\geq A_1$)
7	0.3048	0.50	0.50	0.50
8	0.4672	0.43	0.40	0.40

Common Parameters

$L = 3.67$ m $\qquad J = 76.2$ m/s^3

$\Delta X_T = 0.3048$ m

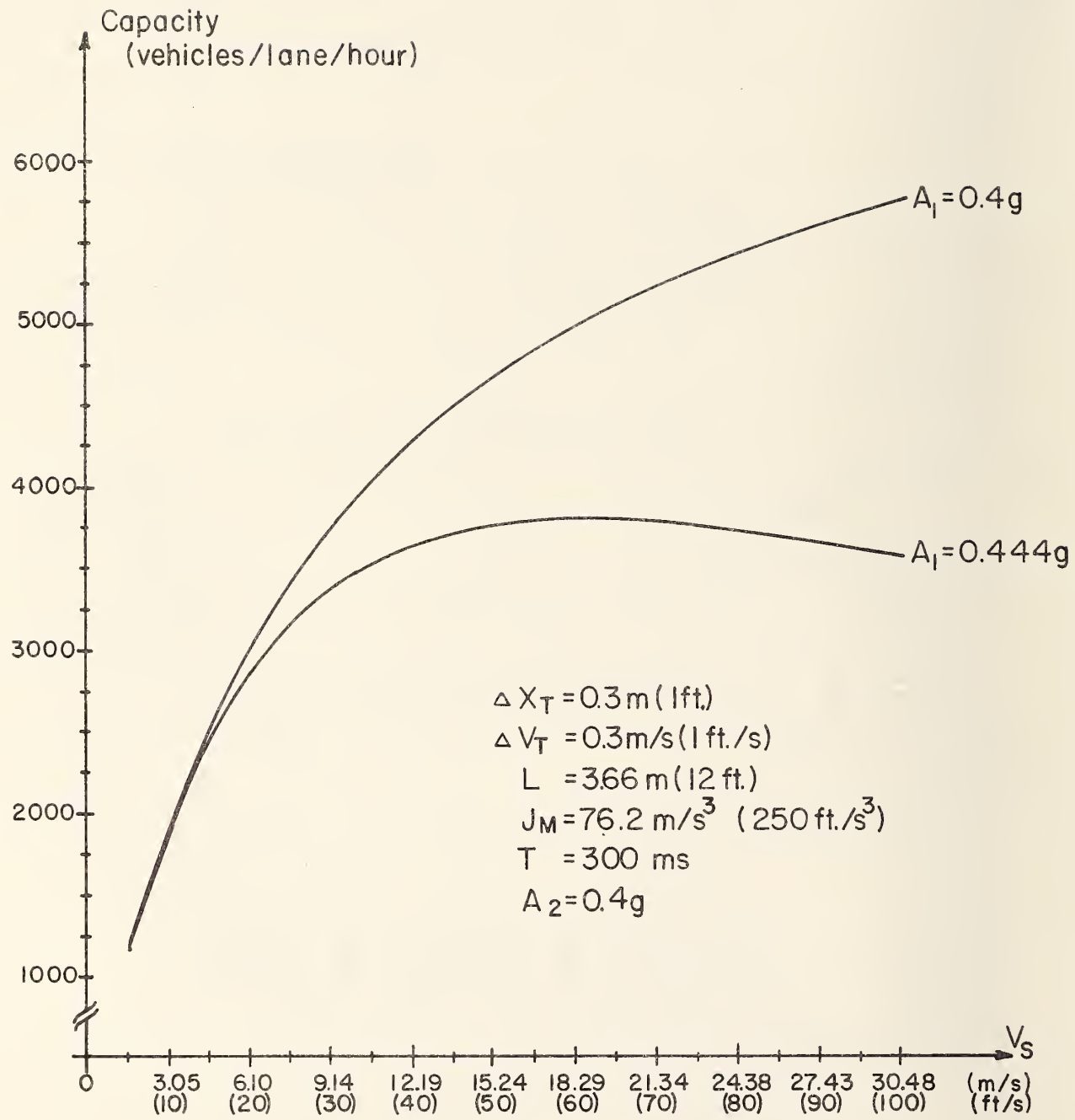

Fig.57 Maximum capacity versus speed for small choices of A_1.

in virtually all emergency braking situations, and the relatively low value of A_1 = 0.444 g. This would probably result in the largest number of accidents for the sets listed, as there would be more possibilities for a failing vehicle's deceleration to exceed this policy choice than it would for the larger A_1's associated with the other sets. The second set includes the same small reaction time of 0.3s, a larger value for A_2 (the specified value of 0.5 g could be achieved in practice with a high probability), and a larger value for A_1. If one could guarantee that following-vehicle decelerations would not be less than A_2 = 0.5 g, this would be a "safer" group than the first one.

The third through the fifth groups also involve small reaction times, $\Delta V_T \leq 0.3048$ m/s, and a somewhat more optimistic choice for A_2 than in the first two sets. Note that A_1 is progressively larger, and thus there would be a diminishing probability for $a_1(t) > A_1$. The result would probably be a fewer number of accidents--if the following vehicles could achieve the specified choice of A_2.

The second approach is to select $A_1 - A_2$ small (or $A_2 - A_1 \geq 0$) with A_1 chosen to be a large value. This is a very attractive theoretical choice, in regard to capacity, as may be noted from Figs. 55 and 56. In addition, this would be a relatively safe choice as, in practice, $a_1(t)$ would rarely exceed the large policy choice for A_1, and the number of rear-end collisions would be relatively small. The principal difficulty here is assuring, with a high degree of probability, that following-vehicle deceleration ($a_2(t)$) will be sufficiently large (i.e., $a_2(t) = A_1$). At present, the best means of accomplishing this appears to be via augmented braking which is reportedly under development

at the General Motors Corporation.

This approach is illustrated by Group 6 in Table 5. The parameter choices shown result in a substantial capacity, well in excess of 3600 veh/lane/hr over a wide speed range. In addition, the requirements on T and ΔV_T need not be as stringent as in the first approach.

The third approach involves selecting $A_1 - A_2$ small with A_1 as a moderate value (e.g., 0.4 - 0.6 g). This approach could only be effective if vehicle decelerations were properly limited, even in highly abnormal situations, by both proper vehicle and roadway/roadside design. The last two groups in Table 5 correspond to this case. Here again, the requirements on T and ΔV_T are not as stringent, and the required capacity would be achieved over a wide speed range.

In selecting the parameter groups of Table 5, it was assumed that braking would occur on dry pavement. On very wet pavement, the achievable braking rates would obviously be less (e.g., A_2 = 0.4 g could be a reasonable choice). However, lead-vehicle decelerations would also be less. The first parameter group of Table 5, and a capacity-versus-speed curve in Fig. 57, could apply to this case. Again, if $a_1(t) > 0.444$ g (the selected A_1), then rear-end collisions could occur.

E. Summary and Discussion

Some conditions under which a high-capacity, automated highway system can safely operate have been specified. This has been in the context of a uniform-spacing headway policy where the intent is to avert

collisions in the presence of "reasonable" lead-car decelerations.

Seven parameters are associated with this policy, with four of these (A_1, A_2, T, and ΔV_T) being especially critical quantities. Therefore, in the primary analysis (which pertained to both the point-following and the car-following modes of operation), only these four were considered in detail.

Three approaches to parameter selection were specified with each involving design tradeoffs and/or extensive future work on vehicle subsystems and sensor development. However, regardless of the approach employed, it was observed that the allowable ranges of parameter selection were severely restricted by the capacity-versus-speed requirement.

In the first approach, the emphasis was on technological development to reduce various time delays and to improve the accuracy with which various state variables (especially ΔV_T) could be measured. A greatest-lower-bound, minimum performance choice for A_2 was made, and then A_1 was selected to achieve the required capacity-versus-speed relationship. The first five sets listed in Table 5 are typical of the choices which may be made here.

To select a desired large value for A_1, a small value of T and/or ΔV_T would be required. The reduction of these quantities to very low values will be difficult to accomplish, as the former is comprised of detection, communication, and braking actuator delays which, collectively, probably cannot be reduced below 0.3s (indeed, this value may be too optimistic) while the latter, which is an "instantaneous" value, can only be measured accurately by a time-averaging operation--thus imparting

an additional delay.

In the second approach, the focus was on achieving $(A_1 - A_2)$ small with A_1 large. Then the requirements on such quantities as T and ΔV_T need not be as restrictive as in the first approach. In general, one could achieve higher capacities as is illustrated in Figs. 56 and 57, or safer operation at lower capacities within the capacity requirement. The principal difficulty lies in assuring that following-vehicle braking will be sufficiently large. The required research focus would be the achievement of a large, maximum "guaranteed" level of braking performance over a wide range of expected operating conditions. One promising approach would be augmented braking.

The third approach also involved achieving $A_1 - A_2 \doteq 0$, but with A_1 selected as a moderate value. The required research emphasis would be in limiting vehicle decelerations, even in highly abnormal situations. This would require an intensive effort; however, in view of the potential benefits involved--a large capacity over a wide speed range, less restrictions on ΔV_T and T, and a substantial reduction in accidents--this would seem to be a worthy subject for future development.

CHAPTER VI

SUMMARY AND FUTURE EFFORTS

A. Summary and Conclusions

The control required for an automated highway system can be achieved via a hierarchy wherein a centralized computer would oversee network operations with this including the coordination of activities in the individual geographic regions comprising the network. A second level of control would be at the regional level. Each regional controller would supervise the activity of a number of sectors and control the vehicles in those sectors via appropriate commands to the sector computers which comprise the third level of control. The fourth, and lowest, level of control is that of the individual vehicle. In this study, the focus is on the following essential aspects of the latter two levels:

a) The specification of the desired state of each vehicle;

b) The determination of the actual state of each vehicle;

c) Communications between each vehicle and sector-control; and

d) The control of each individual vehicle.

Each of the facets can be viewed in the context of either longitudinal or lateral control.

During the past year, which was the first year of a planned three-year program, The Ohio State University efforts were focused principally on the development of a physical test facility which

will be employed to study control and communication problems at, and below, the sector level. These studies would be focused on the automatic control of high-speed, traffic (to 28.4 m/s) operating at time headways as small as 1 s.

Within this framework, the principal accomplishments over the first year of this study include:

a) The implantation of sources to provide each controlled vehicle with a continuous measure of its lateral and longitudinal state over the complete extent of the 6.4 km, ski-pad facility at the Transportation Research Center of Ohio (TRCO). (Some 27,500 m (90,000 ft) of wire were inserted in specially cut slots in the pavement and sealed in place);

b) The development and laboratory testing of an approach employing audio frequencies and a "flattened" helical information source to provide continuous, absolute position information, within an accuracy of ±0.33 cm, to a string of moving vehicles; and

c) The design of a vehicle longitudinal controller for both normal and emergency modes of operation, and the preliminary evaluation of that controller under full-scale conditions.

In addition, substantial progress was made on the following:

a) The design and evaluation of a steering controller which is adaptive to changes in vehicle speed; and

b) The development of a sector-level controller which is comprised of a commercially available microprocessor and a considerable amount of special-purpose hardware.

These items will be discussed in a subsequent report.

The secondary accomplishments included the reevaluation of a headway safety policy for automated highway operations, and the development of a methodology to determine the accident costs associated with a particular policy choice.

The second-year efforts will be focused on the following six topics with the primary emphasis being on the first four:

a) The continued development of the automated vehicle test facility at TRCO;

b) The implementation of a sector-level controller;

c) Studies in automatic longitudinal control under both normative and emergency conditions;

d) Studies in vehicle lateral control with an emphasis on lane-changing operations; and

e) The specification and development of a sector-level communication system; and

f) The instrumentation of a third test vehicle.

REFERENCES

1. Anon., in Personal Rapid Transit III, Audio Visual Library Service, University of Minnesota, Minneapolis, Minnesota, 1976.

2. Anon., Proceedings of the First International Conference on Dual-Mode Transportation, Washington, D.C., May 29-31, 1974.

3. Gardels, K., "Automatic Car Controls for Electronic Highways," General Motors Research Laboratories, General Motors Corporation, Warren, Michigan, GMR-276, June 1960.

4. TRW Systems Group, "Study of Synchronous Longitudinal Guidance as Applied to Intercity Automated Highway Networks," Final Report prepared for the Office of High Speed Transportation, Department of Transportation, September 1969.

5. Stefanik, R. G., and Kiselewich, S. J., "Evaluation of the Operating Conditions of a Detroit Dual-Mode Vehicle Network," presented at the 1972 SAE Automotive Engr. Congress, Jan. 1972, SAE Paper 720272.

6. Wilson, D. G., Ed., "Automated Guideway Transportation Between and Within Cities," Urban Systems Laboratory Rpt. No. FRA-RT-72-14, Mass. Institute of Technology, Cambridge, Mass., Feb. 1971 (PB 206-269).

7. Giles, G. C., and Martin, J. A., "Cable Installation for Vehicle Guidance Investigations in the New Research Track at Crowthorne, JAM Road Research Lab., Crowthorne, England, Rpt. RN/40 57/CGG.

8. Oshima, Y., Kikuchi, E., Kimura, M., and Matsumoto, S., "Control System for Automobile Driving," Proceedings Tokyo IFAC Symposium, 1965, pp. 347-357.

9. Fenton, R. E., et al., "One Approach to Highway Automation," Proceedings of the IEEE, Vol. 46, No. 4, April 1968, pp. 556-566.

10. Fenton, R. E., et al., "Advances Toward the Automatic Highway," Highway Research Record, No. 344, Washington, D. C., Jan. 1971, pp. 1-20.

11. Fenton, R. E., and Olson, K. W., "An Investigation of Highway Automation," Rpt. EES 276-6, Dept. of Elec. Engr., The Ohio State University, Columbus, Ohio, March 1969.

12. Anon., "An Investigation of Highway Automation," Rpt. EES 276A-12 Dept. of Elec. Engr., The Ohio State University, Cols., Ohio, April 1971.

13. Fenton, R. E., Ed., "An Investigation of Highway Automation," Rept. No. 276A-15, Dept. of Elec. Engr., The Ohio State University, Columbus, Ohio, September 1974.

14. Olson, K. W., et al., "Studies in Vehicle Automatic Lateral Control--Theory and Experiment," Appendix I to "An Investigation of Highway Automation," Rpt. 276A-16, Dept. of Elec. Engr., The Ohio State University, Columbus, Ohio, September 1974.

15. Fenton, R. E., et al., "Studies in Synchronous Longitudinal Control," Transportation Control Laboratory Rpt. EES 276A-17, Dept. of Elec. Engr., The Ohio State University, Cols., Ohio 43210, September 1974.

16. Fenton, R. E., Ed., "Fundamental Studies in the Automatic Longitudinal Control of Vehicles," Final Report on DOT-OS-40100, Transportation Control Laboratory, The Ohio State University, Columbus, Ohio, 43210, July 1975 (Available from NTIS).

17. Anon., "Practicality of Automated Highway Systems," Final Report on Contract DOT-FH-11-8903, CALSPAN Corp. Buffalo, N.Y., Nov. 1977 (This report will be available from NTIS).

18. Fenton, R. E., Ed., "Fundamental Studies in the Longitudinal Control of Automated Ground Vehicles," Final Report on DOT-FH-8874, Transportation Control Laboratory, The Ohio State University, Columbus, Ohio 43210, Dec. 1976 (Available from NTIS).

19. Takasaki, G. M., "A Sector Computer for Automated Highway Operations," Transportation Control Laboratory Working Paper 78-1, The Ohio State University, Columbus, Ohio 43210, July 1978.

20. Cormier, W. H., "Studies in Automatic Lateral Control," Transportation Control Laboratory Working Paper 78-2, The Ohio State University, Columbus, Ohio 43210, August 1978.

21. Athans, M., et al., "A System of Optimal and Suboptimal Position and Velocity Control for a String of High-Speed Vehicle," Proceedings of the 5th International Analogue Computation Meetings.

22. Bender, J. G., and Fenton, R. E., "On Vehicle Longitudinal Dynamics," Traffic Flow and Transporation, G. F. Newell, Ed., American Elseivier Publishing Co., Inc., New York, 1972, pp. 33-46.

23. Takasaki, G. M., Vehicle Synchronous Longitudinal Control in Normal Situations, Master of Science thesis, The Ohio State University, Columbus, Ohio, December 1974.

24. Takasaki, G. M., Some Vehicle and Sector Aspects of Automated Ground Transportation, Ph.D. dissertation, The Ohio State University, Columbus, Ohio, March 1978.

25. D'Azzo, J. J., and Houpis, C. H., Feedback Control Systems Analysis and Synthesis, Second Edition, McGraw-Hill, New York, 1966.

26. Chu, P. M., "Longitudinal Controller Studies -- Controller Design and Evaluation," Report 75-1, Transportation Control Laboratory, Dept. of Electrical Engineering, The Ohio State University, Columbus, Ohio, September 30, 1975.

27. Chan, S. P., Chan, S. Y., and Chan, S. G., Analysis of Linear Networks and Systems, Addison-Wesley, Reading, Massachusetts, 1972.

28. Godfrey, M. G., "Headway and Switching Strategies for Automated Vehicular Ground Transportation Systems," Report 76106-4, Engr. Projects Lab., Dept. of Mechanical Engineering, M.I.T., Cambridge, Massachusetts 02139, November 1, 1966 (PB 173 644).

29. Anon., "Automated Highway Systems," High-Speed Ground Transportation Study, TRW Systems, Inc., Redondo Beach, California, April, 1970.

30. Bender, J. G., and Fenton, R. E., "Synchronous Longitudinal Control for Automated Ground Transport -- Some Practical Limitations," Proceedings of 1972 WESCON, Sept. 19-22, 1972, Los Angeles, Calif.

31. Lenard, M., "Safety Considerations for a High Density Automated Vehicle System," Transporation Science, Vol. 11, No. 1, May, 1970, pp. 138-158.

32. MacKinnon, D., "High Capacity Personal Rapid Transit System Developments," IEEE Trans Veh Tech, Vol. VT-24, No. 1, February, 1975, pp. 8-14.

33. Rule, Ronald G., "The Dynamic Scheduling Approach to Automated Vehicle Macroscopic Control," Transportation Control Laboratory Report EES 276A-18, The Ohio State University, Columbus, Ohio, Sept., 1974.

34. Fenton, R. E., and Chu, P. M., "On Vehicle Automatic Longitudinal Control," Transporation Science, Vol. 11, No. 1, February, 1977, pp. 73-91.

APPENDIX A

SPECIFICATIONS

FOR

TRCO SKID PAD INSTRUMENTATON

(Pavement Installations)

A. Introduction

A section of the skid-pad facility at the Transporation Research Center of Ohio (TRCO) was instrumented for automated vehicle testing. These specifications were concerned with one aspect of this installation--the cutting of slots in the skid pad surface, the installation of electrical wires in those slots, and their subsequent sealing.

B. Overview of Wire Installation

An overview of the closed-loop, wire installation is shown in Fig. A-1. This loop, which is some 21,300 ft in extent, includes a path along each turn-around loop and two straight sections which include the two middle test surfaces. The wires are installed in lane center in these surfaces as most users would tend to approximately center their vehicle in a lane before braking were initiated. This vehicle would straddle the wires, braking would be accomplished on an uncut surface, and damage to the sealant and wires should be minimized.

The wires are also installed in lane center on each of the turnaround loops, thus making passing possible. In the region

between the test surface and a turnaround, it was not possible, because of the converging nature of the lanes, to install the wires in lane center. Instead a nearly straight path, which crossed 1 or 2 existing cut lines, was employed as shown in Fig. A-1.

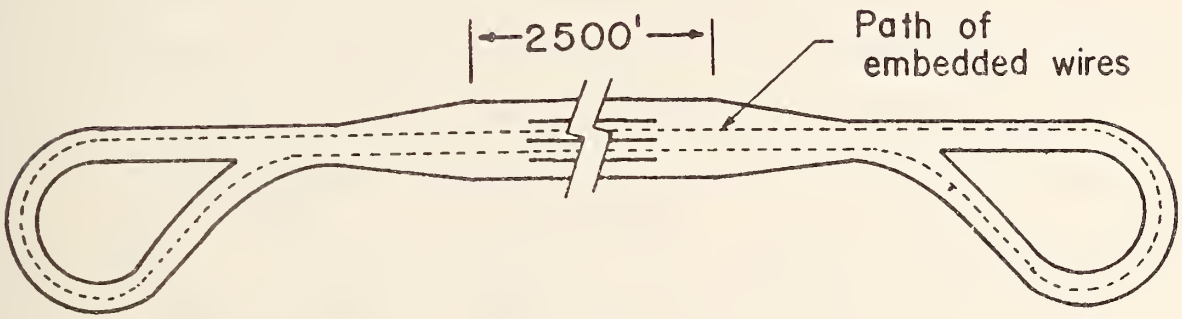

Fig. A-1. Geometrics of an automated vehicle facility.

A detailed view of a typical section of this loop is shown in Fig. A-2. This consists of 3 linear longitudinal slots, with an interslot spacing of 0.5 ft and lateral slots of 2-ft intervals. The width of the two outer lineal cuts was 3/16 (-0, + 1/32) in, that of the middle linear cut was 1/8 (-0, + 1/32) in, and that of the lateral cuts 1/8 (-0, + 1/32) in. Generally the slots were 0.75 in deep and were filled, after the wires were embedded, with a flexible sealant. There were two exceptions to this depth specification. First, so as to provide for the expected expansion and contraction of the wire installed in the center cut, the cut depth was increased to $1\frac{1}{8}$ in for a longitudinal distance of some 5 in

in every 50 ft. The approach to be employed in laying this wire is shown in Fig. A-3.[1]

Every 500 ft, a single line pair was installed is shown in Fig. A-4. As the closed loop encompasses some 20,000 ft, some 40 of these pairs were required. In most cases, the lines were taken directly to roadside as shown in Fig. A-4.[2] However, this was undesirable on the 2500-ft test surface, and the approach detailed in Fig. A-5 was employed. In essence, the lines were not taken to roadside across this surface; Instead they were laid in one of the two "outside" lineal cuts (See Fig. A-2) and subsequently taken to roadside in a nontest surface. As this resulted in an extra wire in that cut, the cut depth was increased to 1 in.

Every 500 ft, a flush-mounted junction box was installed at roadside. This provided access points to the various lines for both excitation and maintainance purposes. This involved a lateral cut across the roadway surface to each box, which precluded any boxes being located adjacent to the 2500-ft test section.

---

[1] The wires laid in the outer linear cuts were in a spatial square-wave configuration wherein enough wire slack was incorporated to eliminate a need for periodic increases in slot depth.

[2] These lines were terminated in small flush-mounted junction boxes. If interconnections between these boxes were necessary, this would be accomplished via wires, approximately 2 in below the surface, around the perimeter of the pad.

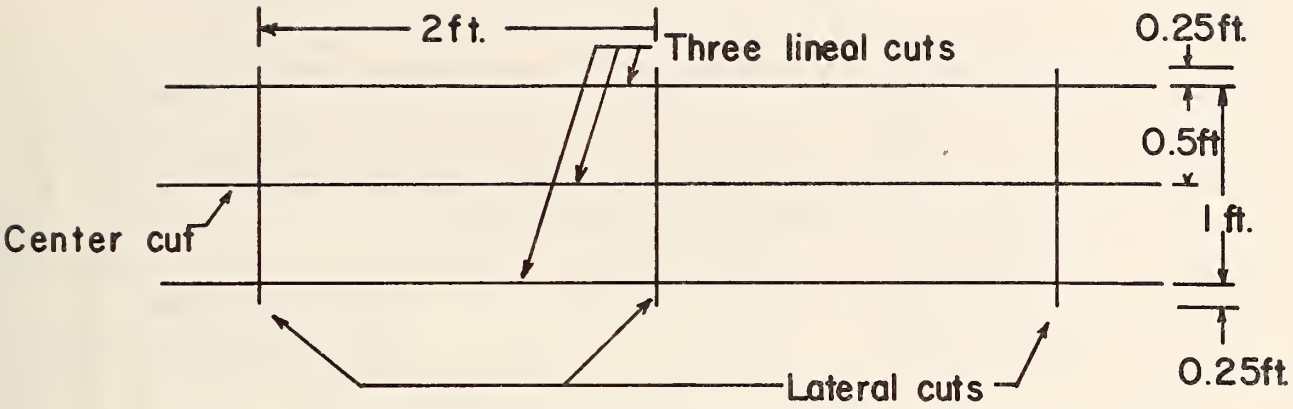

Note: All cuts are a depth of 3/4 in except as noted in text.

Fig. A-2 Detail of saw cuts required for wire embedding.

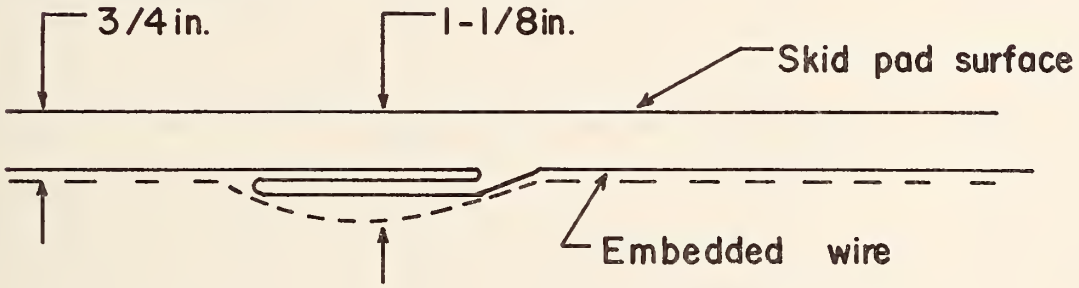

Fig. A-3 Detail of center cut showing approach to accounting for wire expansion/contraction.

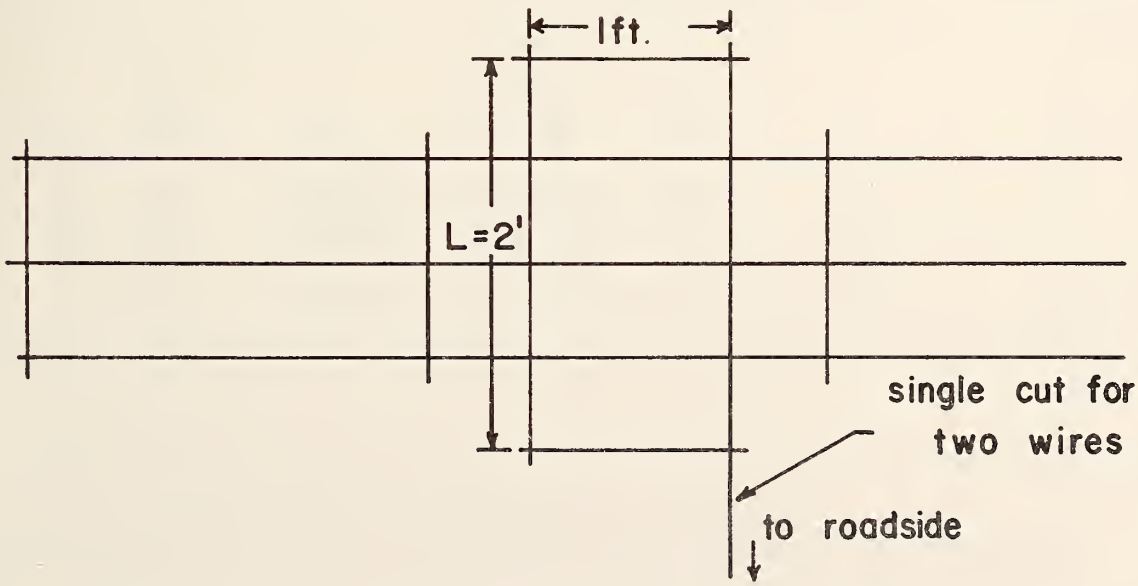

Fig. A-4 Detail of line pair installed every 500 ft.

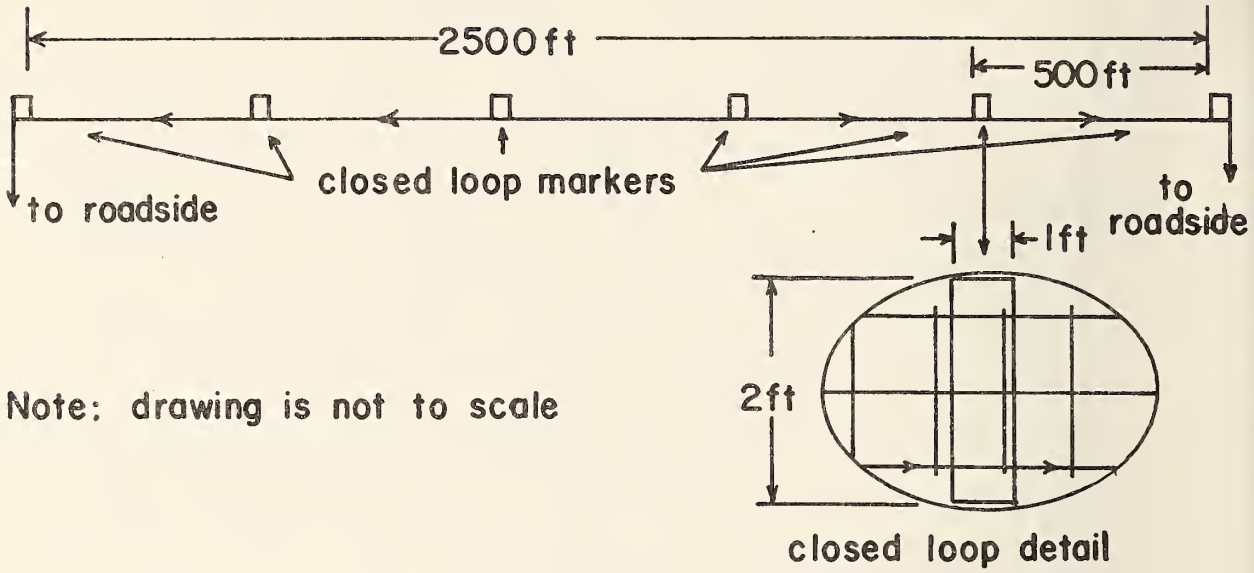

Fig. A-5 Detail of closed-loop markers installed under the test surface.

C. Detailed Specifications

The specifications for each of the required cuts are presented in Table A-1. The sealant was required to satisfy ASTM Tentative Specification D3406-75T.[3]

---

[3] Two of the sealants which meet this specification are NEA-444 (Posh Chemical Company) and Superseal-444 (Superior Products Company, Inc).

TABLE A-1

SPECIFICATIONS ON SLOT CUTS

Cut Type	Location	Position Accuracy	Depth	Width (Accuracy)	Comment
Longitudinal	Center cut--Straightaways	$\pm\frac{1}{8}$ in (1)	$\frac{3}{4}$ in	$\frac{3}{16}$ in ($\pm\frac{1}{32}$ in)	Every 50 ft, the cut depth should be increased to some 1 1/8 in for approx. 5 in.
	Center cut--curving sections	$\pm\frac{1}{4}$ in (1)	$\frac{3}{4}$ in	$\frac{3}{16}$ in ($\pm\frac{1}{32}$ in)	(Same as above)
	2 outer cuts (straight and curving sections)	$\pm\frac{1}{8}$ in (2)	$\frac{3}{4}$ in (3)	$\frac{3}{16}$ in ($\pm\frac{1}{32}$ in)	
Lateral	At 2-ft longitudinal intervals	$\pm\frac{1}{8}$ in (1)	$\frac{3}{4}$ in	$\frac{3}{16}$ in ($-\frac{1}{32}$, +0 in)	See Fig. 6 for cut detail.
	At 500-ft intervals	$\pm\frac{1}{8}$ in (1)	$\frac{3}{4}$ in	$\frac{3}{16}$ in ($\pm\frac{1}{32}$ in)	This encompasses both the closed-loop line pair (See Fig. 4) and the cuts leading to roadside (4).

(1) This accuracy is with respect to the specified reference line.

(2) This accuracy is with respect to the desired distance (6") from the center cut.

(3) On the skid-pad surface (2500 ft in extent), the depth of the cut closest to the roadway edge should be increased to 1 in (-0, +1/32 in).

(4) In 10-12 cases, the cuts lending to roadside will contain up to 6 wires. In these cases, the required saw depth will be 1½ in.

APPENDIX B

AN ACCIDENT-COST, SENSITIVITY ANALYSIS FOR A UNIFORM-SPACING HEADWAY POLICY*

A. Introduction

In recent years, there has been increasing interest in the dual-mode concept which involves the automatic control of individual vehicles on special roadways, termed guideways, and the manual control of those vehicles on conventional roads (1)-(2).[1] This concept can be applied to both intracity and intercity operations, and when applied to the latter, the term automated highway is employed.

The potential advantages of an automated highway system include increased traffic flow, improved safety (at least on the automated part of the system) by replacement of the human driver with a faster reacting and more reliable control system, and the convenience of private door-to-door transportation.

The achievable capacity is closely related to system safety via a headway policy; i.e., a specification of the minimum permitted headway (as a function of speed) for mainline operations. There are three aspects to such a policy:

i) The specification of those abnormal situations in which a collision can be avoided;

---

*This study was performed by Jochen Glimm during his stay at The Ohio State University.

[1]The references for this appendix are listed on pages 182-183.

ii) The specification of the probability of a collision occurring (i.e., the probability of abnormal situations beyond those included in (i)); and

iii) The severity and "cost" of each collision.

In Chapter V, the first of these was evaluated in the context of achieving a high capacity ($\geq$ 3600 vehicles/lane/hr) over a range of typical highway speeds---13-30m/s (30-67 mph). These conditions are those which are generally felt to be essential for the successful operation of an automated highway system. The second aspect could be achieved if an appropriate system-level model were available. As its development would require a detailed knowledge of both system components and system operations, the required effort cannot be satisfactorily completed at this time. The third aspect can be evaluated for various accident situations, and it is the subject of this Appendix.

B. Summary of Headway Policy

Consider a platoon of identical vehicles traveling on a single lane of highway (see Fig. B-1). At time t = 0, this platoon is assumed to be in a worst-permissible normal state; i.e., the lead vehicle is moving with an initial speed of $v_1(t) = V_S - \Delta V_T$, the following vehicles ($i = 2,3,\ldots n$) with a speed of $v_i(t) = V_S + \Delta V_T$ and the distance between the lead and second vehicle is the minimum

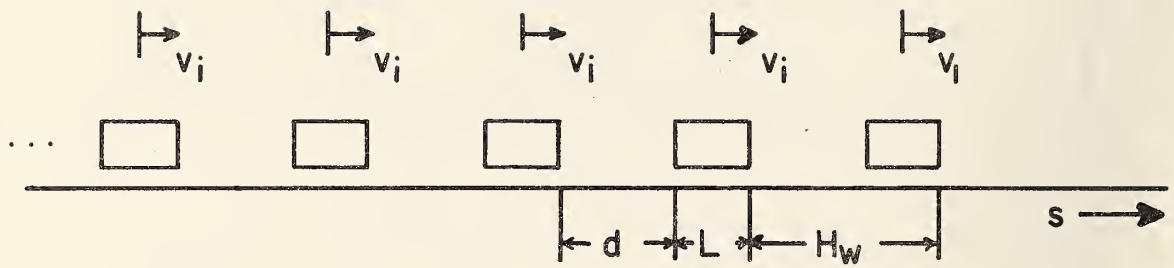

$$v_1 = v_s - \Delta v_T$$
$$v_i = v_s + \Delta v_T \qquad (i = 2,3,4 \ldots n)$$
$$H_w = v_s \cdot H_t - 2\Delta x_t$$

Fig. B-1. Initial state of a platoon of vehicles.

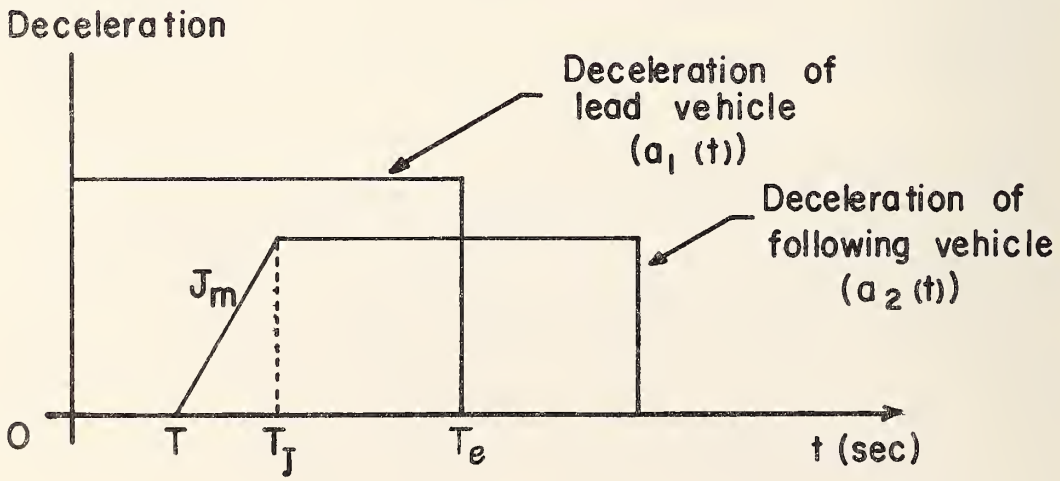

Fig. B-2. Deceleration trajectories of the lead and following vehicle .

permitted value of[2] $H_w = V_s \cdot H_t - 2\Delta X_T - L$ (B-1)

With the platoon in this state, the lead vehicle brakes, at a rate of $a_1(t)$, at time t=0. The second vehicle, after a delay T due to detection, communication, and braking reaction times, also brakes but at a rate of $a_2(t)$. Note from Fig.B-2 that a jerk limit (J_m) is in effect until a constant deceleration is achieved. The other following vehicles similarly brake (with the same final rate) with the time at which braking is initiated being dependent on the type of control (series or parallel) employed.[3]

Under the conditions specified here, the condition for no collisions is (1)

$$V_s H_t \geq L + 2\Delta X_T + (V_s + \Delta V_T)(T + \frac{A_2}{J_m}) - \frac{1}{6}\frac{A_2^3}{J_m^2} + \frac{\left[V_s + \Delta V_T - \frac{1}{2}\frac{A_2^2}{J_m}\right]^2}{2A_2} - \frac{(V_s - \Delta V_T)^2}{2A_1} \quad \text{(B-2)}$$

---

[2] All symbols employed here are defined in Table B-I.

[3] A parallel system is one wherein emergency brake commands are transmitted to all following vehicles simultaneously, and T is the same for all trailing vehicles. This is generally associated with a point-following approach to vehicle control. In a series system, each vehicle must sense the braking of its nearest forward neighbor, and thus the total delay T_T before the ith vehicle brakes would be the sum of the individual delays; i.e.,

$$T_T = T + \sum_{j=3}^{i} T_{j-1,j}$$

where $T_{j-1,j}$ is the reaction delay between the j-1 and j-th vehicles. For the assumed initial condition, $T_{j-1,j}$ has the same value T_c for $j \geq 3$ and $T_T = T + (i-2)T_c$. The relationship of T to T_c depends on the emergency detection mechanism employed. In some cases (e.g., if a relative-deceleration threshold were included in the specification of an emergency), $T \simeq T_c$ and $T_T = (i-1)T$. This was the case considered in this paper. A series system would be associated with a car-following approach to vehicle control.

TABLE B-1

GLOSSARY OF SYMBOLS

Symbol	Definition
$a_1(t)$	Deceleration profile of the lead vehicle
$a_2(t)$	Deceleration profile of the following vehicles
A_1	Policy choice for lead-vehicle deceleration
A_2	Policy choice for deceleration of following vehicle
A_{col}	Vehicle deceleration after impact with its nearest forward neighbor
g	Deceleration due to gravity
J_m	Jerk limit
V_i	Speed of ith vehicle at impact
v_i	Initial speed of ith vehicle in a platoon
$\Delta V_{i+1, i}$	Relative impact speed between the (i + 1) and the ith vehicles
V_s	Normal steady-state speed of vehicle platoon
V_{com}	Common velocity of two colliding vehicles after impact
v	Impact speed between a vehicle and a fixed barrier
ΔV_T	Velocity threshold for initiation of emergency action
V_{max}	Velocity for normalized cost function
VSTWF	Velocity-step-function weighting factor
δV_j	A range of speeds along a speed axis (j = 1,2,...r)

TABLE B-1

GLOSSARY OF SYMBOLS

(continued)

Symbol	Definition
m_j	Number of collisions in the velocity range δV_j
r	Number of speed ranges along a speed axis
ΔX_T	Position threshold for initiation of emergency action
H_w	Required headway distance between vehicles
x	Deformation of a vehicle after a collision
S_{stop}	Stopping position of vehicle
L	Vehicle length
T	Delay due to detection, processing, and braking reaction lags
T_{col}	Time of collision
T_e	Stopping time of lead vehicle
T_J	End of jerk time
T_{stop}	Stopping time of vehicle
H_t	Time headway
k	Accident cost factor (all accidents)
k_F	Accident cost factor (fatal accidents)
k_{NFI}	Accident cost factor (non-fatal, injury-only accidents)
k_{PDO}	Accident cost factor (property-damage only accidents)

TABLE B-1

GLOSSARY OF SYMBOLS

(concluded)

Symbol	Definition
CI_i	Collision index between the i + 1 and ith vehicles
S_c	Accident-cost, severity index
S_{tc}	Total cost of current traffic accidents
n	Number of vehicles in a platoon
q	Maximum number of preceding vehicles which are influenced by a collision behind them
Δ	Relative deviation variable
ε_i	Factor of additional damage to the i preceding vehicles caused by the collision of the (i + 1)st and i vehicles
Veh_{max}	Maximum number of vehicles set into the program

Here, $a_1(t)$ and $a_2(t)$ have been specified as A_1 and A_2, respectively (e.g., policy choices of deceleration for which Eqn. (B-2) would be satisfied). When this equation is not satisfied (e.g., lead-car deceleration $a_1(t) > A_1$), one or more collisions may result.

There are seven parameters in Eqn. (B-2) with two (ΔX_T, ΔV_T) associated with the performance of the vehicle longitudinal controller, two (J_m and A_2) with the physical capabilities of the vehicle, two (T and H_t) which are largely associated with network operations, and one (A_1) which is a "policy" choice for the deceleration of the lead vehicle. In the context of the capacity required for automated highway operations, H_t is relatively insensitive to ΔX_T and J_m and quite sensitive to ΔV_T, T, A_1, and A_2 (See Chapter V). As this requirement is equivalent to $H_t \leq 1$ s over the range of interest, the allowable ranges for the latter four parameters are severely restricted.

C. Collision Dynamics

Various attempts have been made to develop a reasonable, but simple accident or collision model; i.e., a specification of the acceleration- and velocity-time histories of a following vehicle after it has collided with a lead vehicle. Such a model is primarily employed to reconstruct motor-vehicle accidents; i.e., to give a physical picture of what happens in and after collisions, the movements of both vehicles and their occupants, and especially the types of injuries which are most likely to occur.

The nature of vehicle motion after a collision has been considered by several authors. For example, Lenard (3) studied two types of accidents -- the derailment of a moving vehicle and the

failure to detect a stalled vehicle ahead of a platoon of moving vehicles. The former was simulated by assuming a large deceleration of the lead vehicle at a constant rate. The collision of any following vehicle with the preceding vehicle was modeled by letting the velocity of the former assume the velocity of the latter at the instant contact was established. In the second type, the lead vehicle was assumed to collide with the stalled vehicle and thereafter come to a halt at a constant rate of deceleration within a fixed time interval. For all subsequent collisions, it was assumed that the colliding vehicle instantaneously assumed the velocity of the preceding vehicle.

Grime and Jones (4) conducted a laboratory evaluation of car collisions and found that in head-on impacts with rigid barriers the deformation (x) of the front of a car was approximately

$$x = 0.07\ (v - 4) \qquad (m)$$

[e.g., for v = 22.35m/s (50 mi/h), x = 1.27 m (50 in)]. Surprisingly, this is a linear function. The deceleration during an impact between a vehicle, traveling at 16.54 m/s (37 mi/h), and a barrier was an average of 10 to 20g with peak values up to 50g, and the impact time before stopping was approximately 0.1 s. Also, the collisions were almost inelastic; i.e., the coefficient of restitution was as small as 0.05 - 0.1.

Elsholz (5) conducted a laboratory crash test between a moving and a stalled vehicle. He determined that the average deceleration was 15g (peak values ≅ 40g) during an impact time of 0.1 s. He also

reported that both vehicles had a common velocity 0.11 s after impact, and a total (2-vehicle) deformation of 1.15m.

Schmid (6) notes that at an impact velocity of 19.44 m/s (43.7 mi/h), the deformation of one vehicle will be 1 m provided the vehicle decelerated at an average rate of 20g during the 0.1 s of impact.

Finally, Plotkin (7) indicated that the use of conservation of momentum for accident reconstruction is generally not advantageous because reconstructed velocities before impact differ from the results obtained from crash tests by some 30%. This phenomenon is explained by considering that, upon collision, forces are produced which tend to rotate both the vehicles about their respective pitch axes. Thus, some energy is transferred through the tires into the ground.

Based on such findings, the accident collision model shown in Fig. B-3 was developed. Here, a trailing vehicle, upon colliding with the preceding vehicle, assumes the shown acceleration and velocity profiles. Note that the velocity of the former is zero at time T_{stop} (i.e., the collision is with a slowly moving or stationary lead vehicle), corresponding to a worst-case situation, in which the vehicle would not progress appreciably after the collision.

This simplified representation of what is undoubtedly a very complex motion is only intended to match reported "end" conditions (i.e., the position of the colliding vehicle as a function of the absolute collision speed) some 100 ms after the instant of collision T_{col}, and not to represent events within the collision interval.[4] It was convenient to employ two fixed parameters, VSTWF and A_{col}, rather than a single,

---

[4] As the accident severity measure subsequently adopted doesn't depend on events <u>within</u> T_{stop}-T_{col}, this choice appeared reasonable.

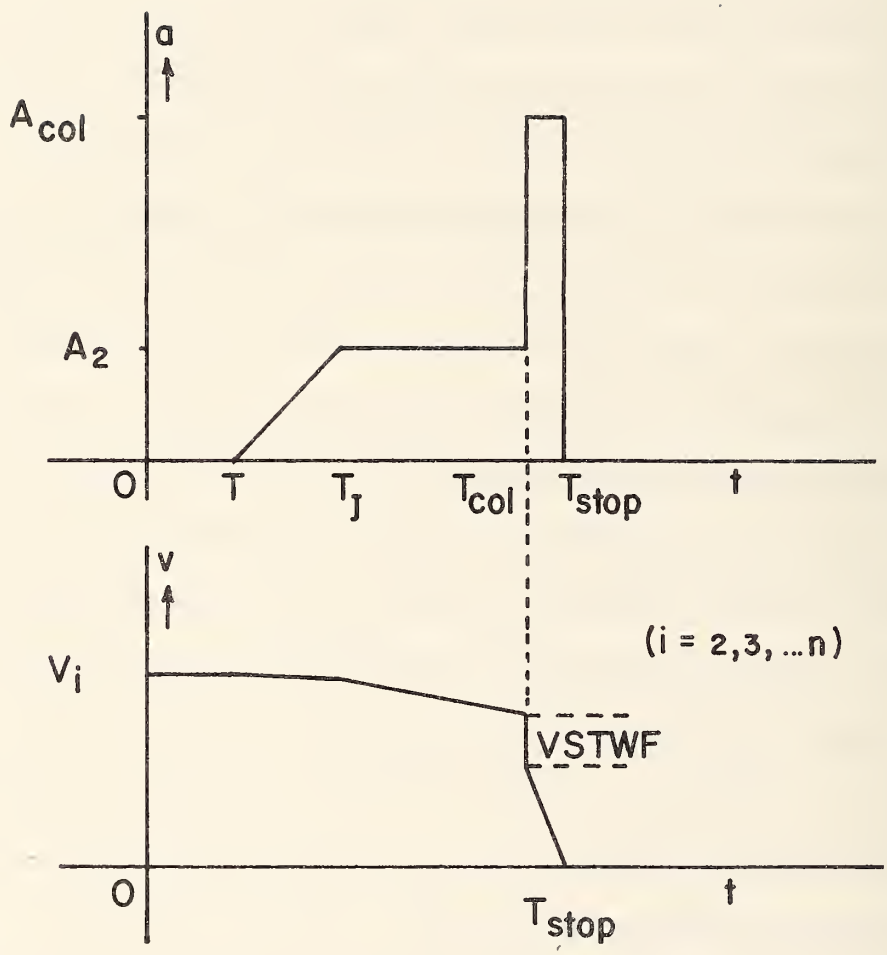

Fig. B-3. Deceleration and velocity trajectories of a following vehicle when a collision occurs.

velocity dependent one for this purpose.

This same model can be applied to the collision of the third vehicle with the combined mass of the first two, the collision of the fourth vehicle with the combined mass of the first three and so on.[5]

D. Evaluation of Accident Severity Data

a) Accident Severity Measures

An accident severity index should be consistent with current accident data. In accordance with the study of Carlson (12), it should be a function of both the relative speeds of the colliding vehicles and their absolute speeds. Thus, in many cases the damage done during the initial impact is only a part of the total damage -- especially if the vehicles' absolute speeds were relatively high.

In a general study, which involves multiple collisions within a platoon, one should therefore account for damage related to both the absolute and relative speeds of colliding vehicles. However, here virtually all collisions (as noted in the study reported in Section E) occurred between a moving vehicle and a composite mass comprised of one or more stopped vehicles. Thus, severity measures were only considered

---

[5] After a large number of collisions, a large, "combined" mass (e.g., 20 vehicles) is present and a "brickwall" situation exists. It is probable that virtually no longitudinal motion of this mass will occur for successive collisions and , in this regard, the model would lead to slightly "optimistic" results.

for this case.

Lenard (3) has suggested three indices to provide a measure of the severity of an accident involving a platoon of n vehicles ($n \geq 2$):

$$S_1 = \sqrt{\sum_{i=1}^{n-1} \left(\Delta V_{i+1,i}\right)^2} \tag{B-3}$$

$$S_2 = \sqrt{\sum_{i=1}^{n-1} \max_{i-n} \left(\Delta V_{i+1,i}\right)^2} \tag{B-4}$$

$$S_3 = \sqrt{\sum_{i=1}^{n-1} \sum_{j=i}^{n-1} \left(\Delta V_{j+1,j}\right)^2} \tag{B-5}$$

Here $\Delta V_{i+1,i} = v_{i+1} - v_i$; i.e., the relative impact speed between the (i + 1) and the i vehicles.

Since the energy of a collision is proportional to the square of the differential collision velocity, S_1 appeared to be a reasonable choice. S_2 was selected on the basis that a light impact followed by more severe ones to the rear of the first vehicle would damage the lead vehicle more severely than a light impact followed by no other collisions. The lead vehicle is increasingly damaged by all successive collisions.

The basic idea associated with S_3 is reasonable; however, the magnitude of this damage, as expressed by (B-5) appears too large, because of the mass relationship between the colliding (i + 1)st vehicle and the previously stopped i vehicles. Thus, for example,

the tenth vehicle would probably cause very little damage to the first vehicle -- possibly none at all. However, if S_3 were rearranged so that

$$S_3 = \sqrt{\sum_{i=1}^{n-1} i \cdot \left(\Delta V_{i+1,i}\right)^2}, \qquad \text{(B-6)}$$

then the collision of the (i + 1)st vehicle with the combined mass of the i preceding ones would be weighted some i times the collision of the first two vehicles.

This problem may be overcome by replacing the factor i by $1 + \varepsilon_i$ in Eqn. (B-6) so that

$$S_3^{\,1} = \sqrt{\sum_{i=1}^{n-1} \left(1 + \varepsilon_i\right)\left(\Delta V_{i+1,i}\right)^2} \qquad \text{(B-7)}$$

One meaningful approach to selecting ε_i would be to assume that the additional damage to the composite mass of the stopped vehicles may be accounted for by choosing

$$\varepsilon_i = \sum_{j=1}^{\min(i,q)} (j+1)^{-1}$$

In effect, when the composite mass becomes much greater than the mass of the ith colliding vehicle (e.g., q = 10), the total effect of each succeeding collision is assumed to be the same. Unfortunately, no data were available so that reasonable values for the ε_i could be selected.

Thus, these were selected as zero, and S_3^1 reduced to S_1 (Eqn. (B-3)).[6]

b) Accident Cost Function

The quantity S_1 is consistent with the empirical data associated with colliding vehicles; in addition, it would be convenient if it could be expressed in a generally interpretable form (e.g., nondimensional units or dollars per unit) for comparison purposes. Toward this end, it is convenient to employ S_1^2 rather than S_1.

The accident dollar costs required are not directly available from current accident data. The latter are inextricably mixed across a variety of causes and research intentions, and it appears impossible to isolate those data which could be applied to the case of interest. It was thus necessary to employ a broad, nondiscriminatory type of averaging and infer appropriate costs.

i) An Overview of Accident Cost Data

An overview of accidents and accident cost data from several studies covering the years of 1953 through 1974 is shown in Table B-II. Note that these data are highly variable depending on locale, year, etc. Furthermore, average values of accident costs, fatal and nonfatal injuries, property damage, and accident type percentages vary widely. (This is true even when the effects of inflation are considered.)

Only a few authors provide information on the relationship between the number of accidents and impact speed. One of these is Vecellio

---

[6]Some justification for this expedient choice was that multiple-collision effects were incorporated into a subsequently presented "dollar" cost function.

TABLE B-2

OVERVIEW OF ACCIDENT DATA

Date	Source	Accident Classification			
		Fatal	Nonfatal Injury	Property Damage Only	All
		No.	No.	No.	No.
1961	Transportation Engineering Center, The Ohio State University (14)				
	No. of Accidents	1,434	113,167	723,872	838,473
	Average Cost ($)	236	833	118	222
1961-65	Vecellio (15)	(Costs: N/A)			
	No. of Accidents	139	3,314	N/A	N/A
1968	Smith and Tamburri (16)	(No. of Accidents: N/A)			
	Average Cost ($)				
	1953 Mass.	5,213	862	203	382
	1955 Utah	3,690	1,277	299	499
	1964 Illinois	8,950	2,200	360	1,190
1974	Abramson (18)	(No. of Accidents: N/A)			
	Average Cost ($) (including indirect cost)	3,693	1,932	310	700
1973	Accident Facts for 1972 (19)				
	No. of Accidents	48,800	1,400,000	15,600,000	17,050,000
	Average Cost ($)	N/A	N/A	N/A	1,138
1972	Böttger (20)	(No. of Accidents: N/A)			
	Average Cost ($)	54,270	1,884	N/A	690

TABLE B-2

OVERVIEW OF ACCIDENT DATA

(concluded)

Date	Source	Accident Classification			
		Fatal	Nonfatal Injury	Property Damage Only	All
		No.	No.	No.	No.
1972	Transp. a. Traffic Eng. Handbook (21)	(No. of Accidents: N/A)			
	Average Cost ($)	82,000	3,400	480	
1977	Calspan (22)	(Cost: N/A)			
	Per 10^9 vehicle-miles	35.8	1,310	N/A	N/A
	Per 10^9 occupant-miles	19.3	706	N/A	N/A
	Per 10^9 occupant-hours	680	24,856	N/A	N/A

N/A: Figure Not Available.

(15) who obtained the function shown in Fig. B-4. Note the relatively large numbers of accidents at very low speeds (< 5 m/s) and at very high speeds (> 20 m/s).

The detailed study of Solomon (17) included a cost distribution-vs-speed function for the period of 1955-58. This function is comprised of a bias and a quadratically increasing term with speed. The approximate speed preceding accidents, based on North Carolina reports from 1972, is contained in Accident Facts 1973 (19). A corresponding distribution of the number of accidents versus speed is as shown in Fig. B-5. Note that the shape of the density function is similar to that of Fig. B-4, although the cumulative distribution functions show some differences. However, no detailed information on the individual average cost of fatal, nonfatal injury, or property damage accidents are given. Nevertheless, these few empirically obtained distribution functions were useful in specifying a cost function for this study.

ii) A Suggested Cost Function

In view of Eqn. (B-3), a collision index (CI_i) could be defined as

$$CI_i = k \cdot \Delta V_{i+1,i}^2 \qquad i = 1,2,..,n-1$$

for a collision between a moving vehicle and a stationary vehicle. In order to avoid unwanted dimensions, it seems reasonable to normalize this function. An obvious choice would be

$$CI_i = k \left[\frac{\Delta V_{i+1,i}}{V_{max}}\right]^2$$

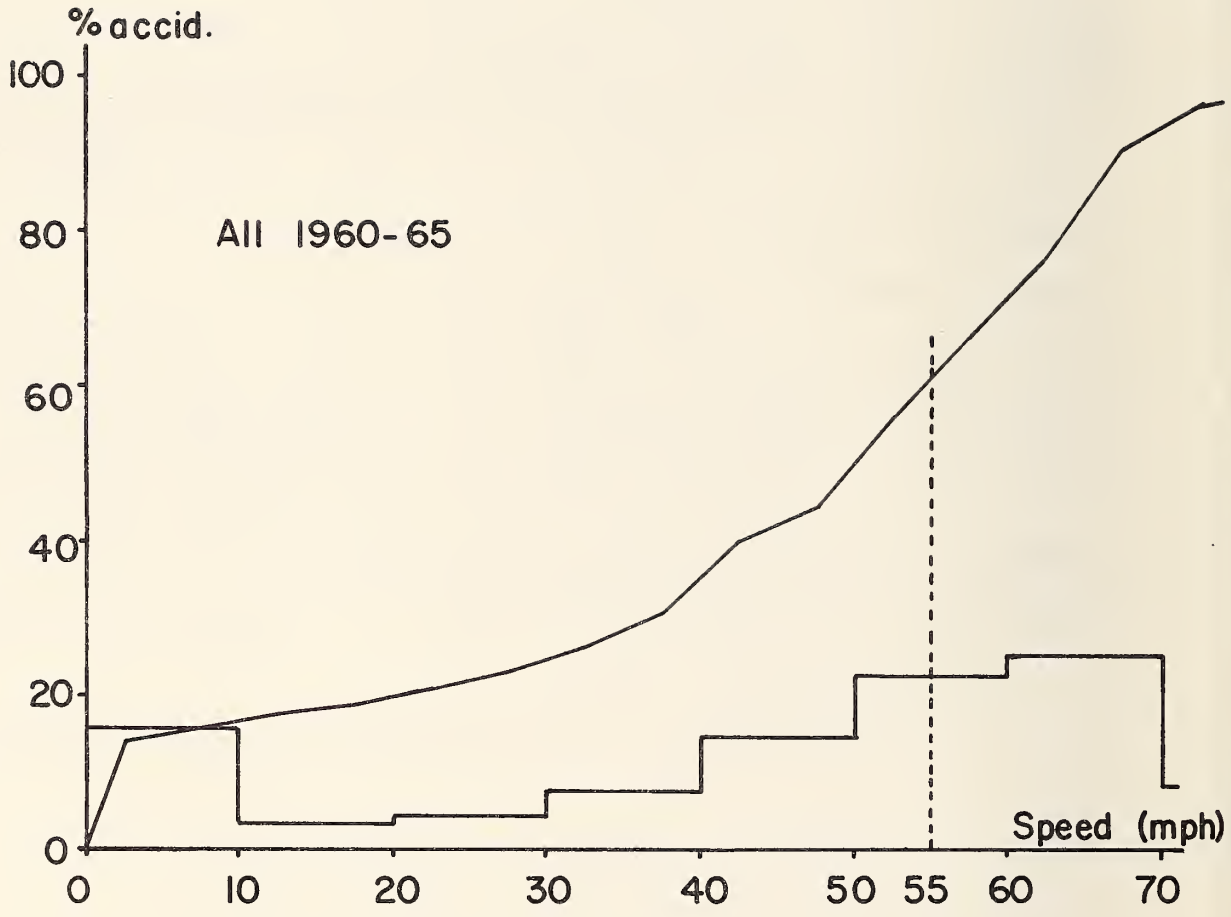

Fig. B-4. The number of accidents versus speed (Reference 15).

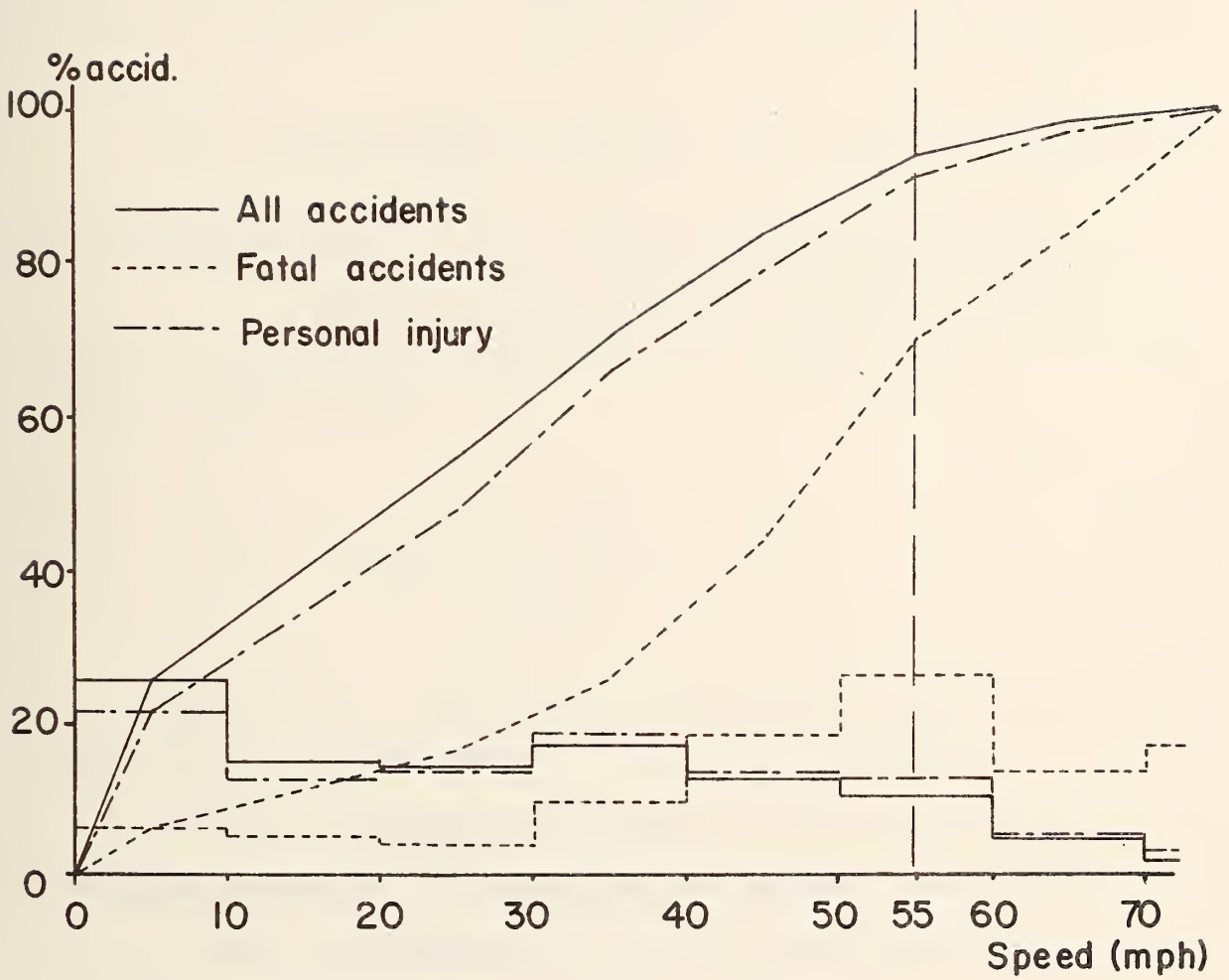

Fig. B-5. The number of accidents versus speed preceding accidents (Reference 19).

A standardized value for V_{max} must be employed so that meaningful comparisons between collision indices of different system configurations and/or headway policies can be made.

Another approach is to relate accident data to an index that has a monetary value

$$CI_i = k \cdot \Delta V^2_{i+1,i} \tag{B-8}$$

where k has the units of dollars/$(m/s)^2$. Then, available accident data and costs could be related to the platoon case.

The selected severity index, expressed in units of dollars, would be

$$S_c = k \sum_{i=1}^{n-1} \Delta V^2_{i+1,i} \tag{B-9}$$

iii) Cost Function Weighting Factor

Consider a distribution of accidents versus relative speed, and let the speed axis be divided into r segments -- δV_1, δV_2,..,δV_r. If the number of accidents occurring with an approximate relative impact speed of δV_j were m_j, then the corresponding cost would be

$$k\, m_j\, (\delta V_j)^2$$

and the total cost would be

$$S_{tc} = k \sum_{j=1}^{r} m_j\, (\delta V_j)^2$$

With the appropriate data (i.e., the m_j and δV_j), k could be determined via

$$k = \frac{S_{tc}}{\sum_{j=1}^{r} m_j \, (\delta V_j)^2}$$

In the subsequent simulation study, it was noted that virtually all collisions were between a moving vehicle and a composite group of already stopped vehicles. Thus, the colliding vehicle's absolute speed at impact was equal to the relative collision speed. Then, for the purposes of interest here,

$$k = \frac{S_{tc}}{\sum_{j=1}^{r} m_j \, V_j^2} \qquad \text{(B-10)}$$

To account for the few cases where $V_j > \delta V_j$, one can make a conservative choice of k.

In 1972, the North Carolina accident distribution versus speed was as shown in Fig. B-5. Assuming that this relationship is generally valid, and employing the specified value of $S_{tc} = 19.4 \times 10^9$ dollars for 1972 (19), then Eqn. (B-10) can be employed to determine

$$k = 4.75 \quad \$/(m/s)^2 \qquad [0.95 \ \$/(mi/h)^2]$$

This result is a weighted average for all types of accidents--fatal, nonfatal injury, and those involving property damage only. As data are also available in (19) for each of these individual catagories, one

can use a corresponding modification of Eqn. (B-10) to obtain

k_f	= 42.73 ($/(m/s)^2)	(8.54 $/(mi/h)^2)	(fatal accidents)
k_{NFI}	= 16.91 ($/(m/s)^2)	(3.38 $/(mi/h)^2)	(nonfatal accidents)
k_{PDO}	= 2.85 ($/(m/s)^2)	(0.57 $/(mi/h)^2)	(property-damage-only accidents)

A conservative choice, which at least partially accounts for the considerable cost increases from 1972 to 1977, the additional affects of a collision on already stopped preceding vehicles, and the difference between absolute and relative impact velocity might be:

$$k = 1 \ \$/(ft/s)^2 \qquad \text{(B-11)}$$

This is equivalent to

$$k = 11 \ \$/(m/s)^2 \qquad \text{(B-12a)}$$

or

$$k = 2.2 \ \$/(mi/h)^2 \qquad \text{(B-12b)}$$

E. Simulation Study

Platoon stopping dynamics were evaluated via a digital-computer simulation. The state of the platoon when the lead vehicle braked was as specified in Section B. If Eqn. (B-2) were satisfied, no rear-end collisions would occur, and each vehicle would be stopped by its brakes. However, if this equation were not satisfied (e.g., lead-car deceleration > A_1), then rear-end collisions would occur. In such a case, a

vehicle's motion after collision would be as specified in Fig. B-3. The severity of all collisions was evaluated from Eqns. (B-9) and (B-12).

The quantity S_c is a function of 11 parameters---9 associated with the headway policy equation (Eqn. B-2) and two with the accident model (Fig. B-2). It was not feasible to exhaustively investigate the influence of each of these; therefore, several were fixed. These were V_s, which was selected as the highest envisioned operating line speed of 26.8 m/s (88 ft/s), L = 3.66 m (12 ft) (a reasonable length for a future, lightweight fuel-efficient vehicle), H_t = 1 s (the approximate required operating condition), ΔX_T = 0.305 m, ΔV_T = 0.305 m/s, J_m = 76.2 m/s^3, A_{col} = 98.1 m/s^2 (10g) and VSTWF = 0.5. The quantities ΔX_T and ΔV_T were specified based on reported measurement and vehicle tracking capabilities, and the last three quantities were selected via a sensitivity analysis as is subsequently described.

The parameter sets considered (see Table B-3) satisfied the capacity-versus-speed requirement and were intended to encompass the range of choices which would be available in practice.

Two general configurations were considered--one in which a serial buildup of reaction delay was present, and one with a single parallel delay.

TABLE B-3

PARAMETER SETS FOR A HEADWAY POLICY

Symbol	Units	1	2	3	4	5
		(Fig. B-10)	(Fig. B-11)	(Fig. B-12)	(Fig. B-13)	(Fig. B-14)
A_1	m/s^2	7.26 (0.74g)	6.74 (0.687g)	6.43 (0.655g)	6.15 (0.626g)	5.61 (0.572g)
A_2	m/s^2	5.89 (0.6g)	5.89 (0.6g)	5.89 (0.6g)	5.89 (0.6g)	5.89 (0.6g)
T	s	0.3	0.4	0.5	0.6	0.8

Fixed Parameters

V_s = 26.8 m/s H_t = 1 s

L = 3.66 m J_m = 76.2 m/s^3

ΔX_T = 0.305 m ΔV_T = 0.305 m/s

a) Outline of Simulation Program

The details of the program employed are presented in a working paper (23); an outline, which will follow the structogram of Fig. B-6, is presented. This program primarily consists of three nested loops:

i) An inner loop where the motion of each vehicle was determined until it stopped--with or without colliding with another vehicle;

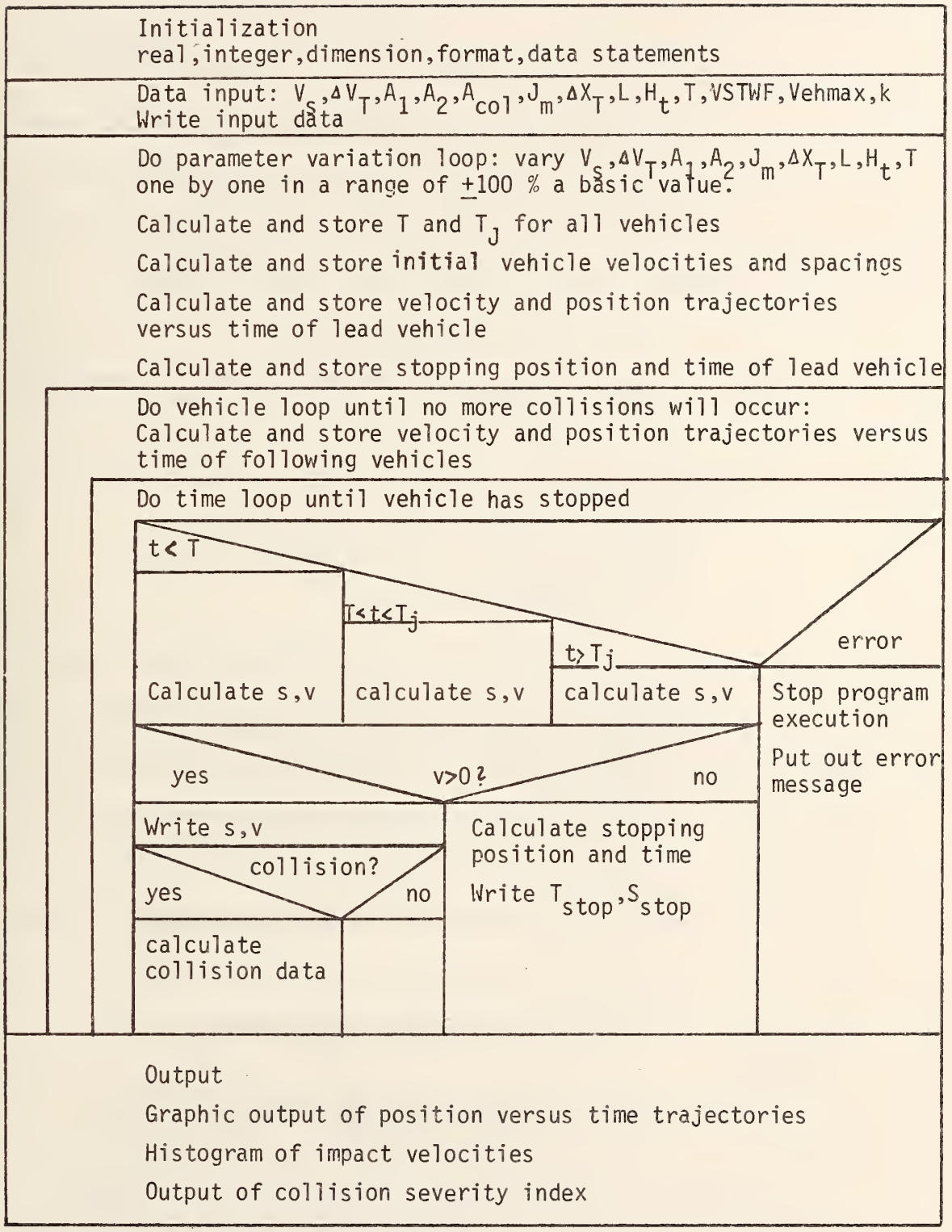

Fig. B-6. Structogram of simulation program.

ii) A second loop, which encompasses the above loop , to count vehicles until no more collisions occur;[7] and

iii) An outer loop which is employed to modify each nonfixed parameter from the specified policy value to ±100% of that value.

The following outputs are available from this program:

i) A printed output of the position of each vehicle versus time;

ii) A graphic display of position and velocity versus time up to 10 vehicles;

iii) A histogram relating the number of collisions to the relative speed at impact; and

iv) The computed values of S_c.

b) Sensitivity Analysis--Accident Model Parameters

The effects on S_c of various choices of A_{col} and VSTWF were evaluated via a sensitivity analysis. Here, a parameter set, which satisfied Eqn. (2) was selected, and $a_1(t)$ was chosen to be greater than A_1 so that collisions would occur. The results for one set of headway policy parameters are shown in Figs. B-7 and B-8. In the former, S_c is plotted versus VSTWF with A_{col} as a parameter and, in the latter, S_c is plotted versus A_{col} with VSTWF as a parameter. Note that for

---

[7] At this point, the procedure is terminated. This approach is more efficient than simply computing the trajectories of a large number of vehicles -- especially when only a few collisions occur.

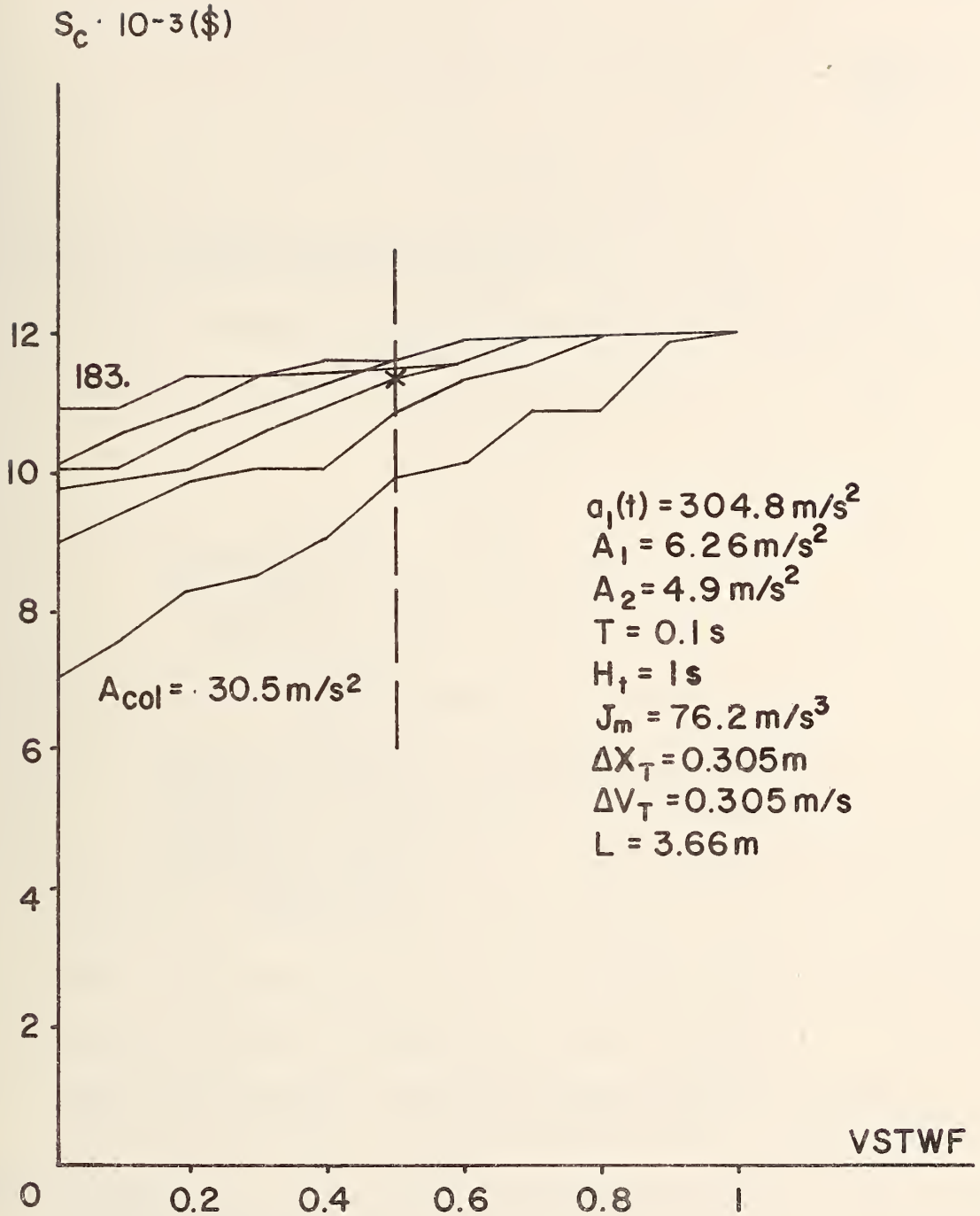

Fig. B-7. Sensitivity analysis of the effects of VSTWF and A_{col} (S_c versus VSTWF).

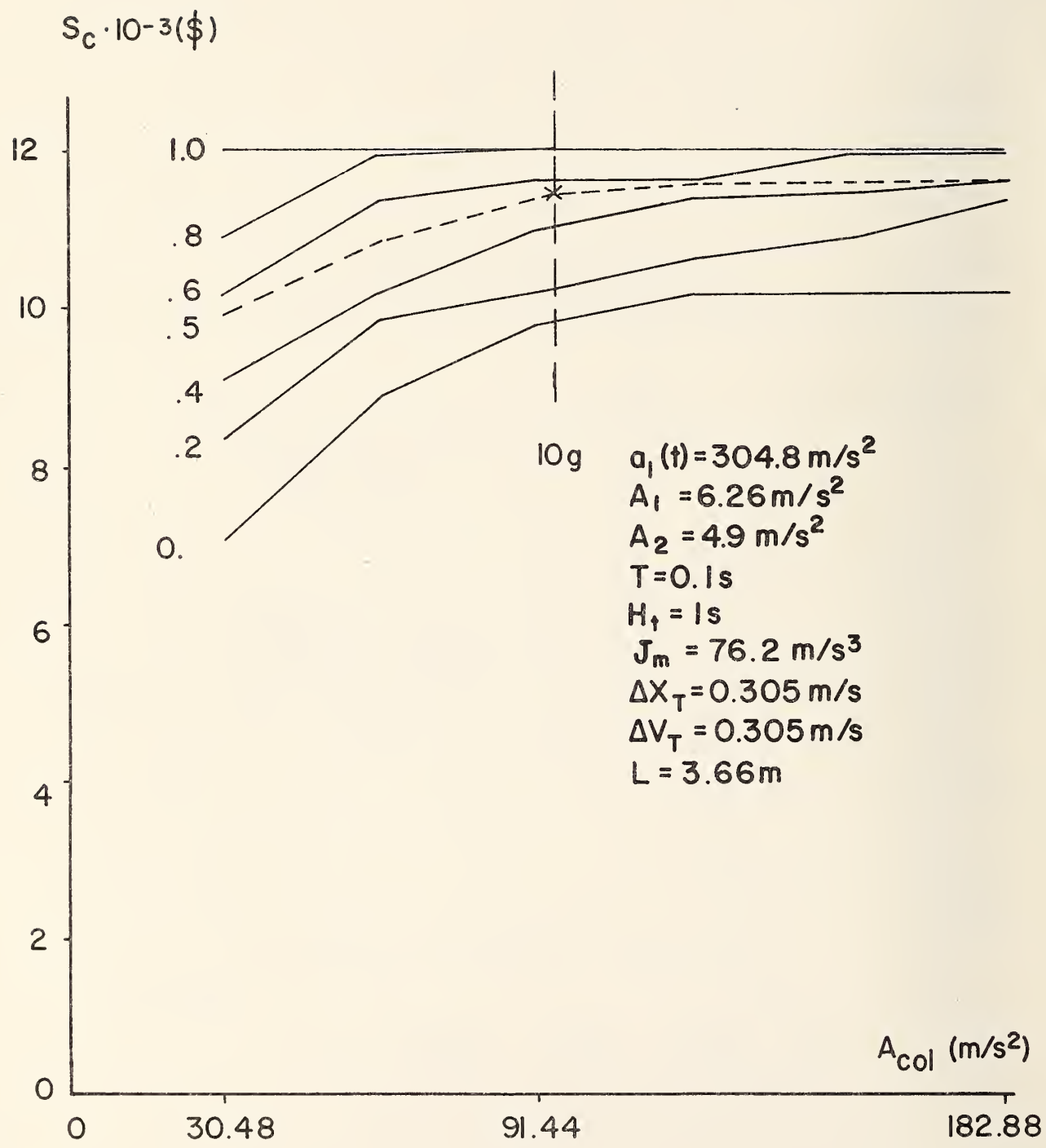

Fig. B-8. Sensitivity analysis of the effects of VSTWF and A_{col} (S_c versus A_{col}).

$$A_{col} > 60 \text{ m/s}^2$$

and

$$0.5 \leq \text{VSTWF} \leq 1.0,$$

S_c is relatively insensitive to the choices of A_{col} and VSTWF. Thus, to reduce the number of parameter combinations, these quantities were selected as

$$\text{VSTWF} = 0.5$$

and

$$A_{col} = 98.1 \text{ m/s}^2 \text{ (10g)}$$

for the remainder of this study.

c) Sensitivity Analysis--Headway Policy Parameters

The behavior of S_c was examined as a function of the variation of each individual parameter in a set. The results were presented in a normalized form in that, for a given parameter set, S_c was plotted versus the normalized variation (Δ) of each parameter with all other parameters fixed. The quantity Δ is thus, variously,

$\frac{\text{Lead-car deceleration}}{\text{Policy choice of } A_1}$, $\frac{\text{Following-car deceleration}}{\text{Policy choice of } A_2}$, $\frac{\text{Time delay}}{\text{Policy choice of } T}$,

or $\frac{\text{Jerk rate}}{\text{Policy choice of } J_m}$. This quantity was varied from 0 to 2, corresponding to a parameter variation of $\pm$ 100% with Δ = 1 being the reference point for which S_c = 0 (i.e., the condition under which the policy constraints were satisfied and no collisions occurred). With

this approach, S_c may be plotted on a single graph as a function of all individual variations.

Consider the plot of S_c versus Δ in Fig. B-9 for which the base parameter set is Set 1 of Table B-3. First, note that both the serial and parallel cases are shown here--the former by dashed lines and the latter by solid ones. Second, note that when all variations are zero (i.e., $\Delta = 1$ for all curves), $S_c = 0$ as expected. Third, S_c is extremely sensitive to positive variations in A_1, T and negative variations in A_2. Fourth, S_c is relatively insensitive for $\Delta > 0.3$ for J_m. The same general trends were obtained for the other basic cases listed in Table B-3, as may be noted from an examination of Figs. B-10-13. Thus, it is convenient to fix J_m as previously noted, and only consider variations in A_1, A_2, and T.

F. Accident Costs

The methodology presented here can be employed to determine accident severity for several accident scenarios. Three of these, which are especially relevant to automated highway operations are:

i) Lead-car braking at a rate greater than the policy choice;

ii) Degraded braking performance of all following vehicles; and

iii) A temporary increase in the reaction delay.[8]

---

[8]This effect would be associated with the parallel system as it would be exceedingly unlikely that the individual delays, associated with each vehicle, would simultaneously change in a serial case.

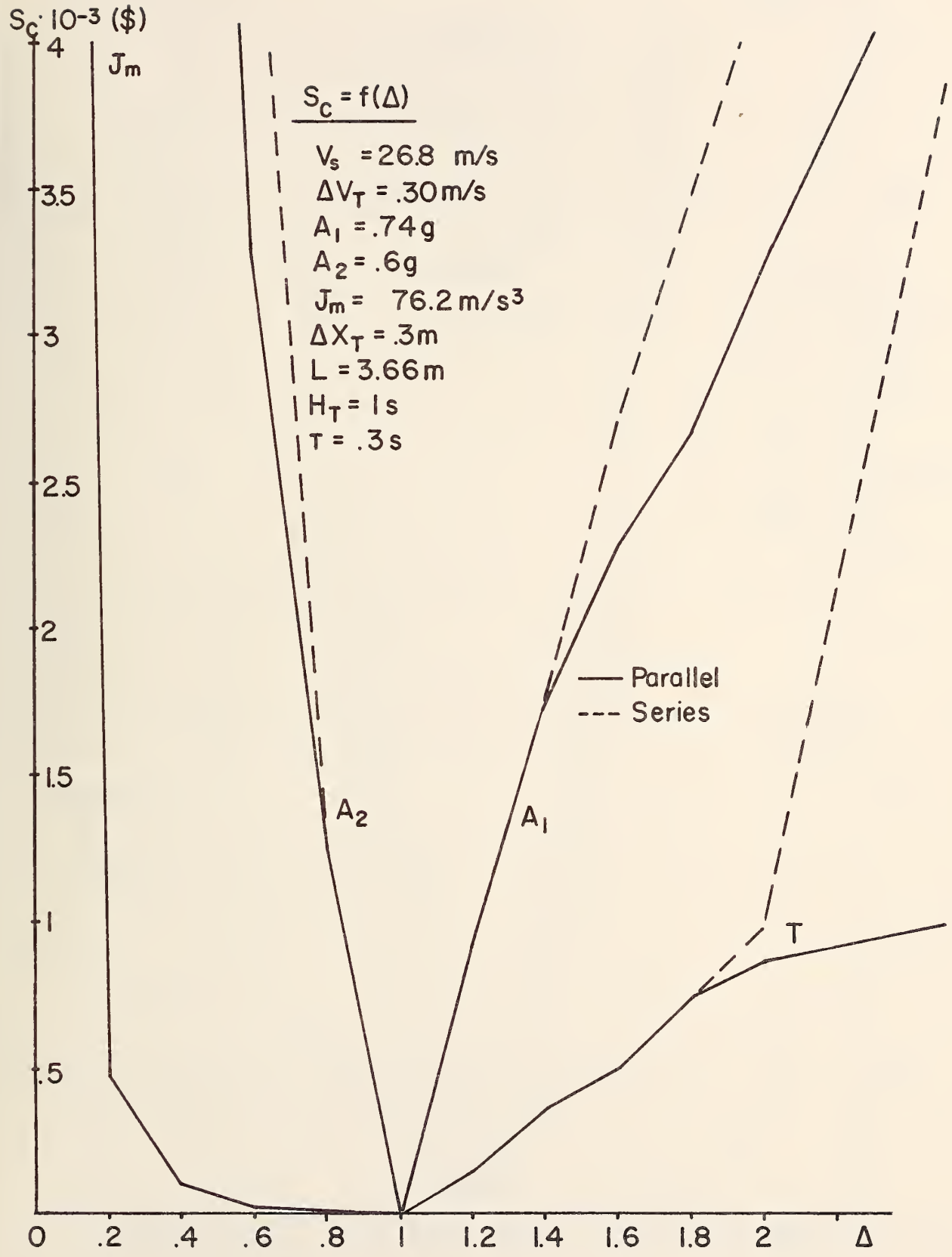

Fig. B-9. S_C versus Δ for Parameter Set 1.

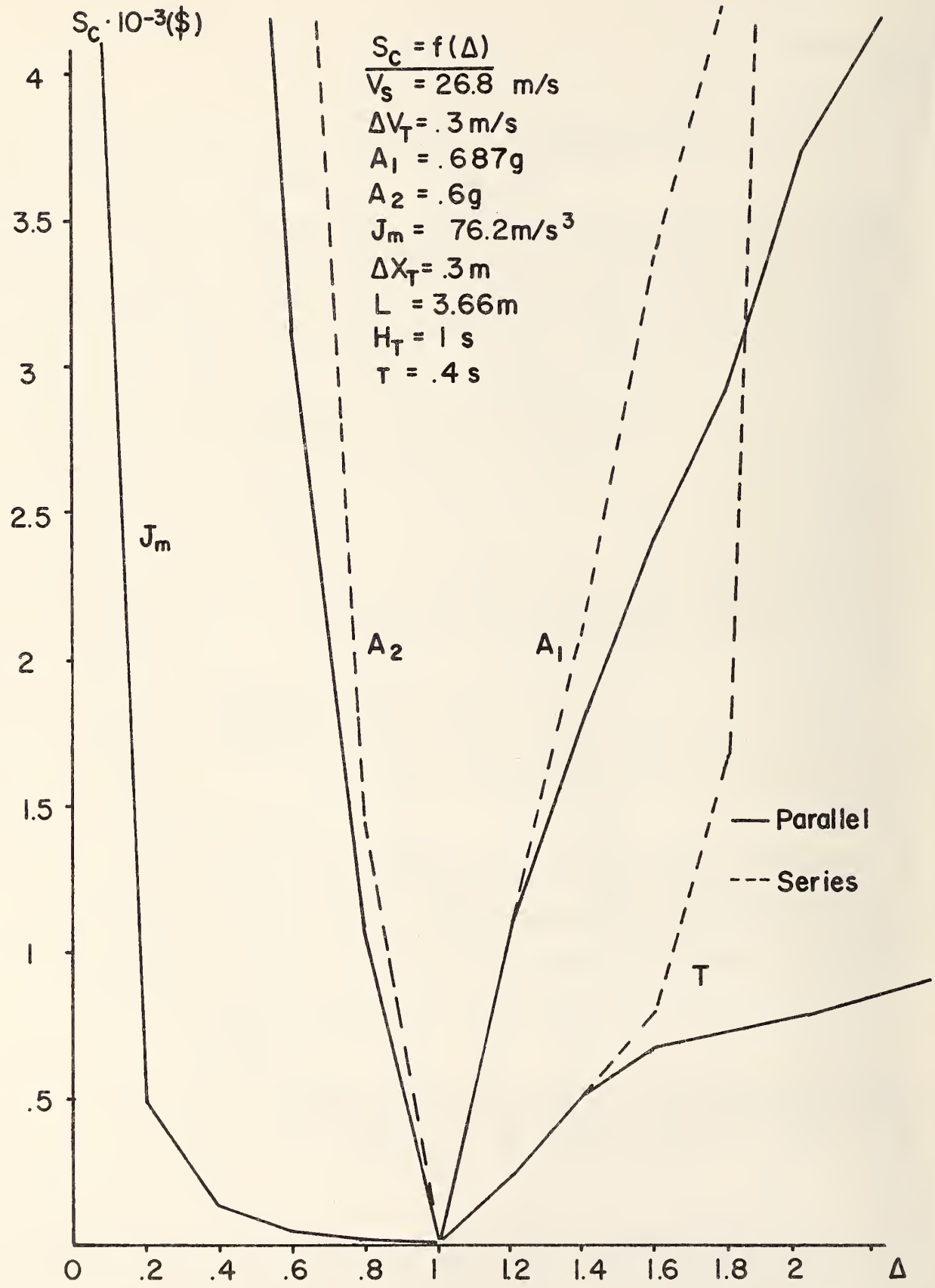

Fig. B-10. S_C versus Δ for Parameter Set 2.

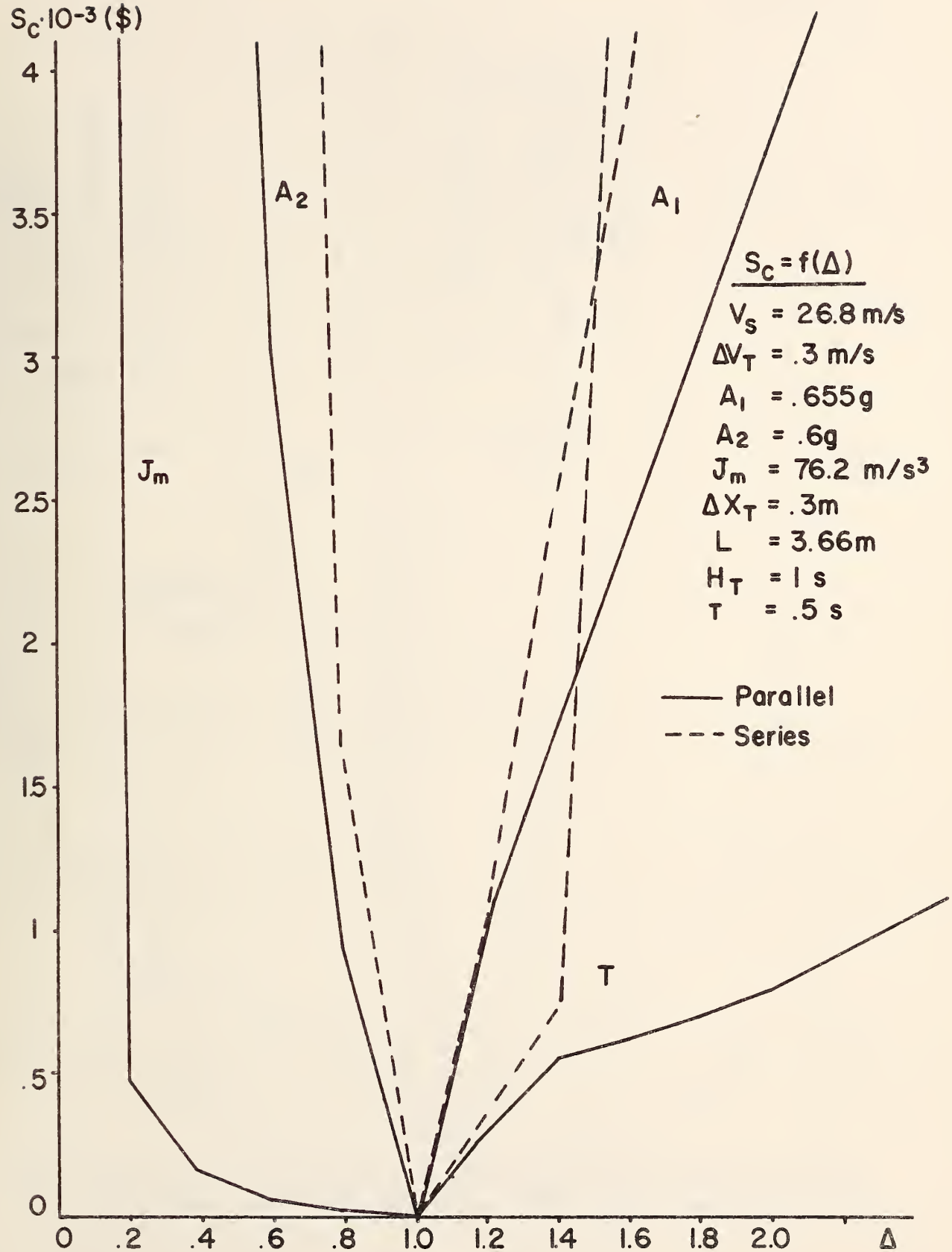

Fig. B-11. S_C versus Δ for Parameter Set 3.

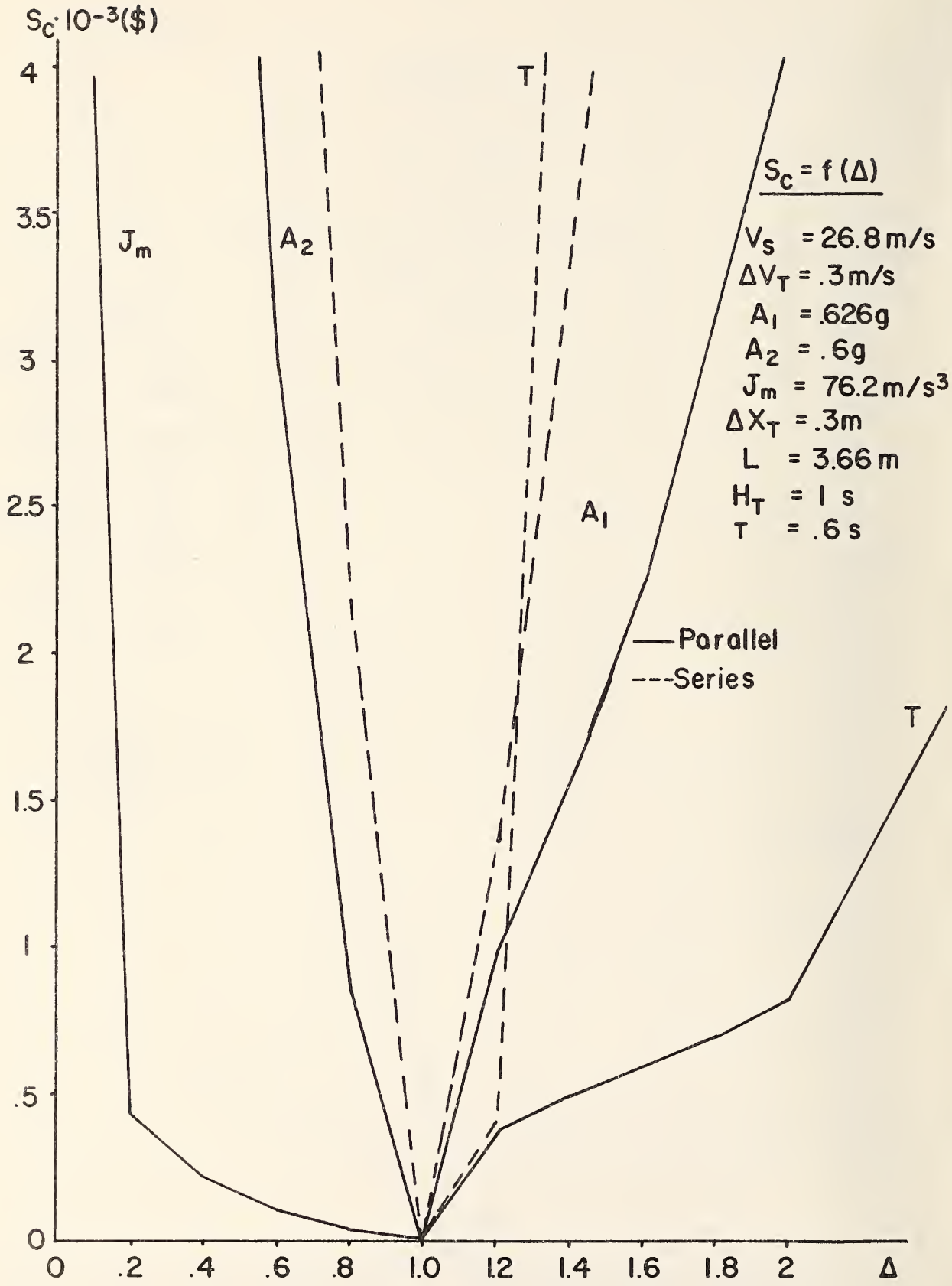

Fig. B-12. S_c versus Δ for Parameter Set 4.

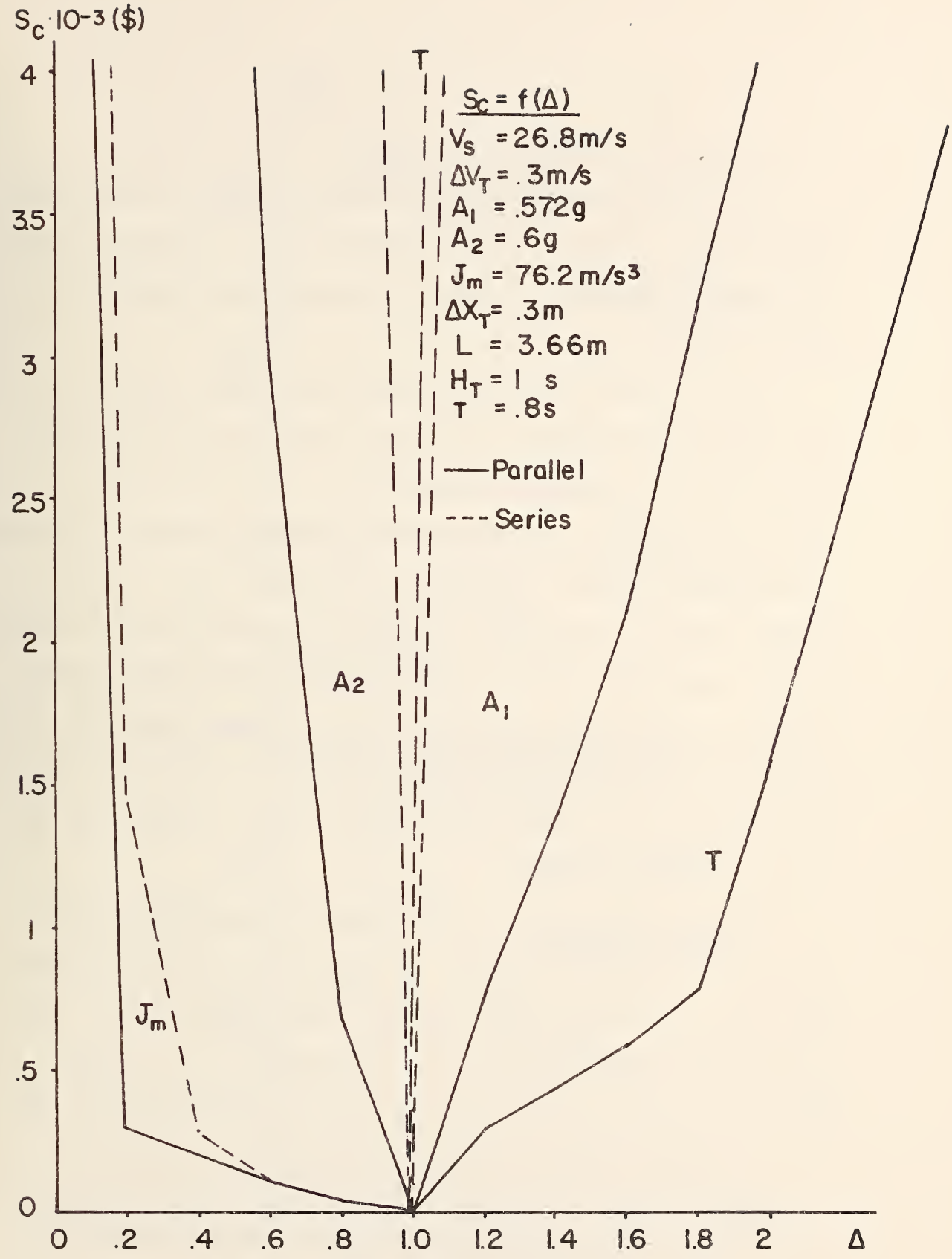

Fig. B-13. S_c versus Δ for Parameter Set 5.

a) Excessive Lead-Vehicle Braking

In a situation in which the lead vehicle brakes at a rate greater than the policy choice of A_1, accidents will occur. This may be seen from Figs. B-9-13, where S_c is seen to increase almost exponentially for $\Delta = [a_1(t)/A_1] > 1$.

It is of interest to view this cost from another viewpoint; i.e., the relationship between S_c and A_1 for a fixed lead-car deceleration. This is done for two actual decelerations--a_1 = 0.8g and 31.06g. The former corresponds to excellent braking on a high-traction, dry-concrete surface,[9] and the latter approximates a "brickwall" stop. These choices encompass the range of virtually all "serious" lead-car decelerations. In practice, the first case should not occur often, and the second (or exceedingly large-g stops which would approximate this case) would be an exceedingly low-probability event in a carefully designed system.[10] Even so, its evaluation provides valuable insights into the relative safety of a policy.

Typical results, which were obtained for the parameter sets of Table B-3 are shown in Fig. B - 14 where S_c is given for both the series and parallel cases. In Fig. B-14a, wherein $a_1(t)$ = 0.8g, S_c decreased with increasing A_1 and was zero for $A_1 = a_1$ = 0.8g. Clearly, A_1 should be chosen as large as is practical; however, this

---

[9] It could also correspond to a variety of abnormal situations; e.g., a vehicle braked by a dragging axle.

[10] This design would, of course, involve a careful weighting of the tradeoffs existing between capacity, safety, costs, etc.

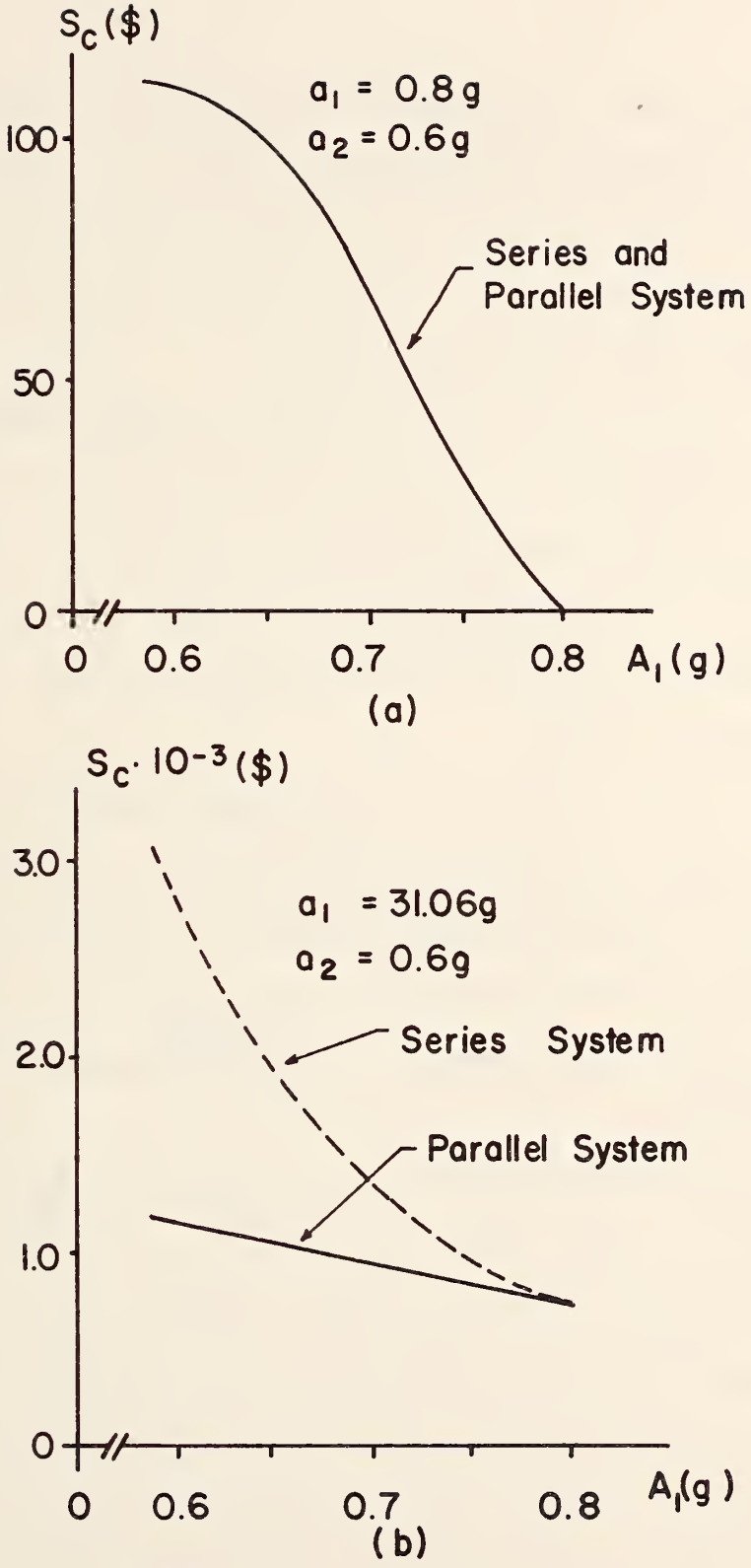

Fig. B-14. Collision severity index for two emergency lead-car decelerations (0.8g and 31.06g).

requires that T be reduced accordingly and/or A_2 be increased. There is a practically achievable lower limit for T as well as a reasonable maximum choice for A_2 (i.e., the maximum value that can be generally guaranteed in practice). Thus, the choice of A_1 is constrained by factors other than accident severity.

In Fig. B-14b, which corresponds to $a_1(t) = 31.06g$, S_c decreased with increasing A_1 for both the parallel and series cases; however, S_c was much less for the former than the latter. This result is similar to that of Lenard (3) for different circumstances, and clearly demonstrates the benefits of warning all vehicles simultaneously of an emergency situation.

b) Lead Vehicle Failure and Degraded Braking of Following Vehicle

Next consider the case where the lead vehicle is decelerated at $a_1(t) = 0.8g$ and accidents are caused by the inability of the following vehicles to decelerate at the policy choice of A_2. Such a case could arise from roadway surface conditions environmentally affected so that $a_2(t) \leq A_2$.

The results, which were obtained for the parameter sets of Table B-3, are shown in Fig. B-15, where S_c is plotted versus A_1 with $a_2(t) = 0.4g$ ($a_2(t) < A_2 = 0.6g$). Accident severity increases with decreasing A_1 and is considerably greater than for the first scenario. This is not surprising as two policy constraints are violated--$a_1(t) \geq A_1$ and $a_2(t) < A_2$--as compared to one for the previous case. These results affirm the need to guarantee $a_2(t)$ at as high a level as possible. It should be noted that S_1^2 is again considerably larger for the serial case.

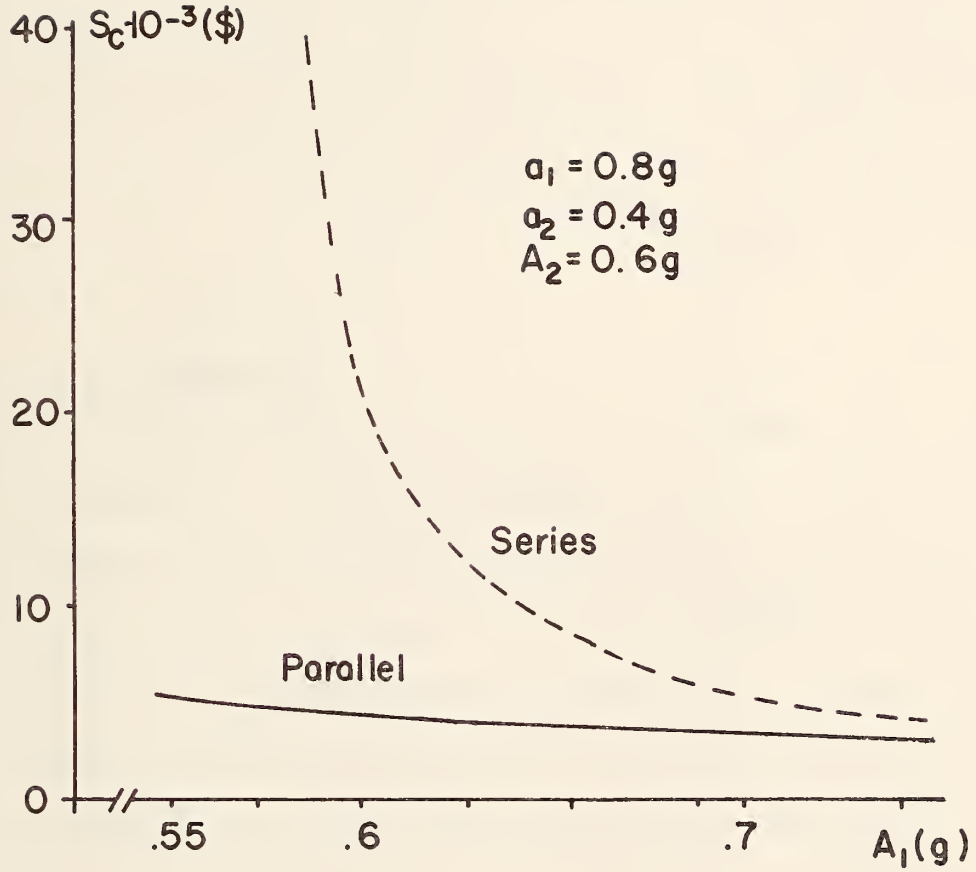

Fig. B-15. S_c versus A_1 with $a_2(t) = 0.4g$.

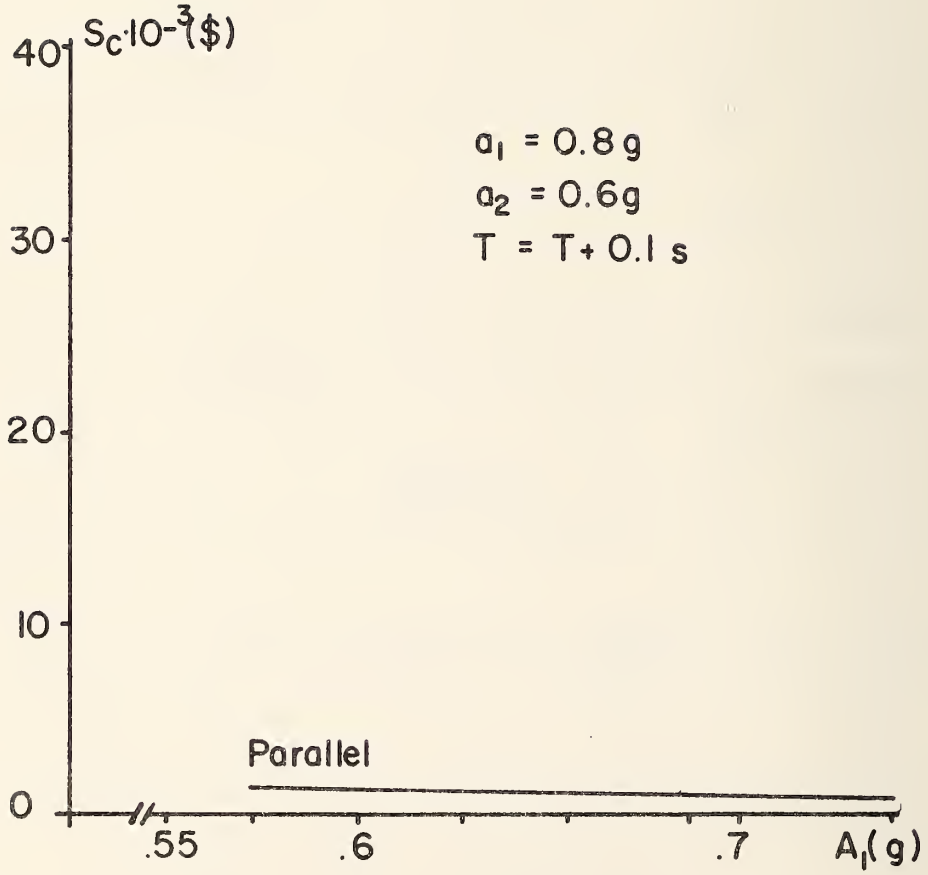

Fig. B-16. Accident cost for an increase in reaction time, T.

c) Increase in Reaction Lag

As a third possibility of considerable practical import, consider a case in which the command to the following vehicles to brake is delayed in excess of the specified value of T by 0.1 s (e.g., as would be due to an unanticipated event). The severity of the resulting accidents for the parameter sets listed in Table B-3 is shown in Fig. B-16, where S_c is plotted versus A_1 for the parallel case only. Here, $a_1(t)$ was 0.8g, and thus two policy constraints were again violated. Even so, S_c is generally lower (e.g., S_c = 1400) than the values obtained for the first two scenarios.

G. Summary and Discussion

Decreases in both the number of accidents and total accident cost are potential advantages of an automated highway system. At present, there is insufficient information to determine the magnitude of the former; however, some insight can be gained into accident severity and/or costs by considering one critical operational situation--the emergency braking of a platoon of closely spaced vehicles. Since high lane capacities ($\doteq$ 3600 veh/lane/hr) are desired, this spacing would correspond to a time headway of approximately 1 s for a uniform-spacing, headway policy.

With this policy, the minimum-permitted, intervehicular spacing is determined by safe, controlled stopping-distance considerations (see Chapter V). The latter are determined by a vehicle's characteristics (e.g., its control system, its braking system, and the vehicle/roadway interface) and network control factors--the primary one being the time delay associated with detecting and notifying vehicles that an accident

has occurred.

In Chapter V, various conditions under which safe, high-capacity operation could be achieved over a wide range of speeds were specified under the condition that the policy conditions were satisfied. If not, accidents (whose severity and/or cost have been of concern here) could result.

This effort was focused on developing a methodology to determine the severity and/or cost of such accidents. A collision model, based on report crash-testing results, was developed, and a measure of accident severity was selected. This was a simplified measure because sufficient accident data were not available to justify a more meaningful and complex choice. An effort was made to relate this measure to a cost in dollars by developing a cost factor, k. This involved a broad averaging of limited cost data -- which pertained to a variety of accident types. With this factor k, one can convert the specified accident measure into a dollar measure, which might be useful for comparison purposes.

The utility of the developed methodology was demonstrated by applying it to three accident scenarios, and resulted in the following observations:

i) A_l (the lead-vehicle deceleration to which the platoon can safely respond) should be as large as possible;

ii) Accident severity was, in some cases, greatly increased when a serial reaction delay (rather than a single parallel delay) was present;

iii) A moderate increase in the parallel reaction delay resulted in a relatively small change in accident severity; and

iv) Accident severity was very sensitive to decreases in the deceleration capabilities of the following vehicles.

Such results, especially in a quantified form, provide useful measures of the effect of making different policy choices (e.g., for A_1).

Several provisos are applicable: First, the accident severity measure employed was overly simplified, and a more meaningful measure would be that of Eqn. (B-7). The principal difficulty with this measure is an appropriate specification of the ε_i which are contained herein. Second, it was not possible to obtain a meaningful conversion of accident severity to accident cost (e.g., the approach employed was based on a broad, nondiscriminatory averaging of very limited accident data from a variety of accident types. A more meaningful cost factor would be based on accidents involving platoons of vehicles). Finally, the analysis contained herein pertains only to one type of accident--the multiple collisions which result when the lead vehicle of a platoon brakes at a rate which is greater than the selected policy value. To assess severity costs for all accident types in a system, much additional information must be available, e.g., the probability that $a_1(t) \geq A_1$ given that a platoon of n vehicles has been formed, the probability of a platoon being in a particular initial state, and the probability of other than rear-end collisions.

There are many possibilities here for future research efforts.

BIBLIOGRAPHY

1. Fenton, R.E., et al, "Fundamental Studies in the Automatic Longitudinal Control of Vehicles," Final Rpt. DOT-TST-76-79, Dept. of Elec. Engr., The Ohio State University, Columbus, Ohio, July 1975.

2. Fenton, R.E., et al, "Fundamental Studies in the Longitudinal Control of Automated Ground Vehicles," Final Rpt. FHWA-RD-77-28, Dept. of Elec. Engr., The Ohio State University, Columbus, Ohio, December 1976.

3. Lenard, M., "Safety Considerations for a High Density Automated Vehicle System," Transportation Science, Vol. 11, No. 1, May 1970, pp 138-158.

4. Grime, G. and Jones, I.S., "Car Collisions - The Movement of Cars and Their Occupants in Accidents," Proc. Instn. Mech. Engrs., Vol. 184, Pt2A, No. 5, 1969-70.

5. Elsholz, F., "Unfallforschung mit Personenkraftwagen," Zeitschrift fuer Verkehrssicherheit, 14, Heft 1, 1968, pp. 55-61.

6. Schmid, C., "Probleme der Fahrsicherheit," Zeitschrift fuer Verkehrssicherheit, 13, Heft 3, 1967, pp. 135-140.

7. Plotkin, S.C., "A Common Momentum Error in Auto Accident Reconstruction," IEEE Transactions on Vehicular Technology, Vol. VT-24, No. 1, Feb. 1975, p. 15.

8. Godfrey, M.B., "Headway and Switching Strategies for Automated Vehicular Ground Transportation Systems," Rpt. PB-173 644, Dept. of Mech. Engr., Massachusetts Institute of Technology, Nov. 1966.

9. Rahimi, A., et al, "Safety Analysis for Automated Transportation Systems," Transportation Science, Vol. 7, No. 1, 1973, pp 1-17.

10. Horn, B.E., "Safety Criteria in Car-Following Situations for Freeway Traffic," Thesis, Dept. of Civil Engr., The Ohio State University, Columbus, Ohio, 1966.

11. Treiterer, J., "Improvement of Traffic Flow and Safety by Longitudinal Control," Transportation Research, Vol. 1, pp 231-251, 1967.

12. Carlson, W.L., "Crash Injury Loss: The Effect of Speed, Weight, and Crash Configuration," Accid. Anal. a. Prev., Vol. 9, pp 55-68, 1977.

13. Huelke, D.F., States, J.D. et al, "The Abbreviated Injury Scale (AIS)," American Association for Automotive Medicine, Morton Grove, Ill., 1976.

14. Anon., "Motorvehicle Accident Costs Analysis in the State of Ohio," Transportation Engineering Center, The Ohio State University, Columbus, Ohio, 1970.

15. Vecellio, R.L., "Ohio Turnpike Accident Analysis 1960-65," Thesis, Dept. of Civil Engr., The Ohio State University, Columbus, Ohio, 1967.

16. Smith, R.N.; Tamburri, T.N., "Direct Costs of California State Highway Accidents," Highway Research Record, No. 225, pp 9-29, 1968.

17. Solomon, D., "Accidents on Main Rural Highways Related to Speed, Driver, and Vehicle," U.S. Dept. of Commerce, Wash., D.C., July 1964.

18. Abramson, P., "An Accident Evaluation Analysis," Transportation Research Record, No. 486, pp 33-41, 1974.

19. Anon., "Accident Facts 1973," National Safety Council, 1973.

20. Böttger, O., "Ueberlegungen zur Erhoehung der Strassensicherheit durch automatische Spurfuehrung und Abstandshaltung," Zeitschrift fuer Verkehrssicherheit, Vol. 18, No. 2, pp 75-86, 1972.

21. Baerwald, J.E., Ed., et al, "Transportation and Traffic Engineering Handbook," Prentice-Hall, Inc., Englewood Cliffs, N.J., Third Edition, 1976.

22. Anon., "Practicality of Automated Highway Systems, Vol. III: Socio-Economic Design Considerations," Final Rpt., prepared for DOT-FHA, November 1977.

23. Glimm, J., "Simulation Program for a Cost Sensitivity Analysis of a Headway Safety Policy," Transportation Control Lab. working-paper 78-1, Dept. of Elec. Engr., The Ohio State University, Columbus, Ohio, 1978.

*U.S. GOVERNMENT PRINTING OFFICE: 1979 626-636/1643 1-3

FEDERALLY COORDINATED PROGRAM OF HIGHWAY RESEARCH AND DEVELOPMENT (FCP)

The Offices of Research and Development of the Federal Highway Administration are responsible for a broad program of research with resources including its own staff, contract programs, and a Federal-Aid program which is conducted by or through the State highway departments and which also finances the National Cooperative Highway Research Program managed by the Transportation Research Board. The Federally Coordinated Program of Highway Research and Development (FCP) is a carefully selected group of projects aimed at urgent, national problems, which concentrates these resources on these problems to obtain timely solutions. Virtually all of the available funds and staff resources are a part of the FCP, together with as much of the Federal-aid research funds of the States and the NCHRP resources as the States agree to devote to these projects.*

FCP Category Descriptions

1. Improved Highway Design and Operation for Safety

Safety R&D addresses problems connected with the responsibilities of the Federal Highway Administration under the Highway Safety Act and includes investigation of appropriate design standards, roadside hardware, signing, and physical and scientific data for the formulation of improved safety regulations.

2. Reduction of Traffic Congestion and Improved Operational Efficiency

Traffic R&D is concerned with increasing the operational efficiency of existing highways by advancing technology, by improving designs for existing as well as new facilities, and by keeping the demand-capacity relationship in better balance through traffic management techniques such as bus and carpool preferential treatment, motorist information, and rerouting of traffic.

3. Environmental Considerations in Highway Design, Location, Construction, and Operation

Environmental R&D is directed toward identifying and evaluating highway elements which affect the quality of the human environment. The ultimate goals are reduction of adverse highway and traffic impacts, and protection and enhancement of the environment.

4. Improved Materials Utilization and Durability

Materials R&D is concerned with expanding the knowledge of materials properties and technology to fully utilize available naturally occurring materials, to develop extender or substitute materials for materials in short supply, and to devise procedures for converting industrial and other wastes into useful highway products. These activities are all directed toward the common goals of lowering the cost of highway construction and extending the period of maintenance-free operation.

5. Improved Design to Reduce Costs, Extend Life Expectancy, and Insure Structural Safety

Structural R&D is concerned with furthering the latest technological advances in structural designs, fabrication processes, and construction techniques, to provide safe, efficient highways at reasonable cost.

6. Prototype Development and Implementation of Research

This category is concerned with developing and transferring research and technology into practice, or, as it has been commonly identified, "technology transfer."

7. Improved Technology for Highway Maintenance

Maintenance R&D objectives include the development and application of new technology to improve management, to augment the utilization of resources, and to increase operational efficiency and safety in the maintenance of highway facilities.

---

* The complete 7-volume official statement of the FCP is available from the National Technical Information Service (NTIS), Springfield, Virginia 22161 (Order No. PB 242057, price $45 postpaid). Single copies of the introductory volume are obtainable without charge from Program Analysis (HRD-2), Offices of Research and Development, Federal Highway Administration, Washington, D.C. 20590.